SYNTHESIS, ANTI HIV-1 REVERSE TRANSCRIPTASE AND CYTOTOXIC ACTIVITY OF PHTHALIMIDE DERIVATIVES

SURATSAWADEE PIYAVIRIYAKUL

A THESIS SUBMITTED IN PARTIAL FULFILLMENT
OF THE REQUIREMENTS FOR
THE DEGREE OF MASTER OF SCIENCE
(PHARMACEUTICAL CHEMISTRY AND PHYTOCHEMISTRY)
FACULTY OF GRADUATE STUDIES
MAHIDOL UNIVERSITY
2007

Thesis

Entitled

SYNTHESIS, ANTI HIV-1 REVERSE TRANSCRIPTASE AND CYTOTOXIC ACTIVITY OF PHTHALIMIDE DERIVATIVES

Suratsawadee Piyaviriyakul

Ms. Suratsawadee Piyaviriyakul
Candidate

Jiraporn Ungwitayatorn

Assoc. Prof. Jiraporn Ungwitayatorn, Ph.D.
Major-Advisor

Chanpen Wiwat

Assoc. Prof. Chanpen Wiwat, Ph.D.
Co-Advisor

Prof. M.D. Jisnuson Svasti, Ph.D.
Dean
Faculty of Graduate Studies

Assoc. Prof. Weena Jirachariyakul, Ph.D.
Chair
Master of Science in Pharmacy
Programme in Pharmaceutical Chemistry
Faculty of Pharmacy

Thesis

Entitled

SYNTHESIS, ANTI HIV-1 REVERSE TRANSCRIPTASE AND CYTOTOXIC ACTIVITY OF PHTHALIMIDE DERIVATIVES

was submitted to the Faculty of Graduate Studies, Mahidol University
for the degree of Master of Science in Pharmaceutical Chemistry and Phytochemistry
on
August 1, 2007

Ms. Suratsawadee Piyaviriyakul
Candidate

Assist. Prof. Weerasak Samee, Ph.D.
Chair

Assoc. Prof. Jiraporn Ungwitayatorn, Ph.D
Member

Assoc. Prof. Chanpen Wiwat, Ph.D.
Member

Prof. M.D. Jisnuson Svasti, Ph.D.
Dean
Faculty of Graduate Studies
Mahidol University

Prof. Ampol Mitrevej, Ph.D.
Dean
Faculty of Pharmacy
Mahidol University

ACKNOWLEDGEMENTS

I am sincerely indebted to my thesis advisor, Associate Professor Dr. Jiraporn Ungwitayatorn, for her kindness, helpful, valuable supervision, guidance and constructive criticism during my entire study.

My sincere and grateful appreciation are also expressed to Associate Professor Dr. Chanpen Wiwat, my co-advisor, for her guidance and correction in bioassay section.

I sincerely wish to thank Assistant Professor Dr. Weerasak Samee, Department of Pharmaceutical Chemistry and Pharmacognosy, Faculty of Pharmacy, Srinakharinwirot University, Nakornnayok for being a chairman of the defense committee.

Acknowledgement, Department of Pharmaceutical Chemistry, Faculty of Pharmacy, Mahidol University, for providing research facilities and supporting the important information. Natural Product Section, Research Division, National Cancer Institute for supporting the cytotoxicity activity test. As well, my special appreciation gives to my fellow graduate students at the Faculty of Pharmacy, Mahidol University, and other persons who have not been mentioned here for their help, friendship and encouragement.

Finally, I wish to express my gratitude and infinite thanks to my family for their love, concern, encouragement and precious spiritual support throughout my life.

Suratsawadee Piyaviriyakul

SYNTHESIS, ANTI HIV-1 REVERSE TRANSCRIPTASE AND CYTOTOXIC ACTIVITY OF PHTHALIMIDE DERIVATIVES

SURATSAWADEE PIYAVIRIYAKUL 4636365 PYPP/M

M.Sc. (PHARMACEUTICAL CHEMISTRY AND PHYTOCHEMISTRY)

THESIS ADVISORS: JIRAPORN UNGWITAYATORN, Ph.D. CHANPEN WIWAT, Ph.D.

ABSTRACT

The novel phthalimide derivatives were designed and synthesized by modifying of the phthalimide structures based on the three-dimentional quantitative structure-activity relationship (3D QSAR), comparative molecular field analysis (CoMFA) and comparative molecular similarity indices analysis (CoMSIA) studies. These derivatives were synthesized using phthalimide and substituted benzyl halide in the presence potassium hydroxide. Six newly synthesized compounds were evaluated for HIV-1 reverse transcriptase inhibitory activity by radioactivity assay at concentration 200 µg/mL using poly(rA).oligo(dT) as template-primer, methyl-[^{3}H]dTTP as substrate and doxorubicin (1.25 mM) as positive control. The synthesized compounds showed low inhibitory activity in the range of 7.9-22.9 % inhibition. Since infection with HIV-1 is associated with an increase risk of developing certain types of cancer, the previously and newly synthesized phthalimide derivatives have been subjected to cytotoxic activity testing using MTT colorimetric method against the cancer cell lines KB and HeLa and normal vero cell line. 1-Phthalimidomethyl-4-*tert*-butylbenzene, compound **36** demonstrated promising cytotoxic activity that was less toxic to normal cells.

KEY WORDS: HIV-1 REVERSE TRANSCRIPTASE INHIBITOR ACTIVITY/ CYTOTOXIC ACTIVITY/ PHTHALIMIDE DERIVATIVES.

87 pp.

การสังเคราะห์ การทดสอบฤทธิ์ต้านเอนไซม์ HIV-1 reverse transcriptase และความเป็นพิษต่อเซลล์มะเร็งของอนุพันธ์ phthalimide (SYNTHESIS, ANTI HIV-1 REVERSE TRANSCRIPTASE AND CYTOTOXIC ACTIVITY OF PHTHALIMIDE DERIVATIVES)

สุรัสวดี ปิยะวิริยะกุล 4636365 PYPP/M

วท.ม. (เภสัชเคมีและพฤกษเคมี)

กรรมการควบคุมวิทยานิพนธ์ : จิรภรณ์ อังวิทยาธร, Ph.D., จันทร์เพ็ญ วิวัฒน์, Ph.D.

บทคัดย่อ

วิทยานิพนธ์นี้ได้ทำการออกแบบและสังเคราะห์อนุพันธ์ของสาร phthalimide โดยอาศัยข้อมูลจากผลของการศึกษาหาความสัมพันธ์เชิงปริมาณระหว่างโครงสร้างทางเคมีและการออกฤทธิ์ของยาแบบ 3 มิติ ด้วยวิธี comparative molecular field analysis (CoMFA) และวิธี comparative molecular similarity indices analysis (CoMSIA) และทำการสังเคราะห์ โดยใช้ phthalimide ทำปฏิกิริยากับสาร substituted benzyl halide โดยมี KOH เป็นตัวเร่งปฏิกิริยา ได้สารอนุพันธ์ใหม่ 6 ตัว จากนั้นทดสอบฤทธิ์ในการต้านเอนไซม์ HIV-1 reverse transcriptase โดยวิธี radiometric assay ที่ความเข้มข้น 200 µg/mL โดยใช้ poly(rA).oligo(dT) เป็น template-primer และใช้ methyl-[^{3}H]dTTP เป็น substrate และ doxorubicin เป็น positive control ที่ความเข้มข้น 1.25 mM พบว่าสารที่สังเคราะห์ได้มีฤทธิ์ในการยับยั้งเอ็นไซม์อยู่ในช่วง 7.9-22.9 % มีรายงานว่าเชื้อ HIV-1 มีความสัมพันธ์กับอัตราเสี่ยงในการเกิดโรคมะเร็ง จึงนำอนุพันธ์ phthalimide ทั้งหมดมาทำการทดสอบความเป็นพิษต่อเซลล์มะเร็ง 3 ชนิด คือ มะเร็งช่องปาก (KB), มะเร็งปากมดลูก (HeLa) และเซลล์ปกติ (vero) โดยวิธี MTT colorimetric method พบว่ามี อนุพันธ์ **36** แสดงความเป็นพิษต่อเซลล์มะเร็งและไม่เป็นพิษต่อเซลล์ปกติ

87 หน้า

CONTENTS

CONTENTS (cont.)

LIST OF TABLES

Tables **Page**

LIST OF FIGURES

Figures **Page**

LIST OF FIGURES (cont.)

LIST OF ABBREVIATIONS

Å	angstrom
ABC	abacavir
AIDS	acquired immunodeficiency syndrome
APV	amprenavir
Arg	arginine
Asn	asparagine
Asp	aspartic acid
ATH-8	atherosclerosis 8
ATZ	atazanavir
AZT	zidovudine
cm^{-1}	per centimeter
ºC	degree Celsius
CTB	CellTiter Blue
CC_{50}	50% cytotoxic concentration
CoMFA	comparative molecular field analysis
CoMSIA	comparative molecular similarity indices analysis
cpm	count per minute
CYP3A4	cytochrome P450 3A4
3D	three dimension
d	doublet
Da	Dalton
δ	chemical shift
d4T	stavudine
ddC	zalcitabine
ddI	didanosine
DMSO	dimethyl sulfoxide
DNA	deoxyribonucleic acid
DLV	delavirdine

LIST OF ABBREVIATIONS (cont.)

EC_{50}	50% effective concentration
EC_{90}	90% effective concentration
EI	electron impact
EFV	efavirenz
env	envelope glycoprotein
et al	and others
ETC	emtricitabine
fAPV	fosamprenavir
FDA	Food and Drug Administration
FTIR	Fourier transform infrared spectroscopy
g	gram
gag	group-specifc antigen
Gly	glycine
gp	glycoproteins
HAART	highly active antiretroviral therapy
HeLa	human cervical carcinoma
His	histidine
HIV-1	human immunodeficiency virus subtype 1
^{1}H NMR	proton nuclear magnetic resonance
IC_{50}	50% inhibitory concentration
i.e.	that is
Ile	isoleucine
IND	indinavir
%IR	percentage of inhibitory ratio
J	coupling constant
KB	human epidermoid carcinoma
Kcal	kilo calorie
kDa	kilo Dalton

LIST OF ABBREVIATIONS (cont.)

LDH	lactate dehydrogenase
Leu	leucine
LPV	lopinavir/ritronavir
LTR	long terminal repeat
Lys	lysine
MCF-7	epithelial breast cancer
mg	milligram
MHC	Major histocompatibility complex
mL	milliliter
mM	millimolar
mmol	millimole
m.p	melting point
MS	mass spectrometry
mRNA	messenger ribonucleic acid
m.o.i.	multiplicity of infection
MT-4	human lymphocyte
MTT	3- (4, 5-dimethylthiazol-2-yl)- 2, 5-diphenyltetrazolium bromide
nef	negative effector
NFV	nelfinavir
nm	nanometer
NNRTIs	non-nucleoside reverse transcriptase inhibitors
NRTIs	nucleoside reverse transcriptase inhibitors
NVP	nevirapine
OD	optical density units
Oligo(dA)	oligodeoxyadenylic acid
Oligo(dC)	oligodeoxycytidylic acid
Oligo(dG)	oligodeoxyguanylic acid
Oligo(dT)	oligodeoxythymidylic acid

LIST OF ABBREVIATIONS (cont.)

PBMC	peripheral blood mononuclear cells
Phe	phenylalanine
PIs	protease inhibitors
pol	polymerase enzyme activity
poly(rA)	polyadenylic acid
PR	protease
QSAR	quantitative structure-activity relationship
rev	regulatory of expression of virion protein
RNA	ribonucleic acid
RNaseH	ribonuclease H
RT	reverse transcriptase
RTV	ritonavir
s	singlet
SAR	structure activity relationship
SQV	saquinavir
SRB	sulforhodamine B
3TC	lamivudine
T20	enfuvirtide
TAR	transactivation response
tat	transactivator of transcription
TDF	tenofovir
Thr	threonine
TIBO	tetrahydrobenzodiazipinone
TMC114	darunavir
TPV	tipranavir
Trp	tryptophan
Tyr	tyrosine
UV	ultraviolet

LIST OF ABBREVIATIONS (cont.)

Val	valine
vero	african green monkey kidney cell
vif	viral infectivity factor
vpr	viral protein R
vpu	viral protein U
μg	microgram
μL	microlitre
μM	micromolar

CHAPTER I

INTRODUCTION

Acquired immunodeficiency syndrome (AIDS) is the most fatal disorder for which no complete successful chemotherapy has been developed so far (1). An asymptomatic period precedes AIDS in which the immune system becomes progressively compromised and unable to fight opportunistic infections and certain cancers (2). Human immunodeficiency virus subtype 1 (HIV-1), a retrovirus, has been found to be prevalent in causing this disease. The HIV pandemic poses one of the greatest challenges to global public health. In estimated 39.5 million people are living with HIV and approximately 4.3 million new infections in 2006 with 2.8 million (65%) of these occurring in sub-saharan africa and important increases in eastern europe and central asia (3). Infection with the HIV-1 is associated with an increased risk of developing certain cancer, particularly Kaposi's sarcoma, non-Hodgkin's lymphoma, Hodgin's disease, cervical cancer and 20 other cancer types (4-7). Recent data report that HIV inhibitors are also potent antiangiogenic, antitumor of Kaposi sarcoma and MCF-7, decrease proliferation of human myelocytic leukemia cell (8-11).

HIV-1 reverse transcriptase (HIV-1 RT) has a vital role in the life cycle of the virus by catalyzing the transformation of the viral single-stranded RNA genome into a double-stranded DNA genome needed for viral genome integration. Two classes of HIV-1 RT inhibitors (HIV-1 RTIs) are used in clinical practice. The first HIV-1 RTIs identified are the nucleoside reverse transcriptase inhibitors (NRTIs), which constitute the backbone of the first line therapeutic intervention. After conversion to their triphosphates, which are the pharmacologically active species within cells, the nucleoside analogs mimic the natural substrates of the enzyme. However, since the analogs lack the 3'-OH group necessary for DNA chain elongation, they prematurely terminate the transformation of the viral RNA into DNA. Eight nucleoside HIV-1 RTIs, i.e., zidovudine (AZT), didanosine (ddI), zalcitabine (ddC), stavudine (d4T), lamivudine (3TC), abacavir (ABC), tenofovir (TDF) and emtricitabine (ETC) were

approved for treatment of HIV infection and are a cornerstone in highly active antiretroviral therapy (HAART) (12-14). Generally, in vivo nucleoside analogs are extensively distributed throughout the body but with limited penetration into the central nervous system. Furthermore, they are rather rapidly cleared from the systemic circulation with apparent half-life usually less than 3 hours. However, the effectiveness is limited by side effects, including bone marrow suppression, pancreatitis, peripheral neuropathy, cardiac and skeletal muscle myopathy, hepatitis steatosis, lactic acidosis, etc (12, 14). The second class are non-nucleoside reverse transcriptase inhibitors (NNRTIs). Unlike nucleoside analogs, NNRTIs bind into an allosteric site, the highly hydrophobic pocket, of the p66 subunit. This pocket is different but close to the polymerase active site of the RT enzyme. NNRTIs binding induces conformational change in some residues, which is probably critical for the polymerase function thereby leading to a noncompetitive inhibition of the enzyme. NNRTIs are attractive because they are highly specific and inactive against cellular polymerase, therefore, no nucleoside-related toxicity. Many structurally distinct families of NNRTIs have been identified. Three HIV-1 NNRTIs, i.e., nevirapine (NVP), delavirdine (DLV) and efavirenz (EFV) were approved for treatment of HIV infection (12-13, 15).

The HIV-1 protease (HIV-1 PR) is also an attractive target to a crucial step in the replication cycle of the viral involving the processing by virus-encoded protease of the viral *gag* and *gag-pol* polyproteins into structural proteins and enzymes essential for the proper assembly and maturation of fully infection virion. Inhibition of HIV-1 PR resulting in noninfectionus particle is attractive strategy to block the progression of HIV infection. Elucidation of the tertiary structure of HIV-1 PR has aided the rational design and development of protease inhibitors. Most HIV-1 PR inhibitors are peptidomimetic, therefore they are difficult to synthesize, and often have poor bioavailability. Although the active site of the enzyme is fairly symmetric, not all inhibitors are symmetric. The flexibility of the peptidomimetic inhibitor backbones appears to facilitate binding with the enzyme. Ten HIV-1 PR inhibitors, i.e., saquinavir (SQV), ritonavir (RTV), indinavir (IND), nelfinavir (NFV), amprenavir(APV), lopinavir/ritronavir (LPV), atazanavir (ATZ), fosamprenavir

(fAPV), tipranavir (TPV) and darunavir (TMC114) were approved for treatment HIV infection (12, 16-19).

Conceptually, the use of agents to block viral entry is also an attractive modality in the treatment of HIV infection. HIV fusion inhibitor, enfuvirtide (T20), the peptidic compound that blocks fusion by directly binding to gp41was recently licensed by the United States Food and Drug Administration (FDA) for treatment of HIV infected individuals, including those who failed to respond to prior antiretroviral therapy (12, 20-21).

The NNRTIs are our research group interest. The aim of this thesis is to synthesize more compounds in the phthalimide series with modifying structures based on the previous 3D QSAR studies, i.e., comparative molecular field analysis (CoMFA) and comparative molecular similarity indices analysis (CoMSIA) (22). Based on the steric contour map from CoMFA and hydrophobic contour map from CoMSIA, more new compounds in phthalimide series, were synthesized and evaluated for their HIV-1 RT inhibitory. Since several studies have reported that some HIV-1 RT inhibitors, e.g., AZT also exhibited antitumor activity (9,11), the synthesized phthalimide derivatives were subjected to cytotoxic activity test as well.

CHAPTER II

LITERATURE REVIEW

A. AIDS and molecular biology of HIV-1 virus

1. Acquired immunodeficiency syndrome (AIDS)

The human immunodeficiency virus (HIV), that causes acquired immunodeficiency syndromes (AIDS), was first identified 20 years ago. Similarly, there are currently two recognized strains of HIV, HIV-1 and HIV-2. HIV-1 is more virulenty, more easily transmitted and is the causes of the majority of HIV infections globally, while HIV-2 is less easily transmitted and is largely confined to West Africa (1-3). According to the latest figures published in the UNAIDS/WHO 2006 AIDS epidemic update, an estimated 39.5 million people are living with HIV. There were 4.3 million new infections in 2006 with 2.8 million (65%) of these occurring in sub-saharan africa and important increases in eastern europe and central asia (3).

HIV primarity infects viral components of the immune system such as $CD4^+$ T cell, macrophages and dendritic cell (23). It also directly and indirectly destroys $CD4^+$ T cell. As $CD4^+$ T cell are required for the proper functioning of the immune system, when enough $CD4^+$ T cell has been destroyed by HIV, the immune system function poorly, leading to AIDS. Many of the problems faced by people infected with HIV result from failure of the immune system to protect from apportunistic infections and cancers (24-25).

2. The viral genome

The genomic complexity and heterogeneity of HIV underlie its pathogenicity. The 9 kilobase single-stranded HIV RNA genome consists of ten open reading frames encoding structural genes, i.e., *gag, env, pol*, regulatory genes i.e., *tat*, *rev*, and accessory genes i.e., *nef, vif, vpr,* and *vpu* (Figure 1) (25). The structural genes are essential for retroviral replication, for instances, the *gag* gene encodes the precursor for virion capsid proteins and the *env* gene encodes the two major envelope glycoproteins,

gp120 and gp 41. These glycoproteins become embedded all over the host cell membrane and this membrane ultimately becomes the viral envelope as the virus "buds" out of cell as it completes its maturation process (25-26). The *pol* gene encodes the viral enzymes protease, reverse transcriptase, and integrase. These enzymes are produced as a *gag-pol* precursor polyprotein, which is processed by viral protease. The regulatory genes are required for control of the viral replication cycle. The *tat* gene acts as a potent transcriptional activator by binding to the transactivation response (TAR) element of the HIV long terminal repeat (LTR) to mediate viral gene expression. The *tat* gene produces proteins which turn on other HIV genes, greatly increasing the activity of the virus. Without *tat,* HIV is largely or totally inactive (26-28). The major role of *rev* is to regulate the expression of HIV proteins by controlling the export rate of mRNAs (28). The accessory genes products perform important functions related to virion maturation, release and infectivity. The *nef* interacts with host cell signal transduction proteins, down regulates expression of cell-surface proteins (CD4 and MHC Class I), and can induce apoptosis in non-infected cells. The *vif* promotes virion maturation and infectivity. The *vpr* is involved in targeting the nuclear localization of preintegration complexes, arrests infected cells at G2 phase of cell cycle, and inhibits cell division (28). The *vpu* acts in the degradation of CD4 in the endoplasmic reticulum and the enhancement of virion release from the plasma membrane (29).

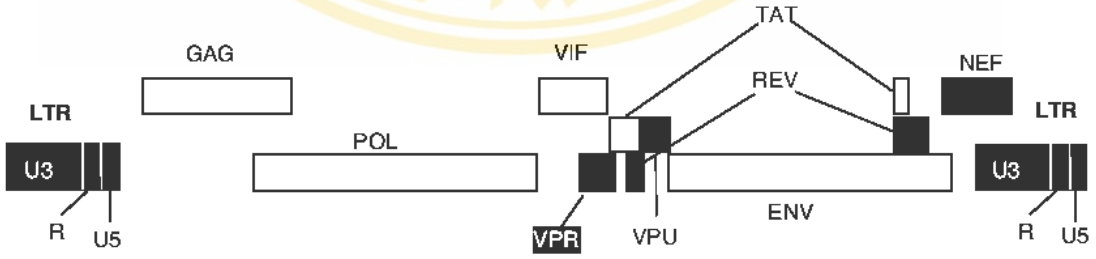

Figure 1. The viral genome of HIV-1 (28).

3. HIV-1 virion

The mature HIV-1 virion is a roughly spherical particle with a diameter of approximately 100 nm. The schematic drawing of the HIV-1 virion is shown in Figure

2. The outer surface of the virus is enveloped by a lipid bilayer that is derived from the membrane of the host cell. The envelope is acquired during virion budding and is studded with approximately 72 spikes formed by the two major viral envelope glycoproteins, gp 120 and gp 41. The gp 120 are anchored to the virus via interactions with the transmembrane protein (gp 41). A shell of matrix (p 17) lines the inner surface of the viral membrane and a conical capsid core particle comprising of the capsid protein (p 24) is located in the center of the virus. The capsid particle encapsidates two copies of the unspliced viral genome, stabilized by nucleocapsid protein (p7) and also contains three essential viral enzymes: reverse transcriptase (p64), integrase (p32), and protease (p10) (2, 25, 28). Major histocompatibility complex (MHC) is protein complex on surface of cells. MHC presents antigens to CD4.

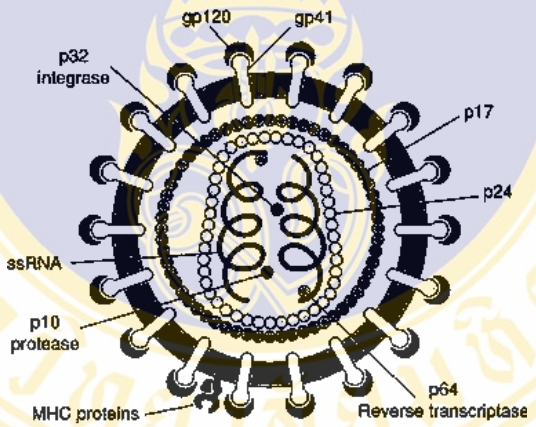

Figure 2. Schematic drawing of the HIV-1 virion (24).

4. The replication cycle of HIV-1

HIV infection begins with the interaction of the HIV glycoprotein (gp) 120 with the CD4 receptor on the surface of the target cell (Figure 3). Following CD4 binding, material change in the HIV gp 120/gp 41 complex is induced by interaction of gp 120 with the chemokine receptors CCR5 or CXCR4. This change in conformation exposes gp 41 and allowing it to initiate fusion of the membranes (24). After the fusion of membranes, the nucleocapsid enters the cytoplasm. The viral RNA, still enclosed in the viral capsid, is uncoated in a process aided by capsid proteins (p24) and cellular protein called cyclophilins (23-26). After uncoating process, reverse

transcription of the viral RNA generates a double-stranded DNA copy (cDNA) of the genome. The newly formed HIV DNA enters the host cell nucleus and integrates into the host cell genome via the action of the viral integrase leading to the formation of a provirus. The provirus may remain inactive for several years, producing few or no new copies of HIV. When the host cell receives a signal to become active, the provirus uses a host enzyme called RNA polymerase to create copies of the HIV genomic material, as well as shorter strands of RNA called messenger RNA (mRNA). The mRNA is used as a blueprint to make long chains of HIV proteins. The HIV life cycle final event is the maturation of cell-free particles upon action of HIV-1 protease (HIV-1 PR) (25). HIV-1 PR cleaves the polyproteins into functional enzymes and structural proteins. These matured viruses, if assembled correctly, are then capable of productive function when they encounter appropriate target cells and start the new replication cycles.

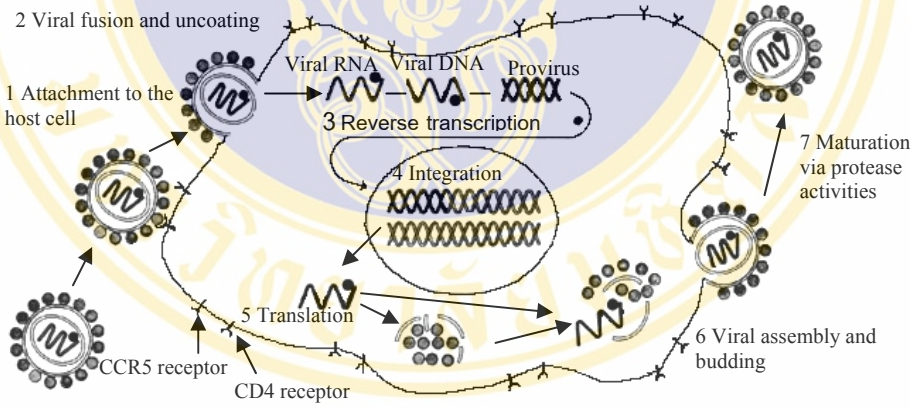

Figure 3. Schematic drawing of the HIV-1 replication cycle (25).

B. The development of anti HIV-1 agents

The current treatment for HIV/AIDS involves utilizing combination of a number of drugs. Although this therapy can suppress viral loads to below detectable levels, suppression has been observed to be reversible, especially once drug therapy is stopped (30-36). In addition, issues of patient adherence, drug toxicity, the emergence of multidrug-resistant phenotypes, and the presence of persistant reservoirs of virus

replication have highlighted the need to develop alternative therapeutic approaches utilizing other targets essential in the viral replication cycle.

Many steps in the HIV life cycle can be considered as a potential target for antiviral chemotherapy. The key in selective antiviral therapy is therefore to identify any process that is essential for the replication of the virus, but not for the survival of the cell. The gained knowledge about the replication cycle of the HIV virus has led to the extraction of virus-specific processes. Predominantly, scientists have focused their attentions on the following processes: 1) viral binding to target cells, 2) virus cell fusion, 3) virus uncoating, 4) reverse transcription of viral genomic RNA, 5) viral integration, 6) gene expression, and 7) protease activity. So far, the two strategies, 4 and 7 have been proven to be the most successful in the search for drugs that can be used for treatment of AIDS (29). These two targets will be described briefly in the following sections.

1. HIV-1 reverse transcriptase

Reverse transcriptase (RT) is essential for the life cycle of HIV. It converts the single stranded genomic RNA into the double stranded DNA version which is subsequently integrated into the host chromosome and passed on to all progeny cells (37-39). The HIV-1 RT molecule is a heterodimer consisting of a 560 residue chain (called p66) and a second chain comprising the initial 440 residues of p66 (called p51). Crystal structures of HIV RT reveal that the p66 subunit folds into five domains named finger, palm, thumb, connection, and RNaseH and that the p51 subunit comprises the first four domain of p66 (Figure 4). Whilst the equivalent domains from each subunit have a broadly similar fold, especially the finger and thumb domains, their relative arrangement in the two subunits is radically different. The p66/p51 HIV-1 RT heterodimer contains one DNA polymerization active site and one RNaseH active site, both of which residue in the p66 subunit at spatially distinct regions. Although the p51 subunit contains the same amino acid sequence that comprises the DNA polymerase domain of the p66 subunit, the polymerase active site in p51 is not functional (40).

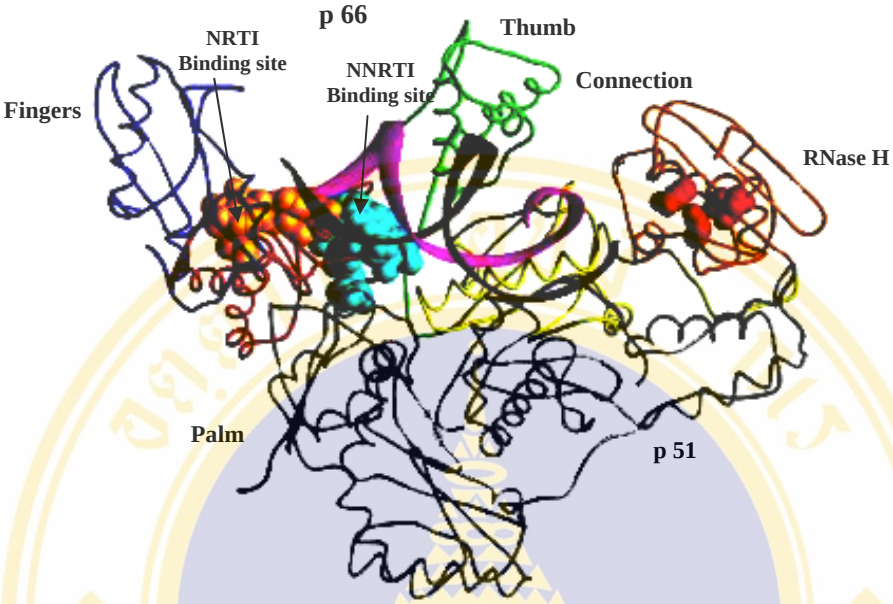

Figure 4. Structure of the HIV-1 RT and the location of the NRTI and NNRTI binding sites (38).

Because of its pivotal role in the HIV life cycle, HIV RT is a primary target for antiretroviral agents. Two major classes of inhibitors that inhibit the polymerase activities of HIV-1 RT have been identified, nucleoside/nucleotide reverse transcriptase inhibitors (NRTIs), and non-nucleoside reverse transcriptase inhibitors (NNRTIs). NRTI binds at the polymerase active site. The polymerase active site, as defined by the three aspartic acid residues Asp 110, Asp 185 and Asp 186 resides in the palm subdomain (37-40). NRTI mimics normal substrates of HIV-1 RT but lack the 3'-OH group required for DNA chain elongation, which causes premature termination of the growing viral DNA strand (40). NNRTI binds to a hydrophobic pocket on HIV-1 RT ca. 10-15 Å from the NRTI site (polymerase active site) and is primarily consisted of Leu100, Lys101, Lys103, Val106, Thr107, Val108, Val179, Tyr181, Tyr188, Val189, Gly190, Phe227, Trp229, Leu234, and Tyr318 in p66 (38). The putative entrance of the pocket is proposed to be located at the interface of the p66/p51 heterodimer and is primarily formed by Pro95, Leu100, Lys101, Lys103, Val179, and Tyr181 of p66 (40-41). The side chains of several residues, especially

those of Tyr181 and Tyr188, assume significant conformational changes on the binding of NNRTIs**.** This binding event alters the conformation of active site residues hampering normal enzymatic activity (41).

2. HIV-1 protease

HIV-1 protease (HIV-1 PR) is a symmetrical homodimer enzyme. It belongs to the family of aspartic proteases, which have two aspartic acid residues at the active site. This was confirmed through pepstatin A inhibition, an aspartic protease selective inhibitor, and by site-directed mutagenesis of the active site Asp25, which led to abolition of the catalytic activity. Examples of the aspartic proteases are pepsin, cathepsin D, renin, chymosin, penicillopepsin, plasmepsins and Rhizopus pepsin. General feature of HIV-1 PR structure is illustrated in Figure 5. Its *C2* symmetric homodimeric structure is consisting of two identical 99-amino acid chains. The active site, with the two catalytic aspartate residues Asp25 and Asp25', is located at the interface between the two monomers. Two β-hairpin structures, called 'flaps', are positioned over the active site. They undergo structural changes on binding of the inhibitor molecule. In the unliganded protease structure, the conformation of the flaps is open, thereby exposing the active site, whereas in the ligand complex, the flaps form a roof over the active site and the ligand. The flaps cover to a large extent of the bound ligand. This arrangement is advantageous for the design of inhibitors, because it offers a large number of tight interactions between the enzyme and the inhibitor. The PR dimer forms a series of subsites, i.e., S_3, S_2, S_1, $S_{1'}$, $S_{2'}$, and $S_{3'}$ which correspond to the binding sites of P_3, P_2, P_1, $P_{1'}$, $P_{2'}$, and $P_{3'}$ residues of substrate, where the scissile bond is located between the P_1 and $P_{1'}$ positions (Figure 5) (42-44).

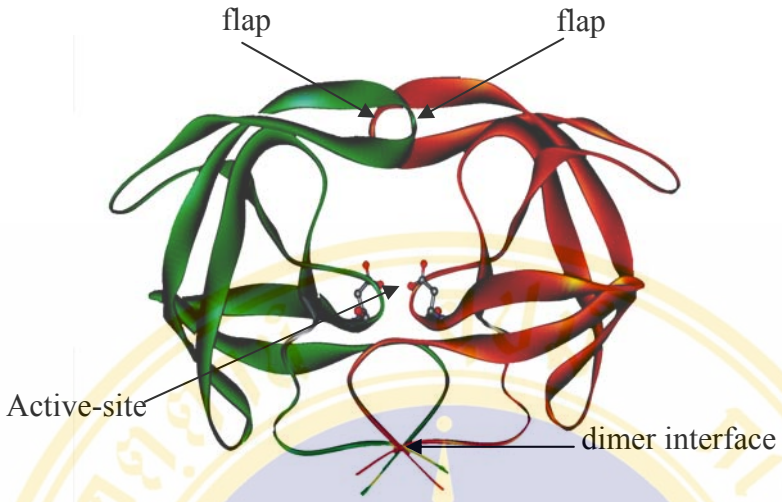

Figure 5. Structure of the HIV-1 PR binding site (42).

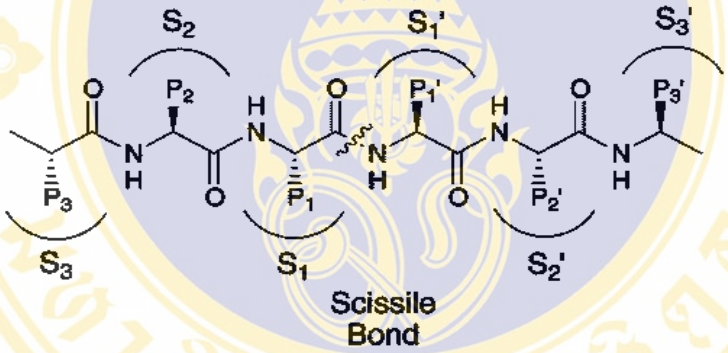

Figure 6. Standard nomenclature for substrate residues and their corresponding binding sites (43).

HIV-1 PR catalyzes the hydrolysis of specific peptide bonds within the HIV-1 *gag* and *gag-pol* polyproteins to generate the various structural and functional proteins essential for viral replication. It cleaves the p55 *gag* precursor into the four structural proteins, forming the core of the virion, p17, p24, p8 and p7. It also processes the p160 *gag/pol* precursor to liberate the structural elements just mentioned, and enzymes of the virus, i.e., the protease itself, the reverse transcriptase, and the endonuclease or integrase. The water molecule that binds between the enzyme (Ile50 and Ile50') and inhibitor is thought to position a peptide substrate, stretching the peptide bond out of

planarity toward a tetrahedral transition state which stabilized by a second water molecule (Figure 7) (44).

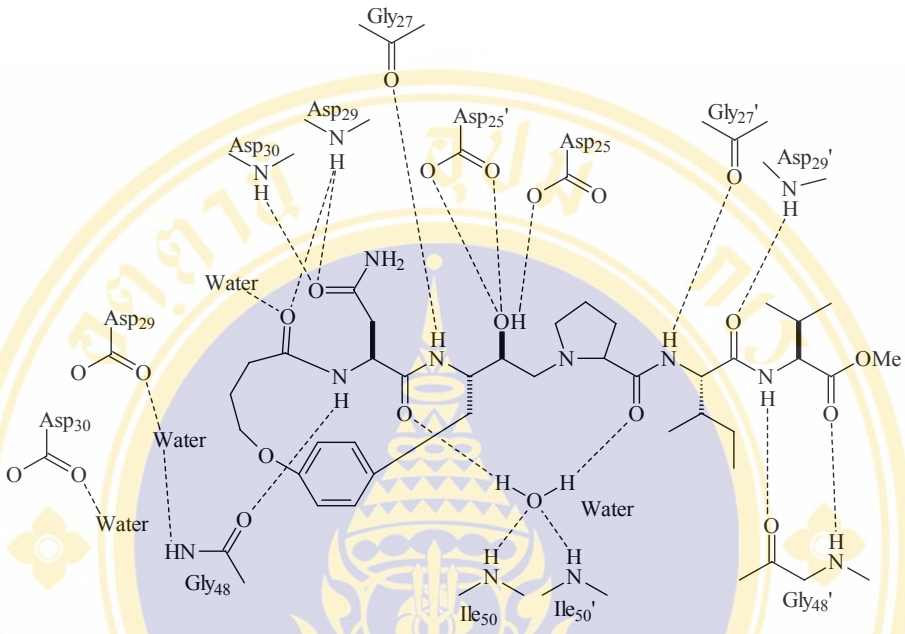

Figure 7. Hydrogen-bonding interactions between a cyclic peptidomimetic inhibitor and HIV-1 PR (44).

C. Antiretroviral agents

Currently, 20 antiretroviral drugs in 3 mechanistic classes were already approved for the treatment of HIV infection, i.e., HIV-1 RT inhibitors, HIV-1 PR inhibitors and HIV entry inhibitors (Table 1).

Table 1. Approved anti HIV-1 drugs.

Class	Generic name	Trade name	Company	Approval
NRTIs	Zidovudine (AZT)	Ritovir	GlaxoSmithkline	1987
	Didanosine (ddI)	Videx	Bristol Mayers Squibb	1991
	Zalcitabine (ddC)	Hivid	Hoffman-LaRoche	1992
	Stavudine (d4T)	Zerit	Bristol Mayers Squibb	1994
	Lamivudine (3TC)	Epivir	GlaxoSmithkline	1995
	Abacavir (ABC)	Ziagen	GlaxoSmithkline	1998
	Tenofovir (TDF)	Viread	Gilead Science	2001
	Emtricitabine (ETC)	Emtriva	Gilead Science	2003
NNRTIs	Nevirapine (NVP)	Viramune	Boeringer-Ingelheim	1996
	Delavirdine (DLV)	Rescriptor	Pharmacia & Upjohn	1997
	Efavirenz (EFV)	Sustiva	DuPont Merck	1998
PIs	Saquinavir (SQV)	Invirase	Hoffman-LaRoche	1995
	Ritonavir (RTV)	Norvir	Abbott Laboratories	1996
	Indinavir (IND)	Crixivan	Merck & Co.	1996
	Nelfinavir (NFV)	Viracept	Pfizer	1997
	Amprenavir (APV)	Agenerase	GlaxoSmithkline	1999
	Lopinavir/ritronavir	Kaletra	Abbott Laboratories	2000
	Atazanavir (ATZ)	Reyataz	Bristol Mayers Squibb	2003
	Fosamprenavir	Lexiva	GlaxoSmithKline	2003
	Tipranavir (TPV)	Aptivus	Boeringer-Ingelheim	2005
	Darunavir (TMC114)	Prezista	Tibotec, Inc.	2006
Fusion inhibitor	Enfuvirtide (T-20)	Fuzeon	Hoffman-LaRoche	2003

1. Nucleoside reverse transcriptase inhibitors (NRTIs)

NRTIs acting as alternative substrates or "false building blocks", they compete with physiological nucleotides, differing from these only by a minor modification in the sugar (ribose) molecule. The incorporation of nucleosides aborts DNA synthesis, as phosphodiester bridges can no longer be built to stabilize the double strand. NRTIs are converted to the active metabolite only after endocytosis, whereby they are phosphorylated to the active triphosphate derivatives. NRTIs are important components of almost all AIDS combination regimens. Although they are potent inhibitors of HIV replication, and are rapidly absorbed when taken orally, they can cause a wide spectrum of side effects. The currently available NRTIs are zidovudine (AZT), didanosine (ddI), zalcitabine (ddC), stavudine (d4T), lamivudine (3TC), abacavir (ABC), tenofovir (TDF), and emtricitabine (ETC), structures as shown in Figure 8.

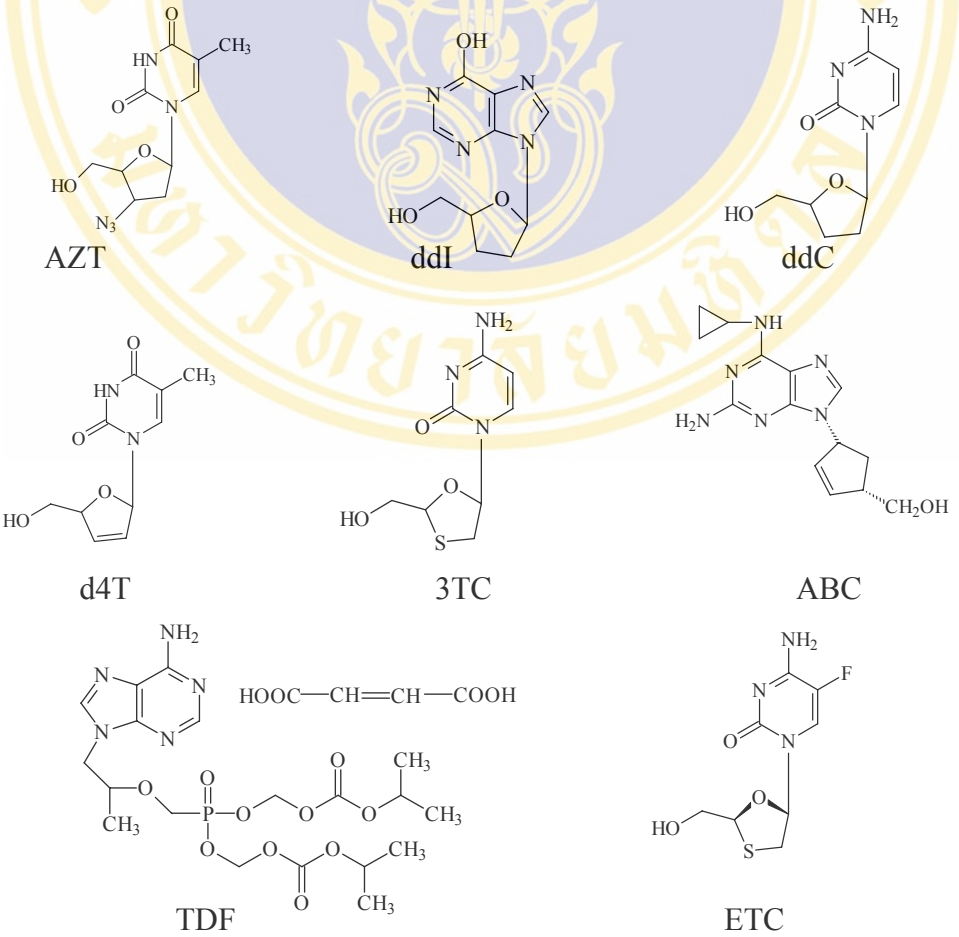

Figure 8. Structures of US FDA approved NRTIs.

3'-Azido-3'-deoxythymidine (AZT, Zidovudine, Retrovir®) was the first antiretroviral agent to be put on the market in 1987 (45). Early therapeutic interventions in asymptomatic individuals showed an initial clinical benefit but was not appear to be maintained for a prolonged period. The anti-HIV-1 activity of AZT stimulated the evaluation of a wide variety of nucleoside derivatives. AZT can cause severe side effect such as bone marrow suppression (46). AZT showed an IC_{50} value of 0.002 μM in MT-4 cells infected at a multiplicity of infection (m.o.i.) of 0.01 (47).

2′,3′-Dideoxyinosine (ddI, Didanosine, Videx®) is a nucleoside analogue that has been well investigated and showed good efficacy in numerous randomized studies (48). Didanosine was approved by the US FDA for the treatment of patients in whom AZT treatment had failed or who had become intolerant to AZT. The most serious side effect of didanosine is pancreatitis (49). Didanosine showed an *in vitro* IC_{50} range from 2.5-10 μM in lymphoblastic cell lines and 0.01-0.1 μM in monocyte/macrophage cell cultures (50).

2′,3′-Dideoxycytidine (ddC, zalcitabine, Hivid®) is an analogue of the nucleoside deoxycytidine. In 1993, ddC was approved for used in combination with AZT for HIV infection. The side effect of ddC is peripheral neuropathy whose symptoms involve tingling, burning, pain or numbness in the hands or feet (51). In laboratory and clinical isolates, ddC showed potent antiviral activity against HIV-1(IIIB) strain on ATH8 cell with IC_{50} value of 30 μM (52).

2′,3′-Didehydro-3′-deoxythymidine (d4T, stavudine, Zerit®) was the second thymidine analog introduced after AZT. Stavudine is one of the more effective nucleoside analogs currently in clinical use for HIV infection. Stavudine was approved by the US FDA for the treatment of patients who are intolerant to zidovudine or didanosine. Stavudine can cause the same side effect as ddC, i.e., peripheral neuropathy (53). Stavudine showed an IC_{50} value of 19 μM in MT-4 cell infected with HIV-1(IIIB) strain (54).

2',3'-Dideoxy-3'-thiacytidine (3TC, lamivudine, Epivir®) has potent antiretroviral activity *in vitro* with good oral bioavailability, and less toxicity than AZT (55). Lamivudine is frequently used as a component in Combivir® (lamivudine and zidovudine) and Trizivir® (abacavir, zidovudine and lamivudine). Its main disadvantage is rapid development of resistance, and a single point mutation (M184V)

is sufficient for loss of effectiveness. The major reported side effects of lamivudine are pancreatitis and peripheral neuropathy (56-57). Lamivudine showed an *in vitro* IC_{50} value of 0.4 μM in MT-4 cells infected at a m.o.i. of 0.01 (57).

Abacavir (ABC, Ziagen®) is a potent and mostly well-tolerated nucleoside with good CNS penetration due to its capable of crossing the blood-brain barrier. It has been well tolerated but the main side effect being hypersensitivity reactions, which sometimes can be dangerous. Strains that are resistant to AZT or lamivudine are generally sensitive to abacavir, whereas strains that are resistant to AZT and lamivudine are not sensitive to abacavir. Abacavir is given orally and has a high bioavailability of 83%. It is metabolized primarily through alcohol dehydrogenase or gluconyl transferase (58-60). When tested with normal human peripheral blood lymphocytes against fresh clinical isolates of HIV-1 obtained from antiretroviral drug-naive patients, the mean 50% inhibitory concentration (IC_{50}) was 0.26 μM (0.07 μg/ml); the corresponding IC_{50} of zidovudine (ZDV), didanosine (ddI), and zalcitabine (ddC) were 0.23, 0.49, and 0.03 μM, respectively (60).

Tenofovir (Viread®) acts as a false building block similarly to nucleoside analogues, targeting the enzyme reverse transcriptase. However, in addition to the pentose and nucleic base it is monophosphorylated, and is therefore referred to as a nucleotide. The more accurate description of the substance is tenofovir disoproxil fumarate which is a prodrug of tenofovir (61). Tenofovir showed an *in vitro* IC_{50} value of 29 μM in PBMC cell infected with HIV-1(IIIB) strain (62).

Emtricitabine (ETC, Emtriva®) is a synthetic nucleoside analogue of cytosine. It is the (-)enantiomer of a thio analogue of cytidine and it differs from other cytidine analogs by a fluorine in the 5 position. Emtricitabine, in combination with other antiretroviral agents, was approved for the treatment of HIV infection in adults age 18 and older. Emtricitabine can cause some side effects, including nausea, vomiting, abdominal pain, lack of appetite, weight loss, difficulty breathing, and fatigue (63-65). Emtricitabine showed an *in vitro* IC_{50} more than 100 μM in PBMC cell infected with HIV-1(LAV) strain (65).

2. Nonnucleoside reverse transcriptase inhibitors (NNRTIs)

NNRTIs were first described in 1990. In contrast to the NRTIs, they are not "false" building blocks, but rather bind directly and non-competitively to the enzyme at a position in close proximity to the substrate-binding site for nucleosides (39-41). A number of competition experiments suggested that various NNRTIs bound to the same or overlapping sites on HIV-1 RT. A crystal structure of RT complexed with the nonnucleoside nevirapine indicated that nevirapine bound in a hydrophobic pocket close to the polymerase active site. Most of NNRTIs binding conformations were in butterfly-like shape (41). Several amino acids residues critical for conferring resistance to other NNRTIs were also located in or near this pocket (especially codon groups 100-108 and 181-190), supporting the suggestion that these inhibitors were binding at similar sites (69). Since NNRTIs target at a nonsubstrate binding site of the RT, they do not require activation through cellular metabolism. The most significant problem with NNRTIs is resistance, with a high risk of cross-resistance. One point mutation on position 103 (Lys103Asp) of the hydrophobic binding site is sufficient to eliminate an entire class of drug. Point mutations may occur very rapidly. Resistance has even been described in maternal transmission prophylaxis, in mothers who had taken nevirapine only once during delivery (69-71). The currently available NNRTIs are nevirapine, delavirdine, and efavirenz, structures as shown in Figure 9.

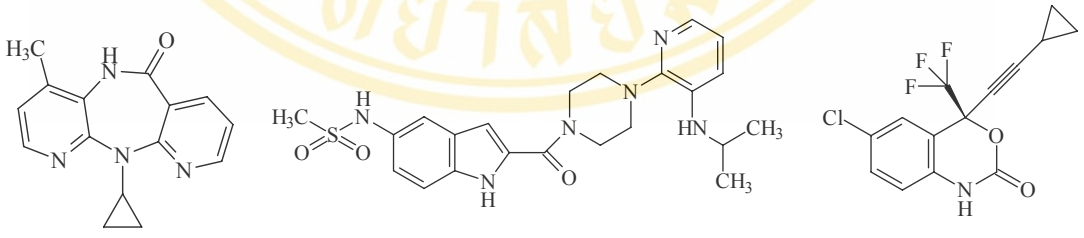

Nevirapine Delavirdine Efavirenz

Figure 9. Structures of the approved NNRTIs.

Nevirapine (Viramune®), the dipyridodiazepinone derivative, was the first licensed NNRTI. Nevirapine was found from a several derivatives of pyridobenzo-diazepinones and dipyridodiazepinones. Structure-activity relationship studies of this

series have demonstrated that the diazepinone N-11 position needs an alkyl group e.g. ethyl or cyclopropyl group and 7-position of the pyridobenzodiazepinones or 4-position of the dipyridodiazepinones requires a lipophilic group such as methyl group (41). In rare cases, it may cause serious hepatic toxicity. Nevirapine was approved by US FDA in 1996. Nevirapine showed IC_{50} value of 0.04 μM in MT-4 cells infected at a m.o.i. of 0.01 (70-71).

Delavirdine (Rescriptor®, U-90152S), the bisheteroaryl piperazine derivative, was the second NNRTI approved by US FDA. The development of delavirdine was based on the modification of the original molecule N-ethyl-2-[4-[4-methoxy-3,5-dimethylphenylmethyl]-1-piperazinyl]-3-pyridinamine (U-80493E). Replacement of the methylene linkage by carbonyl group and phenyl ring by indole ring greatly enhanced the HIV-1 RT inhibitory activity. Delavirdine with two aromatic groups, i.e., 5-methanesulfonamidoindole and 3-isopropylaminopyridine linking with carbonylpiperazine exhibited an IC_{50} of 0.26 μM against HIV-1 RT (wild-type) (72-73). Delavirdine exhibited good absolute bioavailability in preclinical studies and serum drug levels in excess of those needed for in vitro antiviral activity was safely maintained for prolonged periods of time. Delavirdine prevented the spread of HIV-1 in human lymphocytes significantly longer than AZT at the same concentration. Although delavirdine was less effective against the known non-nucleoside-resistant forms of HIV-1 RT (Tyr181Cys and Lys103Asp) as compared to wild-type RT, it still demonstrated significant activity against these mutant RTs in vitro (IC_{50} 8 μM). Due to requiring three times daily dosing, delavirdine is currently rarely prescribed, although it is likely to be approximately as effective as nevirapine and efavirenz (15).

Efavirenz (Sustiva®, Stocrin®) was the third NNRTI approved and the first in which it was demonstrated that NNRTIs were at least as effective as protease inhibitors**.** Efavirenz is a benzoxazinone derivative, consisting of chlorine atom at position 6, trifluoromethyl and cyclopropylethynyl at position 4 of benzoxazinone ring system. Efavirenz has shown good antiviral potency, high oral bioavailability, and favorable profile against a number of mutant RTs. The most common side effects of efavirenz are rash, nausea, dizziness, diarrhea, headache and insomnia and it is contraindicated in pregnancy (74). Lipids are not as favorably affected as with nevirapine, and hepatotoxicity is less frequent. Efavirenz showed IC_{50} value of 80 μM

in MT-4 cell infected with HIV-1 (IIIB) strain and this was the lowest concentration that exhibited signs of cytotoxicity (74-77)

3. HIV-1 protease inhibitors

HIV-1 PIs are compounds which bind to the active site of HIV-1 PR and prevent the processing of viral polyprotein precursors (*gag* and *gag-pol*). This results in the production of immature, non-infectious viral particles, thus inhibiting the replication and proliferation of HIV (43). PIs are almost always used in combination with at least two other anti-HIV drugs. Anti-HIV drug combinations, sometimes called cocktails, can reduce the amount of HIV in the patients's body (78). Several PIs are in clinical trials and eight of them (structures as shown in Figure 10) have been approved for using in AIDS patients.

Saquinavir (Ro 31-8959, Invirase®, Fortovase®), from Hoffmann-La Roche was developed by substrate analogy, with replacement of the scissile dipeptide fragment of the natural substrate with a Phe-Pro hydroxyethylamine transition state insert (79). The basic design criterion relied on the observation that HIV-1 PR cleaves the sequences containing dipeptides Tyr-Pro or Phe-Pro. Mammalian proteases do not cleave peptide bonds followed by a proline; thus, this target promised selectivity. Because reduced amides and hydroxyethylamine isosteres most readily accommodate the amino acid moiety, they were chosen for further studies. Replacement of a proline at the P1' subsite by (S,S,S)-decahydroisoquinoline-3-carbonyl (DIQ) significantly improved the potency of the inhibitors (80). This general approach has previously been used with success by a number of researchers seeking to develop inhibitors of human renin. Following traditional SAR optimization, saquinavir emerged and became the first approved HIV-1 PI in December 1995. Saquinavir inhibits HIV-1 PR with a Ki value of 0.12 nM and shows specificity for that enzyme, with little inhibition of mammalian aspartyl proteases (IC_{50} > 10 mM) (81).

The first available formulation, Invirase®, was a hard gel capsule and provided dismal bioavailability of about 4% due to poor absorption and extensive first pass clearance. Fortovase® is a new version of saquinavir and is better absorbed by the body, it has a stronger anti-HIV effect than Invirase®. The anti-HIV effect of Fortovase® seems to be similar to other available PIs (79-83).

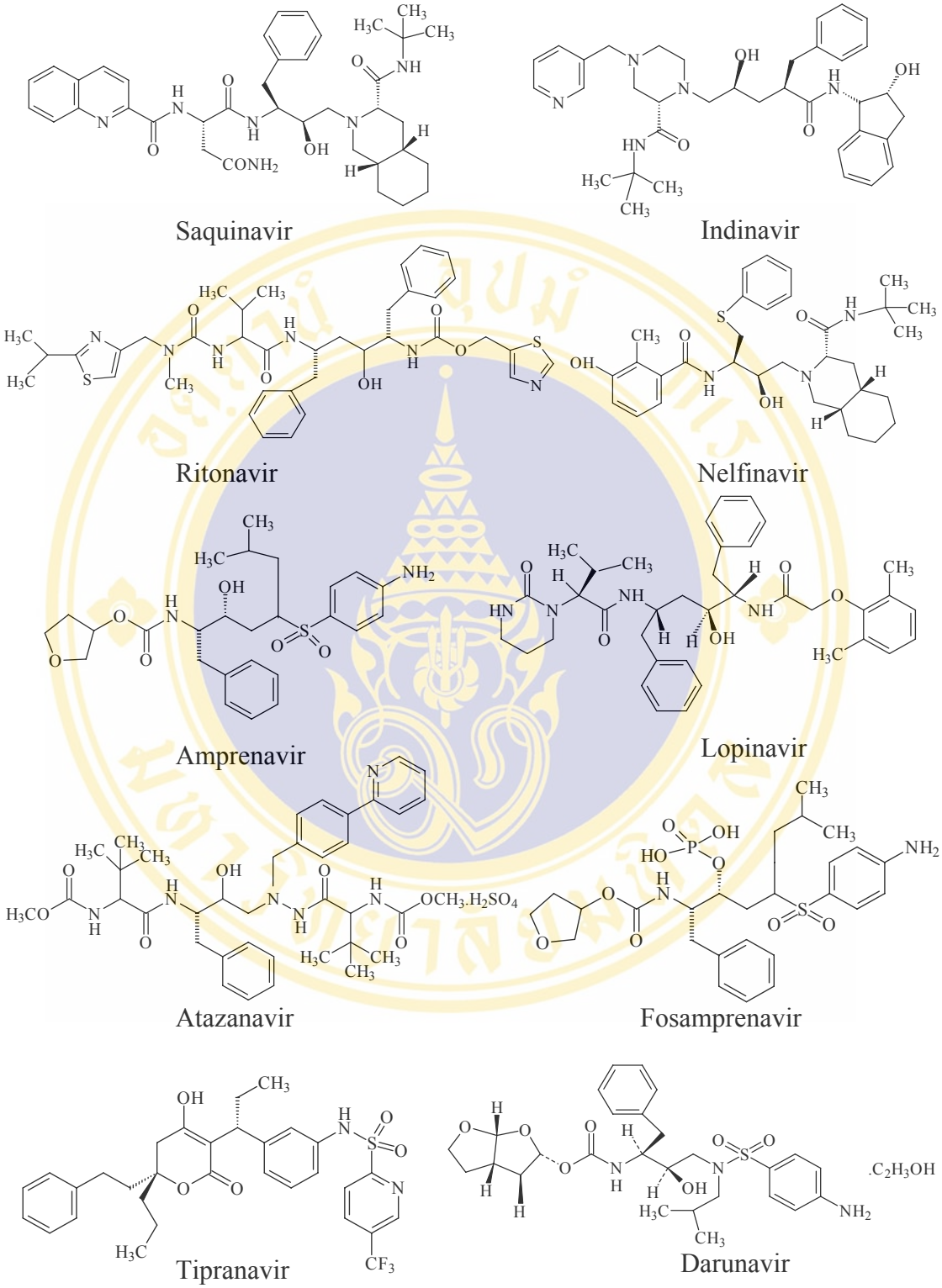

Figure 10. Structures of clinically approved anti HIV-1 PR drugs.

Ritonavir (ABT-538, Norvir®) was the symmetry of HIV-1 PR, and the first symmetric inhibitor (A-77003) from Abbott (84). Researchers at Abbott initially sought to exploit the *C2* symmetry of HIV-1 PR by incorporating *C2* symmetry as an inhibitor design element. After extensive SAR investigation, which also involved partial desymmetrization, ritonavir emerged. The compound showed an IC_{50} value against HIV-1 PR of 25 nM, with property of both an inducer and potent inhibitor of cytochrome P450 3A4. The latter property has been used to advantage for increasing the half-life of coadministered drugs (85-86). Ritonavir achieved FDA approval as Norvir® in February 1996.

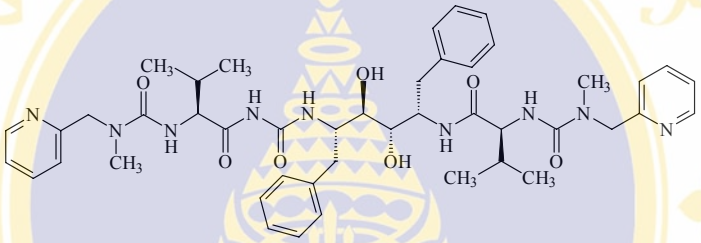

A-77003

Indinavir (MK-639, L-735,524, Crixivan®) was developed by Merck based on a transition-state mimetic concept (87), which had identified potent renin inhibitors based upon the PheΨ[$CHOHCH_2$]Phe transition state insert. In order to improve solubility and bioavailability, the P1/P2 portion of L-685,434 was replaced, first by the Roche P1'/P2' decahydroisoquinoline *tert*-butylamide (saquinavir) to generate L-704,486 (Figure 11), and subsequently by the pyridyl methylpiperazine moiety. Indinavir showed a Ki value against HIV-1 PR of 0.34 nM and is effective in antiviral cell culture with IC_{50} values of 25-100 nM. It is synergistic with both nucleoside and nonnucleoside RTIs, and is unique among currently approved PIs in having a low degree of protein binding in human plasma (88-89). Indinavir therapy has been associated with kidney stones and urinary tract sludging, leading to the recommendation of increased fluid intake during its use. Indinavir was approved by FDA in March 1996 under the trade name Crixivan®

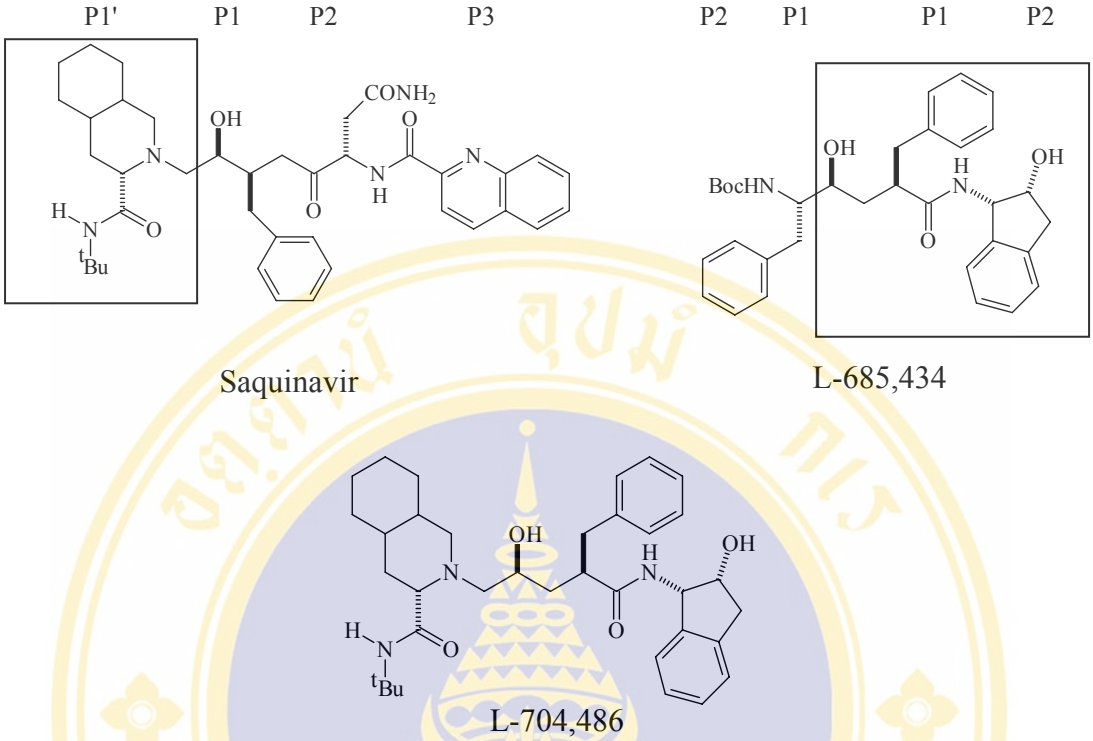

Figure 11. Design concept of indinavir (87).

Nelfinavir (AG-1343, Viracept®) was the first non-peptidomimetic PI, arose through a collaborative effort at Agouron and Lilly from a fusion of small peptidomimetic compounds with the Roche decahydroisoquinoline system. A key discovery during this evolution was the N-terminal 3-hydroxy-2-methylbenzoyl fragment, which subsequently found utility in other PIs (90). Nelfinavir showed a Ki value of 2 nM against HIV-1 PR with more than 78% bioavailability. Nelfinavir was launched in the US in March 1997 under the trade name Viracept® and was the first PI to be indicated for pediatric AIDS (91).

Amprenavir (VX-478, 141W94, Agenerase®) arose at Vertex from a structure-based design approach, which incorporated molecular weight minimization as a key goal. Its central core is identical to that of saquinavir, although both ends are quite different. The P2 group consists of tetrahydrofuran carbamate, whereas the P1'-P2' moieties consist of an isobutylphenyl sulfonamide with an added amide. This design gives amprenavir fewer chiral centers than saquinavir, facilitating synthesis and increasing water solubility to allow oral bioavailability as high as 40%-70%.

Amprenavir inhibited HIV-1 PR with a Ki value of 0.6 Nm (92). In humans, its pharmacokinetic properties, such as more than 70% bioavailability and long half-life (10 hours) are consistent with twice-daily dosing. Amprenavir was FDA approved as Agenerase® in April 1999. Amprenavir in a combination with lamivudine and saquinavir was more potent than lamivudine or saquinavir alone, although less effective than indinavir (92-94).

Lopinavir is a second generation inhibitor from Abbott Laboratories, designed to preserve activity against Val 82 mutant virus arising with ritonavir therapy. The compound is based upon the same core insert as ritonavir but includes highly modified peripheral functionality (95). In particular, the P3 functionality interacts only minimally with Val 82, decreasing the sensitivity of the inhibitor to this particular mutation. Lopinavir showed a Ki value of 1.3 pM against HIV-1 PR and an antiviral IC_{50} value in cell culture of 6-17 nM. Administered alone, lopinavir is rapidly cleared from circulation (96-99). For this reason, the approved product Kaletra® is a formulation of lopinavir containing ritonavir, which blocks the metabolic degradation mediated by cytochrome P450 3A4 (CYP3A4) (98). Lopinavir/Ritonavir (Lopinavir/r, Kaletra®), which contains both lopinavir and ritonavir, has been approved in both capsule and liquid formulations for adults and children greater than 6 months of age with HIV. Ritonavir may increase concentrations of lopinavir by more than 100-fold. This results in blood levels of lopinavir that enhance its effectiveness against HIV (96). The new drug is used in combination with other anti-HIV drugs. Dyslipidemia appears to be a significant problem with lopinavir therapy. Kaletra® was approved in September 2000 (99).

Atazanavir (Reyataz®) is a once-daily PI that received approval by US FDA in June 2003 (100). Structure-activity studies with a series of azadipeptides designed to mimic the transition state of the peptide-cleavage reaction catalyzed by HIV-1 PR identified lead compounds that had either potent antiviral activity against mutant HIV-1 strains or good oral bioavailability, but not both. Lead optimization using X-ray structural data from an inhibitor-protease complex led to the discovery of atazanavir sulphate, which showed excellent antiviral activity with high oral bioavailability and could be used in combination with other antiretroviral agents (101). Atazanavir differs from the peptidomimetic PIs (e.g. saquinavir, nelfinavir) by its *C2* symmetric drug

interaction concerns, chemical structure and was designed and synthesized based on X-ray studies of an enzyme dysazadipeptide complex (101-102). Atazanavir has an EC_{50} of 35 nmol/L against a variety of HIV-1 isolates in different cell types and is a highly selective and effective inhibitor of the HIV-1 PR *in vitro* (Ki, <1 nmol/L) (103).

Fosamprenavir (Lexiva®, Telzir®), is an essentially inactive, highly water soluble phosphate ester prodrug of amprenavir. It was synthesized to enhance oral bioavailability and solubility of amprenavir, thus allowing a reduction in the pill burden and offering the potential for improved patient compliance (104-106). Fosamprenavir calcium is a single stereoisomer with the (3*S*)(1*S*,2*R*) configuration. Fosamprenavir is rapidly and almost completely hydrolyzed to amprenavir and inorganic phosphate by cellular phosphatases in the gastrointestinal epithelium as it is absorbed (107). Fosamprenavir demonstrated efficacy when used as a sole PI administed twice-daily or in combination with ritonavir-boosting is a once-daily regimens in treatment naïve patients. Fosamprenavir appears to have an adverse effect profile similar to that of other PIs (104). The most common adverse event reported were diarrhea, nausea, vomiting, fatigue, headache, abdominal pain, and rash. Coadministration of food with fosamprenavir tablets appears to have little effect on amprenavir absorption. As a result, fosamprenavir may be taken with or without food (105). Fosamprenavir was approved by the FDA on October 20, 2003, for the treatment of HIV infection in adults in combination with other antiretroviral agents (108).

Tipranavir (TPV, PUN-140690, Aptivus®), is a new class of non-peptidic PIs with activity against both wild-type virus and variants resistant to current PIs and is also characterized by a high genetic barrier (109). Tipranavir, a sulfonamide compound containing 5,6-dihydro-4-hydroxy-2-pyrone, was developed from 5-cyano-2-pyridyl sulfonamide derivative, PNU-109112, that exhibited a Ki = 7 pM against recombinant HIV-1 PIs and IC_{50} of 40 μM in HIV-1 IIIB-infected H9 cell (110). Unfortunately, PNU-109112 was found to be convented both in cell culture in vitro, and in animal testing to a product with Ki about four orders of magnitude higher. Tipranavir was subsequently shown to suffer from excessive metabolic clearance, a fate which was later traced to an unusual enzymatic cleavage of the sulfonamide moiety (107). The simple replacement of the cyano group in the pyridyl ring of PNU-

109112 with a trifluoromethyl group conferred metabolic stability and high potency in the product. Tipranavir was resistant to sulfonamide cleavage, and the isomer with 3αR,6R stereochemistry exhibited a Ki = 8 pM against recombinant HIV-1 PR (it also inhibited the HIV-2 PR with Ki <2 nM). Tipranavir was highly specific for the viral enzyme; Ki values were in the μM range for the human aspartyl pretease, cathepsines D and E, and pepsin. In HIV-1 IIIB-infected H9 cell, tipranavir showed antiviral activity with IC_{50} = 30 μM, and IC_{90} = 100 μM (110-112). It was also effective against ten AZT-resistant HIV-1 clinical isolates in primary PMBC, exhibiting a mean IC_{90} value of 0.15 μM (109). In vitro assays, tipranavir was effective against strains of HIV that are highly resistant to indinavir, ritonavir, nelfinavir and saquinavir (111). Tipranavir was approved on June, 2005.

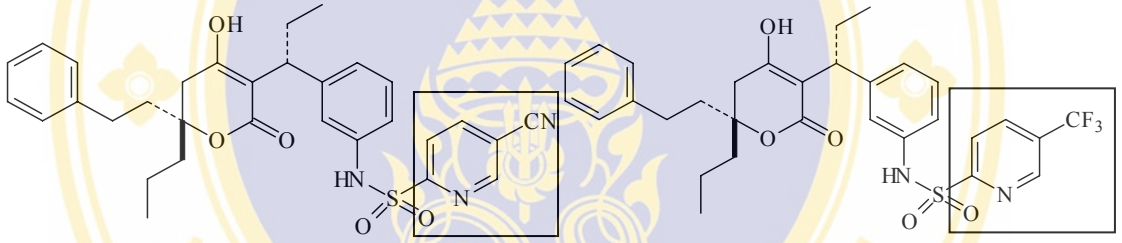

PNU-109112 Tipranavir

Darunavir (TMC114, UPI-94017, Prezista®), a newly class of peptidomic PIs from Tibotec, Inc. Prezista® in the from darunavir ethanolate, was developed from structural analogues of amprenavir (19).

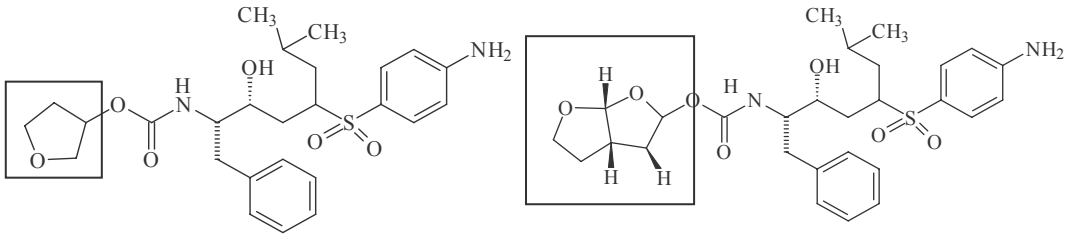

Amprenvir Darunavir

Darunavir showed inhibitory activity against wild-type HIV-1 and HIV-2. In vitro antiviral activity of darunavir against laboratory HIV-1 strains was evaluated in

acutely infected MT-4 cell, in PBMCs and in M/Ms. The EC_{50} of darunavir against different HIV-1 laboratory strains ranged from 1 to 5 nM and the corresponding EC_{90} ranged from 2.7 to 12 nM (113). Moreover, darunavir inhibited replication of HIV-2 with a EC_{50} of 4.2 nM and the EC_{90} of 13 nM, which was comparable with the activity observed against HIV-1 (113). The CC_{50} of darunavir was found to be > 100 μM, from which the selective index (CC_{50}/ EC_{50}) was calculated to be > 20,000 for wild-type HIV (113-115). Darunavir was also potent against multi-PIs-resistant clinical HIV-1 variants isolated from patients who had not response to existing antiviral regiments after having received a variety of antiviral agents (116-118). Darunavir was approved by the FDA on June, 2006.

4. Fusion inhibitors

Enfuvirtide (T-20, DP-178, Pentafuside®), the first in a new class of anti HIV-1 drugs that inhibit the entry of the virus into cells, was approved by the US FDA in March 2003 for treatment of HIV-1 infection in treatment-experienced patients. Enfuvirtide is a synthetic 36 amino acids peptide (Figure 12) corresponding to residues 127-162 of the extracellular portion (ectodomain) of gp41 (or residues 643-678 in the gp160 precursor) of the HIV envelope glycoprotein. The molecular formula of enfuvirtide is $C_{204}H_{301}N_{51}O_{64}$, and its molecular weight is 4492 Da. (20). Considering its large size, the manufacture of enfuvirtide is very complex, currently involving 106 steps in the chemical pathway to give a powder for subcutaneous injection (119). Because of the large size of the molecule and the complexity of the manufacturing process, enfuvirtide is expensive even by antiretroviral standards (119). Although enfuvirtide is the most expensive antiretroviral to date, the cost effectiveness of enfuvirtide has been explored and been demonstrated to be within currently acceptable thresholds for both the US and UK (120). Enfuvirtide was approved for using with other anti-HIV drugs in the treatment of HIV infection and was approved for using in HIV infected adults and children 6 years of age or older whose HIV infection has not been controlled by other anti-HIV drugs.

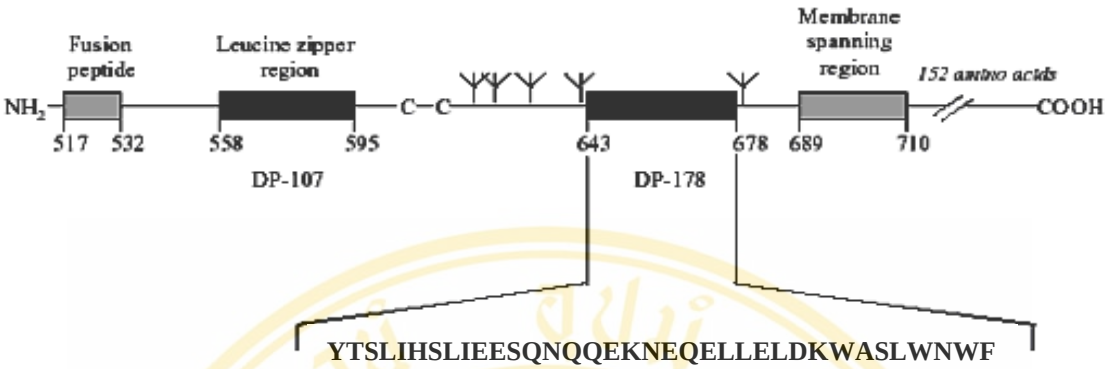

(CH_3CO-Tyr-Thr-Ser-Leu-Ile-His-Ser-Leu-Ile-Glu-Glu-Ser-Gln-Asn-Gln-Gln-Glu-Lys-Asn-Glu-Gln-Glu-Leu-Leu-Glu-Leu-Asp-Lys-Trp-Ala-Ser-Leu-Trp-Asn-Trp-Phe-NH_2).

Figure 12. Structure of enfuvirtide (20, 119).

D. HIV-1 reverse transcriptase inhibitory activity test

The radioactive assay was developed for detection of the inhibitory activity of enzyme reverse transcriptase in virions, using polyadenylic acid [poly(rA)] as the template, oligodeoxythymidylic acid [oligo(dT)] as the primer, and radiolabled thymidine 5'-triphosphate (TTP) as the substrate. HIV-1 RT used in the assay was obtained from an *Escherichia coli* expression system using a genetically engineered plasmid; the enzyme was purified to near homogeneity. The purified recombinant enzyme was sufficiently similar to the viral enzyme that it can be substituted for the latter in drug screening assay (122-123). Reverse transcription process is also specifically dependent on a divalent cation either Mg^{2+} or Mn^{2+}, but the majority of the retroviruses preferentially use Mn^{2+}. The optimal monovalent cation such as KCl is also required for this enzyme. The RTs of retroviruses generally require an optimum pH between 7 and 8 but the major activity is occurred at pH 8.0. Therefore, tris-HCl at pH 8.0 was chosen as the buffer for the assay. In addition, a sulfhydryl-containing compound such as dithiothreiol (DDT) was also used conventionally in RT assay as a reducing agent.

Compounds which bind selectively to the activity site of the enzyme should yield useful response. Unfortunately, such agents are not frequently encountered.

Compounds that bind to proteins in a relatively nonspecific fashion such as polyphenolic compounds are observed to have more generalized effects on a variety of enzyme system. In this case, the inclusion of bovine serum albumin (BSA) as a protective agent in an enzyme assay is optimal.

The general procedure consists of three main steps as follow:

1. Reverse transcriptase reaction

Recombinant HIV-1 RT, template-primer $(rA)_n$-$P(dT)_{12-18}$, substrate (methyl-[^{3}H]dTTP), sample and other reagents were incubate at 37°C for 60 minutes.

2. Stop reaction

The reaction was stopped by boiling the reaction mixture for 10 minutes. Eighty μL of each reaction mixture was applied to Whatman® grade DEAE cellulose paper and dried for 2 hours. The membrane was washed batchwise with (4x7 mL) 3% disodium hydrogenphosphate (Na_2HPO_4) for 5 minutes, followed by 2x7 mL of water for 2 minutes and 2 mL of absolute ethanol for 1 minute. The membrane was dried on the Petri-dish not less than 1 hour.

3. Detection of DNA

The dried membrane was transferred into a vial containing the scintillation cocktail (Ultima Gold, Packard), and radioactivity was measured by liquid scintillation system (TRI-CARB 2100RT, Packard).

The HIV-1 RT inhibition was the inhibition of the incorporation of [^{3}H]-labeled substrate (dTTP) into a polymer fraction in the presence of a synthetic compound. The positive control of the assay was performed in the same manner to the preparation for the synthetic compounds, but an equivalent volume of solvent (DMSO) was added instead. The negative control was performed without the enzyme (124).

E. AIDS and cancer

An asymptomatic period precedes AIDS in which the immune system becomes progressively compromised and unable to fight opportunistic infections and certain cancers (2). AIDS related cancer, that many types of cancer are relatively frequent outcome of HIV. AIDS-associated cancers have focused on the interplay of immunity and viral infections and has increased of cancer pathogenesis. These cancers are sometimes called “AIDS malignancies”. There are many research to stimulate and

to increase knowledge of the underlying pathophysiology of HIV/AIDS-associated malignancies and the development of more effective interventions. There are three major of AIDS malignancies i.e., Kaposi'sarcoma (KS), Cervical cancer and Non-Hodgkin's lymphoma (NHL).

Kaposi'sarcoma (KS) is associated with human herpesvirus 8 (HHV-8). This virus is sometimes called "Kaposi'sarcoma-associated herpesvirus." The virus is likely transmitted through saliva. Fortunately, the number of case of KS has decreased dramatically since the introduction of potent anti-HIV therapy (5, 10, 125).

Cervical cancer is caused by certain types of human papillomavirus (HPV). This virus also can cause genital and oral warts. It is spread by contact with infected areas of the body. Some forms of this virus are low-risk for cancer (like HPV-6 and HPV-11) while other forms are high-risk for cancer (HPV-16 and HPV-18). Woman get regular Pap tests to detect any call abnormalities (dysplasia) that may be caused by this virus and may indicate the beginnings of cancer. This same virus causes anal cancer. Some HIV-treating physicians are using the Pap test to screen for anal cancer in men and women. Successful anti-HIV therapy helps reduce, but does not eliminate, the risk of cervical cancer in women (5-6,125).

Non-Hodgkin's lymphoma (NHL) is associated with Epstein-Barr virus (EBV), a type of herpes virus that infected almost all humans by young adulthood. Lymphoma involves immune cell "B lymphocytes". Since these cell are almost everywhere in the body, tumors can arise in a number of locations (bone, brain, abdomen, lung, etc.) and spread through the body's lymphatic system (5-6, 125).

The national cancer of USA is stimulated to perform the research and increase the knowledges of HIV/AIDS-associated malignancies and the development of more effective interventions (125). The development of cancer is a multistep process through which cells gradually undergo a progressive series of alterations, which include multation and selection for cells with increasing capacity for proliferation, survival, invasion and metstasis (126). The cytotoxic assay activity is the first biological screening for proliferation of cancer and there are many assays for testing for example, sulforhodamine B (SRB) assay, CellTiter Blue (CTB) cell viability assay, lactate dehydrogenase (LDH) cytotoxic assay, 3-(4,5-dimethylthiazol-2-yl)-2, 5-diphenyltetrazolium bromide (MTT) assay (127-130). Currently, several cytotoxic

screening assays are commonly used including MTT assay, CTB assay, LDH assay and SRB assay. The MTT assay has higher sensitivity for detecting cytotoxic effects (127).

F. The cytotoxic activity testing

The MTT assay is commonly applied as a preliminary screen to quantify cell proliferation, viability, sensitivity, and cytoxicity (131-134). The MTT assay is based on the ability of a mitochondrial dehydrogenase enzyme from viable cells to cleave the tetrazolium rings of the pale yellow MTT and form a dark blue formazan crystals which is largely impermeable to cell membranes, thus resulting in its accumulation within healthy cells. Solubilization of the cells by the addition of a detergent results in the liberation of the crystals which are solubilized. The number of surviving cells is directly proportional to the level of the formazan product created (135-137). The color can then be quantified using a simple colorimetric assay. The results can be read on a multiwell scanning spectrophotometer (ELISA reader).

CHAPTER III

CHEMICAL EXPERIMENTAL

A. Equipment and chemicals

1. Equipment

Analytical balance model 2842	Sartorius, USA
Chromato-VUE cabinet (Model CC-60)	UVP Inc., USA
Elemental analyzer (PE 2400 series II)	Perkin Elmer, Germany
FTIR (FTIR 550)	Nicolet, USA
^{1}H NMR (DPX-3000) spectrophotometer	Bruker, Switzerland
Magnetic stirrer (MR 3001K)	Heidolph, Germany
Mass spectrometer (MAT 90)	Finnigan, Germany
Melting point apparatus (model 9100)	Electrothermal , UK
Rotary evaporator	Eyela, Japan

2. Chemicals

Acetone	J.T. Baker
3-(Bromomethyl) benzonitrile	Fluka, Switzerland
Chloroform	Lab Scan
Dichloromethane	Lab Scan
Ethyl acetate	J.T. Baker
Hexane	J.T. Baker
Methanol	Lab Scan
3-Methoxybenzyl chloride	Fluka, Switzerland
2-Methylbenzyl bromide	Fluka, Switzerland
4-Methylbenzyl chloride	Fluka, Switzerland
3-Nitrobenzyl chloride	Fluka, Switzerland
Phthalimide	Fluka, Switzerland
Potassium hydroxide	Merck, Germany

Pyridine	J.T. Baker
Sodium sulfate	Merck, Germany
Silica gel 60 No. 1.07734	Merck, Germany
Silica gel F_{254} (0.2 mm)	Merck, Germany
Sea sand	Fluka, Switzerland

B. Methods

All new compounds were characterized by spectroscopic methods, i.e., infrared (IR) spectroscopy, proton nuclear magnetic resonance (^{1}H NMR) spectroscopy, mass spectrometry (MS) and elemental analysis. IR spectra were recorded on FTIR Nicolet 550, using the potassium bromide pellet technique. ^{1}H NMR spectra were obtained on an ADVANCE 300 MHz Digital NMR Spectrophotometer (Bruker Switzerland DPX-3000). Chemical shifts were reported in ppm related to the internal standard, tetramethylsilane (TMS). The NMR solvent used was deuterated chloroform ($CDCl_3$ δ_H = 7.2 ppm). Mass spectra were determined on a MAT 90 (Finnigan) mass spectrometry using EI method. Percentage of carbon, hydrogen and nitrogen were obtained from a CHNS/O analyzer (Perkin Elmer PE2400 series II) and the results were within 0.4 % of theoretical values. Melting point of all products were determined on an Electrothermal model 9100 capillary melting point apparatus. The crude products were purified by column chromatography using silica gel, E. Merck (70-230 mesh) and recrystallization. Thin layer chromatography (TLC) was carried out on silica gel GF_{254} coated aluminum sheets 20 x 20 cm (E. Merck) with spots visualized by UV light (254 nm). All solvents were reagent grade and when necessary, were purified and dried by standard methods.

1. 1-Phthalimidomethyl-2-methylbenzene

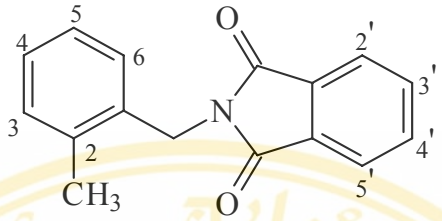

To a solution of phthalimide (2 g, 13.6 mmol) in N,N-dimethylformamide (40 mL) was added 2-methylbenzyl bromide (4 mL, 29.4 mmol) and potassium hydroxide solution (0.31 g, 5.5 mmol) 10 ml. The reaction mixture was refluxed for 6 hours at 190°C. The mixture was extracted with chloroform (30 mL) and water (3x15 mL). The organic phase was dried over anhydrous sodium sulfate, filtered and concentrated in vacuo. The residue was purified by column chromatography (silica gel 60 No. 1.07734) using hexane/ethyl acetate (4:1) as eluent. Recrystallization from chloroform/methanol gave compound **34** (1.50 g, 44.70% yield) as a white needle crystal; mp 158-159°C. IR (KBr) (cm^{-1}): 3466 (overtone C=O), 3087 (aromatic C-H), 2920 (aliphatic C-H), 1705 (C=O), 1424 (C=C), 1319 (C-N); ^{1}H NMR ($CDCl_3$): δ 2.46 (s, 3H, CH_3), 4.85 (s, 2H, CH_2-N), 7.09-7.15 (m, 3H, benzene H3, H5, H6), 7.21-7.25 (m, 1H, benzene H4), 7.67-7.73 (m, 2H, phthalimide H3', H4'), 7.84 (dd, *J* = 3.0, 5.4 Hz, 2H, phthalimide H2', H5'); MS: m/z (relative intensity): M^+251 (100), 236 (19.73), 160 (23.88), 130 (10.43), 104 (53.36), 78 (14.35), Anal. Calcd. for $C_{16}H_{13}NO_2$ (251.28): C, 76.48; H, 5.21; N, 5.57. Found: C, 76.92; H, 5.54; N, 5.43. TLC (ethyl acetate/hexane [1:1]): R_f of phthalimide = 0.471, R_f of 2-methyl benzyl bromide = 0.824, and R_f of compound **34** = 0.612.

2. 1-Phthalimidomethyl-4-methylbenzene

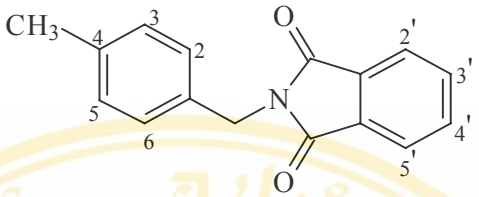

To a solution of phthalimide (0.5 g, 3.40 mmol) in N,N-dimethylformamide (40 mL) was added 4-methylbenzyl bromide (1.0 mL, 7.54 mmol) and potassium hydroxide solution (0.13 g, 2.32 mmol) 10 mL. The reaction mixture was refluxed for 6 hours at 190°C. The mixture was extracted with chloroform (30 mL) and water (3x15 mL). The organic phase was dried over anhydrous sodium sulfate, filtered and concentrated in vacuo. The residue was purified by column chromatography (silica gel 60 No. 1.07734) using hexane/ethyl acetate (2:1) as eluent. Recrystallization from chloroform/methanol gave compound **35** (0.41 g, 43.04% yield) as a white needle crystal; mp 117-118°C. IR (KBr) (cm^{-1}): 3459 (overtone C=O), 3065 (aromatic C-H), 2940 (aliphatic C-H), 1726 (C=O), 1438 (C=C), 1319 (C-N); ^{1}H NMR ($CDCl_3$): δ 2.28 (s, 3H, CH_3), 4.78 (s, 2H, CH_2-N), 7.10 (d, *J* = 7.8 Hz, 2H, benzene H3, H5), 7.31 (d, *J* = 8.1 Hz, 2H, benzene H2, H6), 7.64-7.70 (m, 2H, phthalimide H3', H4'), 7.81 (m, *J* = 3.0, 5.4 Hz, 2H, phthalimide H2', H5'); MS: m/z (relative intensity): M^+251 (100), 236 (60.36), 208 (13.01), 160 (20.34), 130 (26.97), 105 (13.96), 104 (27.04), 77 (15.58). Anal. Calcd. for $C_{16}H_{13}NO_2$ (251.28): C, 76.48; H, 5.21; N, 5.57. Found: C, 76.93; H, 5.45; N, 5.42. TLC (ethyl acetate/hexane [1:2]): R_f of phthalimide = 0.383, R_f of 4-methylbenzyl bromide = 0.617, and R_f of compound **35** = 0.468.

3. 1-Phthalimidomethyl-4-*tert*-butylbenzene

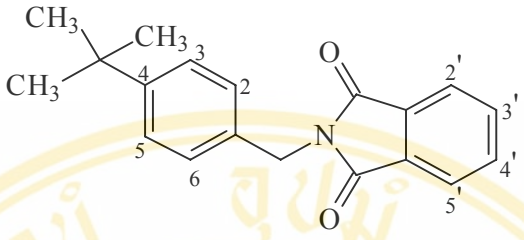

To a solution of phthalimide (1 g, 6.79 mmol) in N,N-dimethylformamide (40 mL) was added 4-*tert*-butyl benzyl bromide (2.4 mL, 13.2 mmol) and potassium hydroxide solution (0.16 g, 2.85 mmol) 10 mL. The reaction mixture was refluxed for 8 hours at 190°C. The mixture was extracted with chloroform (30 mL) and water (3x15 mL). The organic phase was dried over anhydrous sodium sulfate, filtered and concentrated in vacuo. The residue was purified by column chromatography (silica gel 60 No. 1.07734) using hexane/ethyl acetate (4:1) as eluent. Recrystallization from chloroform/methanol gave compound **36** (0.63 g, 31.66% yield) as a white solid crystal; mp 93-94°C. IR (KBr) (cm^{-1}): 3495 (overtone C=O), 3072 (C-H aromatic), 2966 (C-H aliphatic), 1716 (C=O), 1400 (C=C), 1334 (C-N); ^{1}H NMR ($CDCl_3$): δ 1.25 (s, 9H, -C(CH_3)$_3$), 4.79 (s, 2H, 2H, CH_2-N), 7.31 (d, *J* = 8.4 Hz, 2H, benzene H2, H6), 7.36 (d, *J* = 8.4 Hz, 2H, benzene H3, H5), 7.66-7.69 (m, 2H, phthalimide H3', H4'), 7.81 (dd, *J* = 3.1, 5.5 Hz, 2H, phthalimide H2', H5'); MS: m/z (relative intensity): M^+293 (16.31), 278 (100), 236 (28.04), 160 (46.68), 131 (34.90), 130 (11.93). Anal. Calcd. for $C_{19}H_{19}NO_2$ (293.36): C, 77.79; H, 6.23; N, 4.77. Found: C, 77.61; H, 6.75; N, 4.50. TLC (ethyl acetate/hexane [1:2]): R_f of phthalimide = 0.360, R_f of 4-*tert*-butyl benzyl bromide = 0.605 and R_f of compound **36** = 0.500.

4. 1-Phthalimidomethyl-3-methyloxybenzene

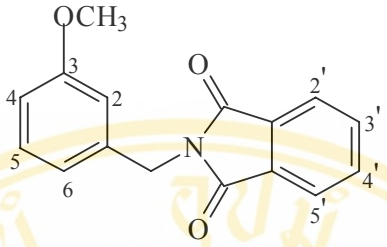

To a solution of phthalimide (2 g, 13.6 mmol) in N,N-dimethylformamide (40 mL) was added 3-methoxybenzyl chloride (4 mL, 29.5 mmol) and potassium hydroxide solution (0.31 g, 5.5 mmol) 10 mL. The reaction mixture was refluxed for 6 hours at 190°C. The mixture was extracted with chloroform (30 mL) and water (3x15 mL). The organic phase was dried over anhydrous sodium sulfate, filtered and concentrated in vacuo. The residue was purified by column chromatography (silica gel 60 No. 1.07734) using hexane/ethyl acetate (4:1) as eluent. Recrystallization from chloroform/methanol gave compound **37** (0.50 g, 13.75 % yield) as a white solid crystal; mp 126-167°C. IR (KBr) (cm^{-1}): 3470 (overtone C=O), 3039 (aromatic C-H), 2953 (aliphatic C-H), 1709 (C=O), 1604, 1499 (C=C), 1393 (C-N); ^{1}H NMR ($CDCl_3$): δ 3.76 (s, 3H, OCH_3), 4.80 (s, 2H, CH_2-N), 6.78 (dd, *J* = 1.9, 8.2 Hz, 1H, benzene H2), 6.95 (d, *J* = 2.4 Hz, 1H, benzene H6), 6.99 (d, *J* = 7.5 Hz, 1H, benzene H4), 7.21 (t, *J* = 8.4 Hz, 1H, benzene H5), 7.66-7.72 (m, 2H, phthalimide H3', H4'), 7.82 (dd, *J* = 3.0, 5.4 Hz, 2H, phthalimide H2', H5'); MS: m/z (relative intensity): M^++H 268 (28.94), 267 (100), 234 (28.26), 206 (30.34), 180 (9.23), 130 (8.82), 77 (10.33). Anal. Calcd. for $C_{16}H_{13}NO_3$ (267.28): C, 71.80; H, 4.90; N, 5.24. Found: C, 71.78; H, 5.11; N, 4.89. TLC (ethyl acetate/hexane [1:2]): R_f of phthalimide = 0.294, R_f of 3-methoxybenzyl chloride = 0.695 and R_f of compound **37** = 0.412.

5. 1-Phthalimidomethyl-3-nitrobenzene

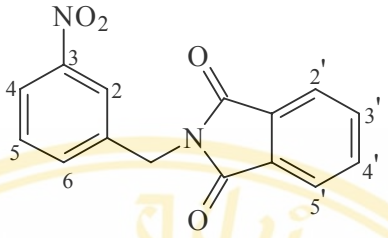

To a solution of phthalimide (2 g, 13.6 mmol) in N,N-dimethylformamide (40 mL) was added 3-nitrobenzyl chloride (5 g, 29.1 mmol) and potassium hydroxide solution (0.31 g, 5.5 mmol) 10 mL. The reaction mixture was refluxed for 8 hours at 190°C. The mixture was extracted with chloroform (30 mL) and water (3x15 mL). The organic phase was dried over anhydrous sodium sulfate, filtered and concentrated in vacuo. The residue was purified by column chromatography (silica gel 60 No. 1.07734) using hexane/ethyl acetate (4:1) as eluent. Recrystallization from chloroform/methanol gave compound **38** (1.31 g, 34.19 % yield) as a white needle crystal; mp 163-164°C. IR (KBr) (cm^{-1}): 3460 (overtone C=O), 3087 (aromatic C-H), 2933 (aliphatic C-H), 1719 (C=O), 1543 (C=C), 1350 (C-N); ^{1}H NMR ($CDCl_3$): δ 4.92 (s, 2H, CH_2-N), 7.49 (t, *J* = 7.8 Hz, 1H, benzene H5), 7.69-7.75 (m, 3H, benzene H6, phthalimide H3', H4'), 7.85 (dd, *J* = 3.0, 5.4 Hz, 2H, phthalimide H2', H5'), 8.11 (dd, *J* = 0.9, 7.8 Hz, 1H, benzene H4), 8.25 (s, 1H, benzene H2); MS: m/z (relative intensity): M^+281 (10.52), 265 (100), 266 (22.83), 235 (67.78), 207 (9.17), 179 (5.01), 130 (5.82), 77 (8.28). Anal. Calcd. for $C_{15}H_{10}N_2O_4.0.5H_2O$ (291.26): C, 61.86; H, 4.15; N, 9.62. Found: C, 62.03; H, 3.61; N, 9.10. TLC (ethyl acetate/ hexane [4:1]): R_f of phthalimide = 0.601, R_f of 3-nitrobenzyl chloride = 0.637 and R_f of compound **38** = 0.562.

6. 1-Phthalimidomethyl-3-cyanobenzene

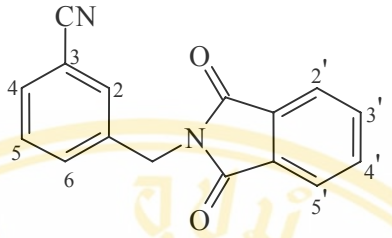

To a solution of phthalimide (1 g, 6.79 mmol) in N,N-dimethylformamide (40 mL) was added 3-(bromomethyl)benzonitrile (2.7 g, 13.8 mmol) and potassium hydroxide solution (0.16 g, 2.85 mmol) 10 mL. The reaction mixture was refluxed for 6 hours at 190°C. The mixture was extracted with chloroform (30 mL) and water (3x15 mL). The organic phase was dried over anhydrous sodium sulfate, filtered and concentrated in vacuo. The residue was purified by column chromatography (silica gel 60 No. 1.07734) using hexane/ethyl acetate (1:2) as eluent. Recrystallization from chloroform/methanol gave compound **39** (1.50 g, 44.70 % yield) as a white solid crystal; mp 148-149°C. IR (KBr) (cm^{-1}): 3466 (overtone C=O), 3072 (aromatic C-H), 2947 (aliphatic C-H), 2242 (C≡N), 1709 (C=O), 1492 (C=C), 1393 (C-N); ^{1}H NMR ($CDCl_3$): δ 4.84 (s, 2H, CH2-N), 7.41 (t, *J* = 7.8 Hz, 1H, benzene H5), 7.54 (d, *J* = 7.8 Hz, 1H, benzene H6), 7.65 (d, *J* = 7.8 Hz, 1H, benzene H4), 7.68 (s, 1H, benzene H2), 7.71-7.75 (m, 2H, phthalimide H3', H4'), 7.84 (dd, *J* = 3.0, 5.4 Hz, 2H, phthalimide H2', H5'); MS: m/z (relative intensity): M^++H 263 (60.95), 262 (100), 244 (66.90), 233 (24.34), 205 (21.82), 130 (10.42), 105 18.95), 77 (8.87). Anal. Calcd. for $C_{16}H_{10}N_2O_2$ (262.27): C, 73.27; H, 3.84; N, 10.68. Found: C, 73.69; H, 3.94; N, 10.59. TLC (ethyl acetate/hexane [4:1]): Rf of phthalimide = 0.576, R_f of 3- (bromo methyl) benzonitrile = 0.706 and R_f of compound **39** = 0.624.

CHAPTER IV

BIOLOGICAL EXPERIMENT

A. HIV-1 reverse transcriptase inhibitory activity test

Radioactivity test

1. Equipments and reagents

1. Analytical balance	Oterling
2. Centrifuge	Hettich Universal
3. Micropipette	Gilson
4. Shaking water bath	Clifton
5. ß-Counter TRI-CARB 2100TR	Packard
6. Recombinant reverse transcriptase (RT)	Calbiochem
7. [methyl-^{3}H]-Thymidine-5'-triphosphate (dTTP)	Amersham
8. Poly.(rA).oligo.(dT)	Amersham
9. Doxorubicin hydrochloride (adriamycin)	Sigma
10. DEAE-cellulose paper disc	Whatman
11. Dimethyl sulfoxide (DMSO)	Sigma
12. Scintillation fluid	Packard
13. Disodium hydrogenphosphate anhydrous	Merck
14. Absolute ethanol	J.T.Baker

2. Methods

2.1 Buffer and reagents preparation

1. Preparation of 10 mL of the buffer mixture solution.

DW	7.57 mL
1 M Tris HCl pH 8.0	1.0 mL

2 M KCl	0.5 mL
1 M $Mg(OAc)_2$	0.1 mL
2 M dithiothreitol (DDT)	0.03 mL
2.5% Nonnidet P-40	0.8 mL

2. Preparation of substrate solution per sample.

Buffer mixture solution	50.25 µL
DW	12.0 µL
[^{3}H] dTTP	0.25 µL

3. Preparation of enzyme solution per sample.

Buffer mixture solution	10.0 µL
BSA	2.0 µL
Recombinant RT	0.1 µL

2.2 Assay of RT (complete system)

The reaction mixture for the standard RT assay (final volume 100 µL) contained the following:

Substrate solution	62.5 µL
Poly(rA).oligo(dT)	10.0 µL
DW	10.4 µL
Sample solution	5.0 µL
Enzyme solution	12.1 µL

The synthesized compound was adjusted to 4 µg/µL with DMSO. The enzyme solution was added immediately before incubation. The reaction mixture was incubated at 37°C for 60 minutes and then terminated by boiling at 100°C for 10 minutes. Eighty µL of each assay mixture was applied at 2.3 cm circular Whatman DE81 cellular paper and dried for 1 hour. The membrane was washed batchwise with (4x7 mL) disodium hydrogenphosphate (Na_2HPO_4), followed by 2x7 mL of water and 2 mL of absolute ethanol. The membrane was dried and then transferred to a vial containing scintillation fluid (5 mL). The radioactivity was measured by a liquid scintillation counter.

2.3 Positive control of inhibitors.

The positive control of inhibitors was performed by using doxorubicin hydrochloride. The reaction mixture (final volume 100 µL) contained the following:

Substrate solution	62.5 µL
Poly(rA).oligo(dT)	10.0 µL
DW	10.4 µL
Doxorubicin hydrochloride (14.5 µg/µL)	5.0 µL
Enzyme solution	12.1 µL

The reaction mixture was incubated at 37°C for 60 minutes and followed the same procedure for the assay of RT.

2.4 Positive control of tested solution (complete system-sample).

The positive control assay consisted of DMSO instead of the synthetic compound. The reaction mixture (final volume 100 µL) contained the following:

Substrate solution	62.5 µL
DW	10.4 µL
DMSO	5.0 µL
Poly(rA).oligo(dT)	10.0 µL
Enzyme solution	12.1 µL

The reaction mixture was incubated at 37°C for 60 minutes and followed the same procedure for the assay of RT.

2.5 Negative control of teased solution (complete system-RT).

The negative control assay consisted of the same constituents as the assay of RT, but RT was omitted. The reaction mixture (final volume 100 µL) contained the following:

Substrate solution	62.5 µL
Poly(rA).oligo(dT)	10.0 µL
Buffer mixture solution	10.0 µL
BSA	2.0 µL
DMSO	5.0 µL

DW 10.5 μL

The reaction mixture was incubated at 37°C for 60 minutes and followed the same procedure for the assay of RT.

2.6 Inhibition of RT activity.

The inhibition of RT incorporation of ^{3}H labeled substrates [^{3}H]dTTP into a polymer fraction by RT in the presence of the samples was calculated as followed:

$$(\%)\ IR = \left[1 - \frac{[cpm(complete\ system)-cpm(complete\ system\text{-}RT)]}{[cpm(complete\ system\text{-}sample)-cpm(complete\ system\text{-}RT)]} \right] \times 100$$

where: (%) IR = percent of relative inhibitory ratio

cpm = count per minute

complete system = reaction mixture which consisted of RT, template-primer, substrate, sample, and other reagents.

complete system-RT = reaction mixture which consisted of template- primer, substrate and other reagents.

complete system-sample = reaction mixture which consisted of RT, template-primer, substrate and other reagents.

All experiments were performed in triplicate. The average of the 2 closely values obtained from the experiment was used to calculate % IR.

B. In vitro cytotoxic activity testing

3- (4, 5-dimethylthiazol-2-yl)- 2, 5-diphenyltetrazolium bromide (MTT) assay

1. Equipments and reagents

1. Cell lines [human epidermoid carcinoma (KB), human cervical carcinoma (HeLa) and african green monkey kidney cell (vero)]
2. Growth medium, minimal essential medium (MEM) Gibco

3. PBS (phosphate buffered saline) Gibco
4. Fetal bovine serum (FBS) Gibco
5. 3- (4, 5-dimethylthiazol-2-yl)- 2, 5-diphenyltetrazolium bromide (MTT) Sigma
6. Dimethyl sulfoxide (DMSO) Sigma
7. 96-well disposable plate Bio Basic
8. Incubator Shel Lab
9. Micropipette Biohit
10. Microplate reader Bio Rad

2. Methods

2.1 Cell lines and culture conditions

Humam epidermoid carcinoma (KB), human cervical carcinoma (HeLa), and african green monkey kidney cell (vero) were maintained in minimal essential medium (Gibco) 10% fetal bovine serum in a 95% air/5% CO_2 atmosphere at 37°C in a humidified incubator. Then the cells were subcultured and followed by trypsinization with 0.25% trypsin-EDTA solution.

2.2 MTT colorimetric assay

Cells at the density of 3,000 cells were seeded in 96 well plate containing 90 µL of growth medium per well. The well plate was incubated for 24 hours at 37°C with 5% CO_2 and 95% air atmosphere. Sample was diluted with DMSO and mix with 5% DMSO in phosphate-buffered saline (PBS). Ten µL of the sample solution was added in 96 well plate. The final concentration was 0.1-100 µg/mL. After incubating for 72 hours, 100 µL of MTT solution (0.5 mg/PBS 1 mL) was added and cells were incubated for 4 hours. One hundred µL of DMSO was added to each culture. Relative cell viability was obtained by scanning with an ELISA reader with a 550 nm filter.

2.3 Data Analysis

The experiments were performed in triplicate. The results were shown as plot between cell viability and concentration. The percentage of cell viability was calculated by following formula.

$$\% \text{ viability} = \frac{(\text{OD of sample at 550 nm})}{(\text{OD of control at 550 nm})} \times 100.$$

Where: % viability = percent of the cell survival

OD = optical density (absorbance) units

CHAPTER V

RESULTS AND DISCUSSION

A. General discussion

A key target in the search for effective drugs for AIDS therapy is the viral enzymes that have critical roles in the life cycle of the HIV-1, i.e., fusion, reverse transcriptase (RT) and protease (PR) enzyme (18-19). NNRTIs are attractive due to their low toxicity and high specificity. The absence of the binding to cellular polymerase of NNRTIs results in considerably lower cytotoxicity than nucleoside analogues. Recently, our research group has designed and synthesized a new class of non-nucleoside analogues in phthalimide series and tested for their HIV-1 RT inhibitory activities (Table 2). In order to investigate in more details in term of structural reguirements for good inhibitory activity of compounds in this series, more derivatives were synthesized with modifying structures based on the previous comparative molecular field analysis (CoMFA) and comparative molecular similarity indices analysis (CoMSIA) studies (22) (Figure 13 and Figure 14).

The steric and electrostatic contour maps from CoMFA and CoMSIA models indicate that bulky substituents should be located at position C-3 and methyl group of pyrazine and the positive charge substituents are preferred at position C-6 of the pyrazine nucleus. This structural requirement is correspond to the CoMSIA hydrophobic contour maps (Figure 14 c) which illustrates the hydrophobic region around position C-3 and methyl group of the pyrazine ring (22). Based on the steric contour map from CoMFA and hydrophobic contour map from CoMSIA, more new compounds in phthalimide series, were synthesized and evaluated for their HIV-1 RT inhibitory. Since there are studies reported that some HIV-1 RT inhibitors, (e.g., AZT) also exhibited antitumor activity (12-14), the synthesized phthalimide derivertives were subjected to cytotoxic activity test as well.

Table 2. Structures of the previously synthesized phthalimide derivatives and HIV-1 RT inhibitory activities (22).

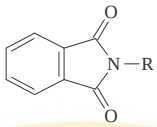

Cpd	R	% inhibition	Cpd	R	% inhibition
1	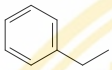	43	14	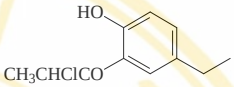	20
2	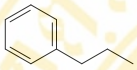	37	15	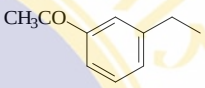	24
3	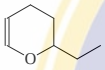	43	16	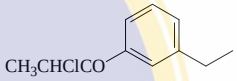	52
4	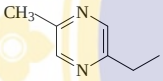	84 (IC_{50} = 120.75 μg/mL)	17	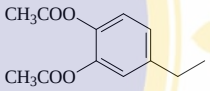	43
5	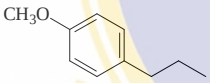	32	18	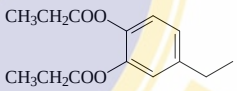	16
6	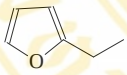	21	19	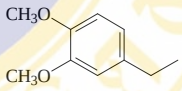	14
7	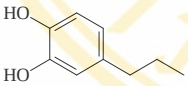	3	20	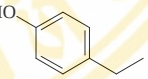	22
8	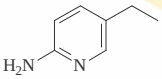	11	21	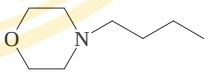	61
9	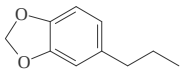	8	22	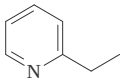	7
10	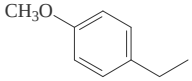	29	23	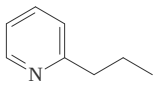	15
11	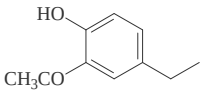	3	24	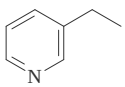	15
12	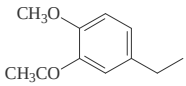	26	25		17
13	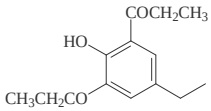	6	26	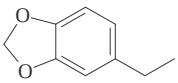	3

Table 2. Structures of the previously synthesized phthalimide derivatives and HIV-1 RT inhibitory activities (continue).

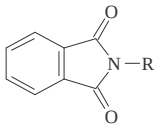

Cpds	R	% inhibitions	Cpds	R	% inhibitions
27	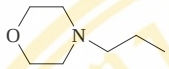	62	31	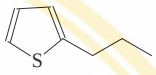	78 (IC_{50} = 98.10 µg/mL)
28	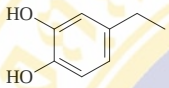	76 (IC_{50} = 60.90 µg/mL)	32	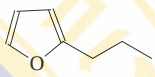	9
29	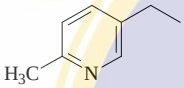	41	33	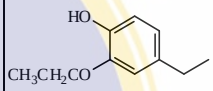	22
30	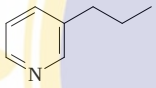	20			

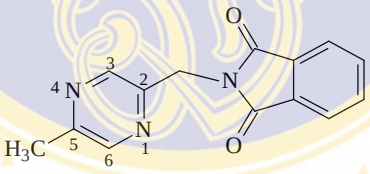

(a) (b)

Figure 13. CoMFA contour maps: (a) steric contour maps: green and yellow Polyhedra indicate regions where more steric bulk or less steric bulk, respectively, will enhance the activity. (b) electrostatic contour map: blue and red polyhedra indicate regions where positively charged or negatively charged substituent will enhance the activity (22).

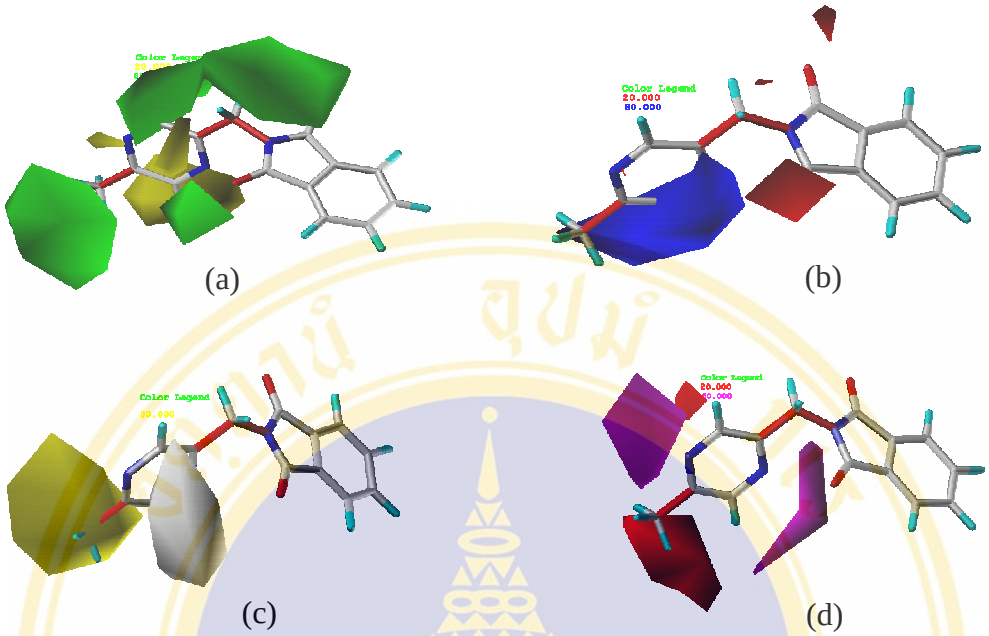

Figure 14. CoMSIA contour maps: (a) steric contour maps. (b) electrostatic contour maps. (c) hydrophobic contour map: yellow and white polyhedra indicate regions where hydrophobic or hydrophilic group, respectively, will enhance the activity, (d) hydrogen bond acceptor ability contour map: magenta and polyhedra indicate regions where hydrogen bond acceptor groups will increase or decrease the activity, respectively (22).

B. Synthesis of phthalimide derivatives

Based on the steric contour map from CoMFA and hydrophobic contour map from CoMSIA studies, more new compounds in phthalimide series, structures as shown in Figure 15 were synthesized.

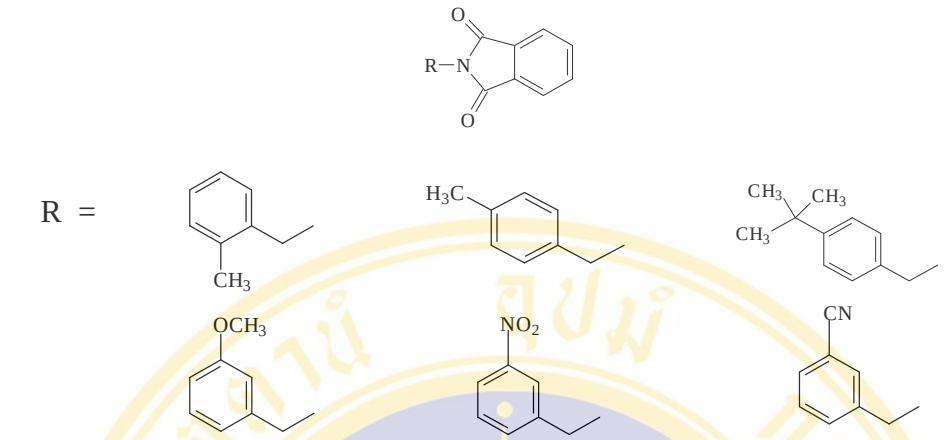

Figure 15. Structures of the newly synthesized phthalimide compounds**.**

The phthalimide derivatives were synthesized by the reaction of phthalimide and substituted benzyl halide in the presence of potassium hydroxide, outline as shown in Figure 16. The synthesized compounds were purified by column chromatography and/or recrystallization and structures of pure compounds were identified by Fourier transform infrared spectroscopy (FT-IR), nuclear magnetic resonance (NMR) spectroscopy, mass spectrometry (MS), and elemental analysis.

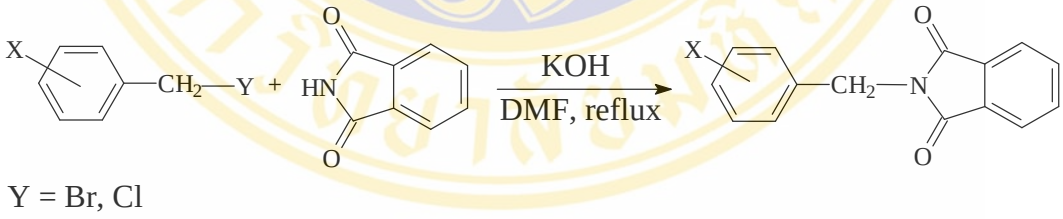

Figure 16. Synthetic outline of phthalimide compounds.

The physical properties data and elemental analysis of the phthalimide compounds are given in Table 3. The products were obtained in between low and moderate percentage yields, approximately 14-45 %.

Table 3. Physical properties of phthalimide derivatives.

Cpds	Structure	Formula	MW	mp (°C)	% yield		%C	%H	%N
34	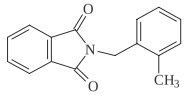	$C_{16}H_{13}NO_2$	251.28	158-159	44.70	Calculated Found	76.48 76.92	5.21 5.54	5.57 5.43
35	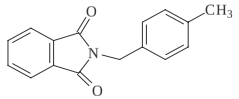	$C_{16}H_{13}NO_2$	251.28	117-118	43.04	Calculated Found	76.48 76.93	5.21 5.45	5.57 5.42
36	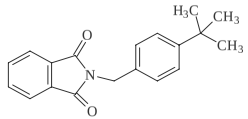	$C_{19}H_{19}NO_2$	293.36	93-94	31.66	Calculated Found	77.79 77.61	6.23 6.75	4.77 4.50
37	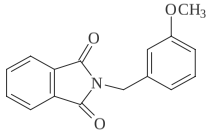	$C_{16}H_{13}NO_3$	267.28	126-127	13.75	Calculated Found	71.80 71.78	4.90 5.11	5.24 4.89
38	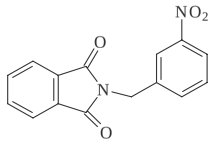	$C_{15}H_{10}N_2O_4$	282.25	163-164	34.19	Calculated Found	61.86 62.03	4.15 3.61	9.62 9.10
39	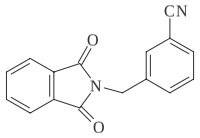	$C_{16}H_{10}N_2O_2$	262.27	148-149	44.70	Calculated Found	73.27 73.69	3.84 3.94	10.68 10.59

The IR spectrum of 1-phthalimidomethyl-4-*tert*-butylbenzene, compound **36** (Figure 17) shows the frequency of aromatic C-H stretching at 3072 cm^{-1}, aliphatic C-H stretching at 2966 cm^{-1}, C=O stretching at 1716 cm^{-1}, aromatic C=C stretching at 1550 and 1400 $cm^{-1}$and C-N stretching at 1334 cm^{-1}.

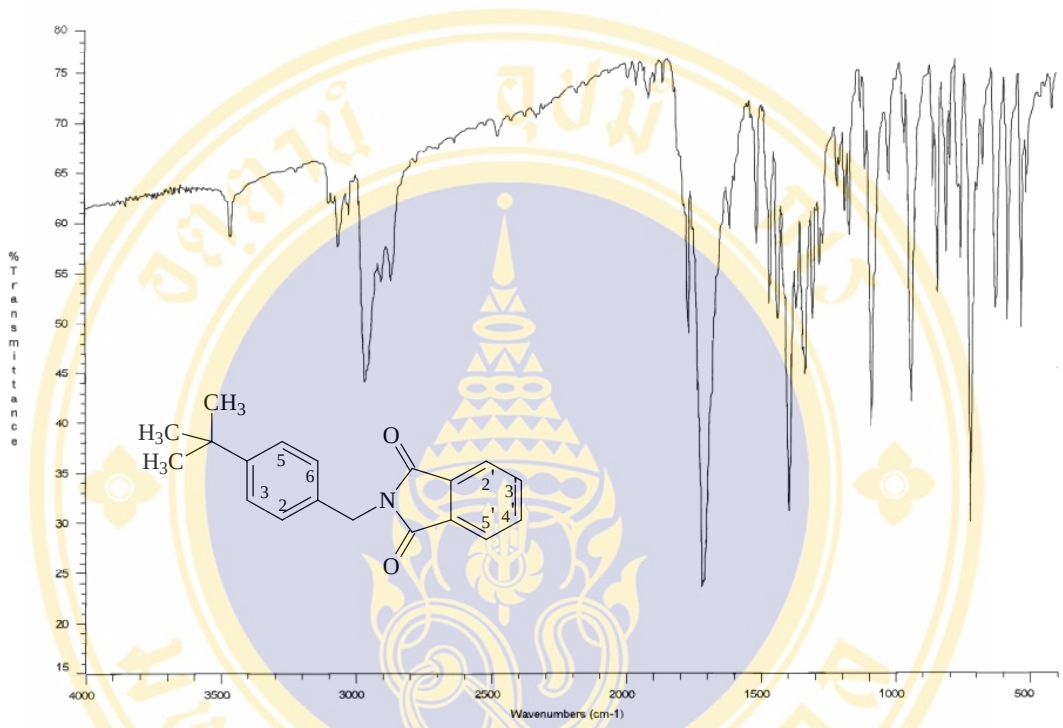

Figure 17. The IR spectrum of 1-phthalimidomethyl-4-*tert*-butylbenzene **36**

The ^{1}H NMR spectrum of compound **36** was shown in Figure 18. The singlet peak at 1.25 ppm represents the nine protons of *t*-butyl group. The singlet peak at 4.79 ppm represents the methylene protons between benzene and phthalimide rings. The doublet peaks at 7.31 ppm represent the two protons at position H2 and H6 of benzene which coupled to protons at position 3 and 5 (H3, H5) respetively (J = 8.4 Hz). The doublet peaks at 7.36 ppm represent the two protons at position H3 and H5 which coupled to protons at position 2 and 6 (H2, H6) respetively (J = 8.4 Hz). The multiplet peaks at 7.66-7.69 ppm show the two protons at positive H3´ and H4´ of the phthalimide nuclei. The doublet of doublet peaks at 7.81 ppm represent two protons at position H2´ and H5´ which coupled to protons at position 3´ and 4´(H3´, H4´) repectively (J = 5.5 and 3.1 Hz).

The EI mass spectrum of compound **36** has characteristic peak at 236, 130, 104, 77 and 76 as shown in Figure 19. The proposed fragmentation mechanism is illustrated in Figure 20.

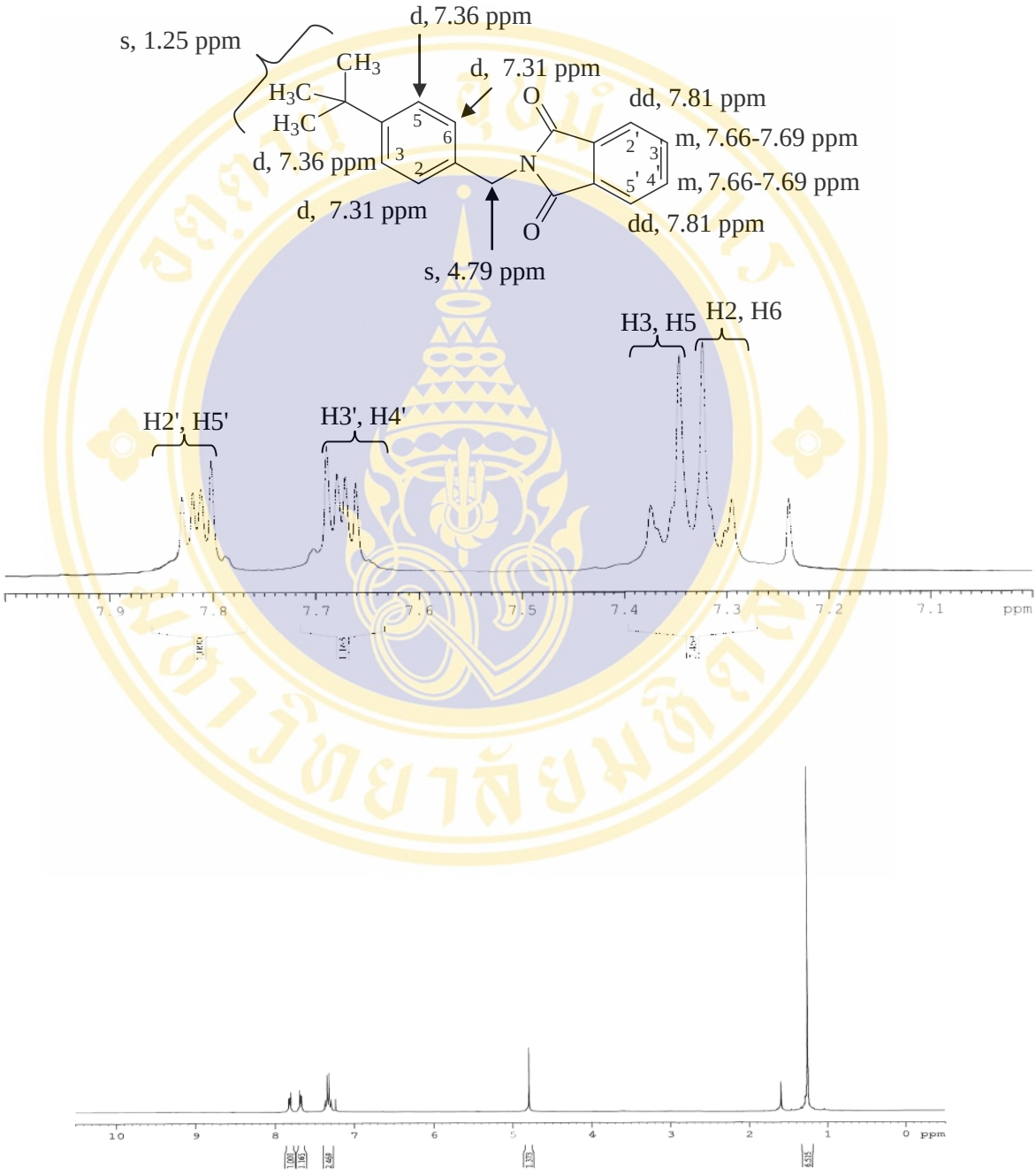

Figure 18. The ^{1}H NMR spectrum (300 MHz, $CDCl_3$) of 1-phthalimidomethyl-4-*tert*-butylbenzene **36**

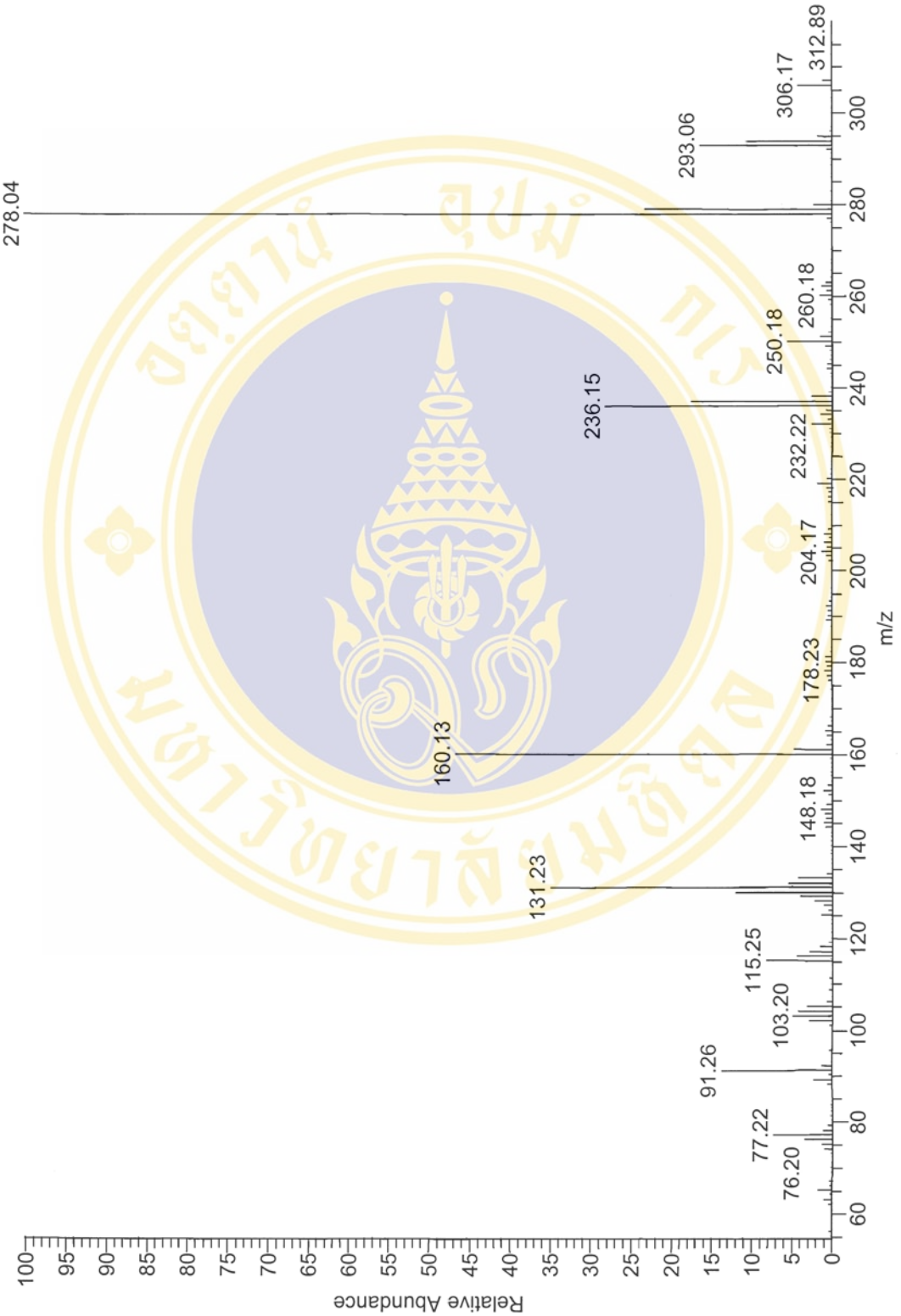

Figure 19. The EI mass spectrum of 1-phthalimidomethyl-4-*tert*-butylbenzene **36**

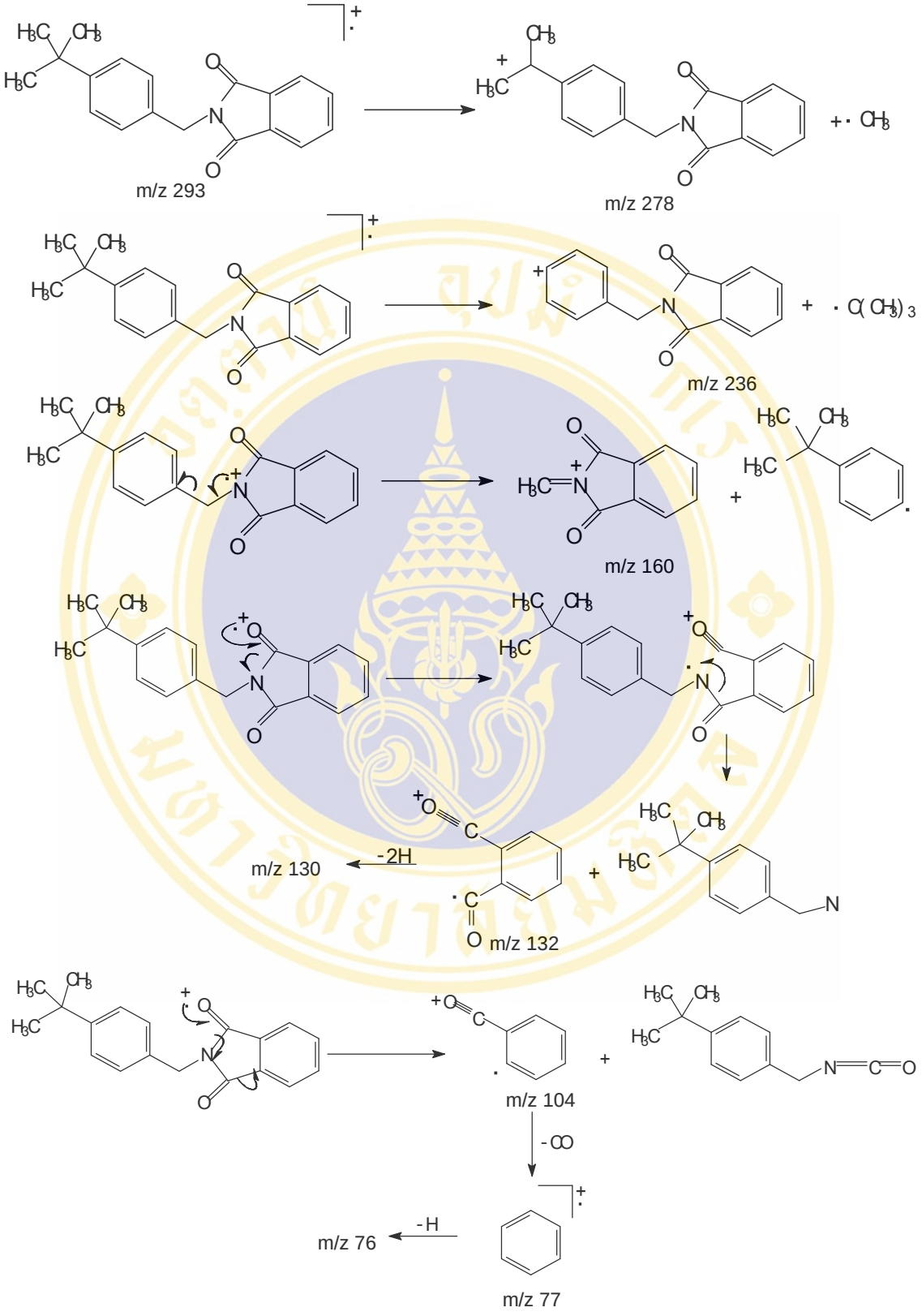

Figure 20. Fragmentation patterns of 1-phthalimidomethyl-4-*tert*-butylbenzene **36**

The IR spectrum of 1-phthalimidomethyl-3-nitrobenzene, compound **38** (Figure 21) shows the frequency of aromatic C-H stretching at 3087 cm^{-1}, aliphatic C-H stretching at 2933 cm^{-1}, C=O stretching at 1719 cm^{-1}, aromatic C=C stretching at 1543 and 1450 $cm^{-1}$and C-N stretching at 1350 cm^{-1}.

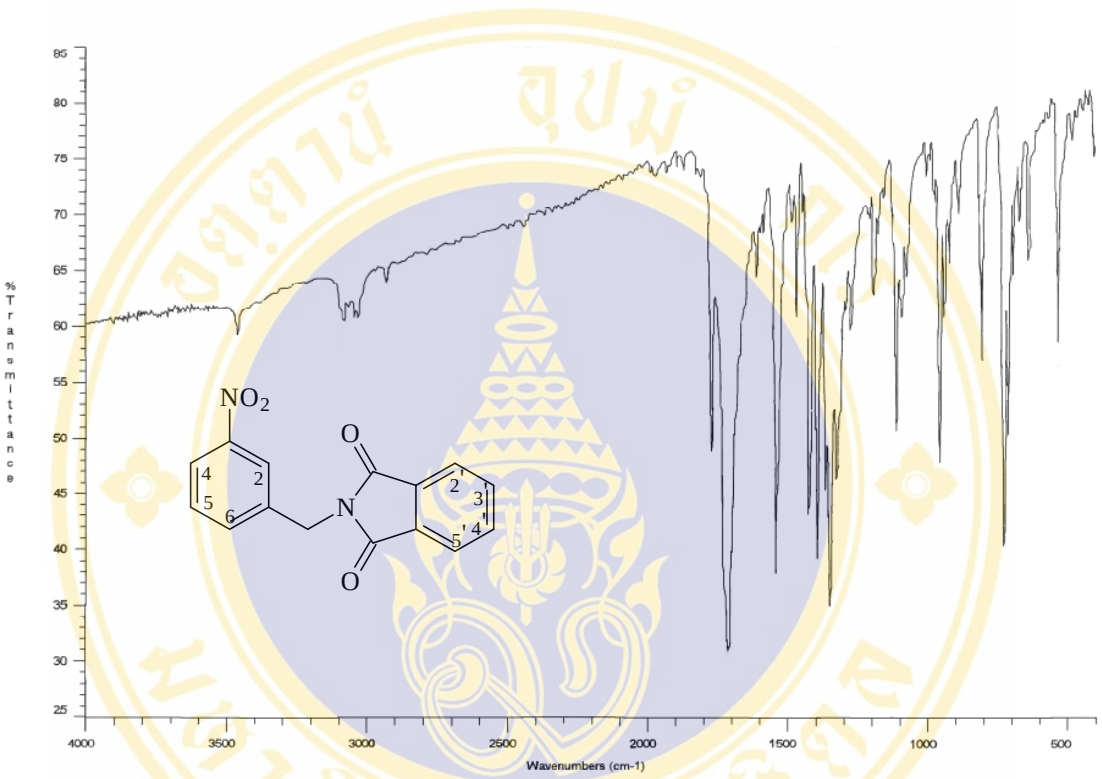

Figure 21. The IR spectrum of 1-phthalimidomethyl-3-nitrobenzene **38**

The ^{1}H NMR spectrum of compound **38** is shown in Figure 22. The singlet peak at 4.92 ppm represents the methylene protons between benzene and phthalimide ring. The triplet peaks (J = 7.8 Hz) at 7.49 ppm represent proton at position H5 of benzene ring which coupled to protons at position 4 and 6 (H4, H6). The multiplet peaks at 7.69-7.75 ppm show the three protons at position H3′ and H4′ of the phthalimide and H6 of the benzene ring. The doublet of doublet peaks at 7.85 ppm represent two protons at position H2′ and H5′ of the phthalimide which coupled to H3′ and H4′ respectively (J = 5.4 and 3.0 Hz). The doublet of doublet peaks at 8.11 ppm represent proton at position H4 of benzene ring coupling to H5 (J = 7.8 Hz) and H6 (J = 0.9 Hz). The singlet peak at 8.25 ppm represents proton at position H2 of the benzene ring.

The EI mass spectrum of compound **38** has characteristic peak at 236, 130, 104, 77 and 76 as shown in Figure 23. The proposed fragmentation mechanism is illustrated in Figure 24

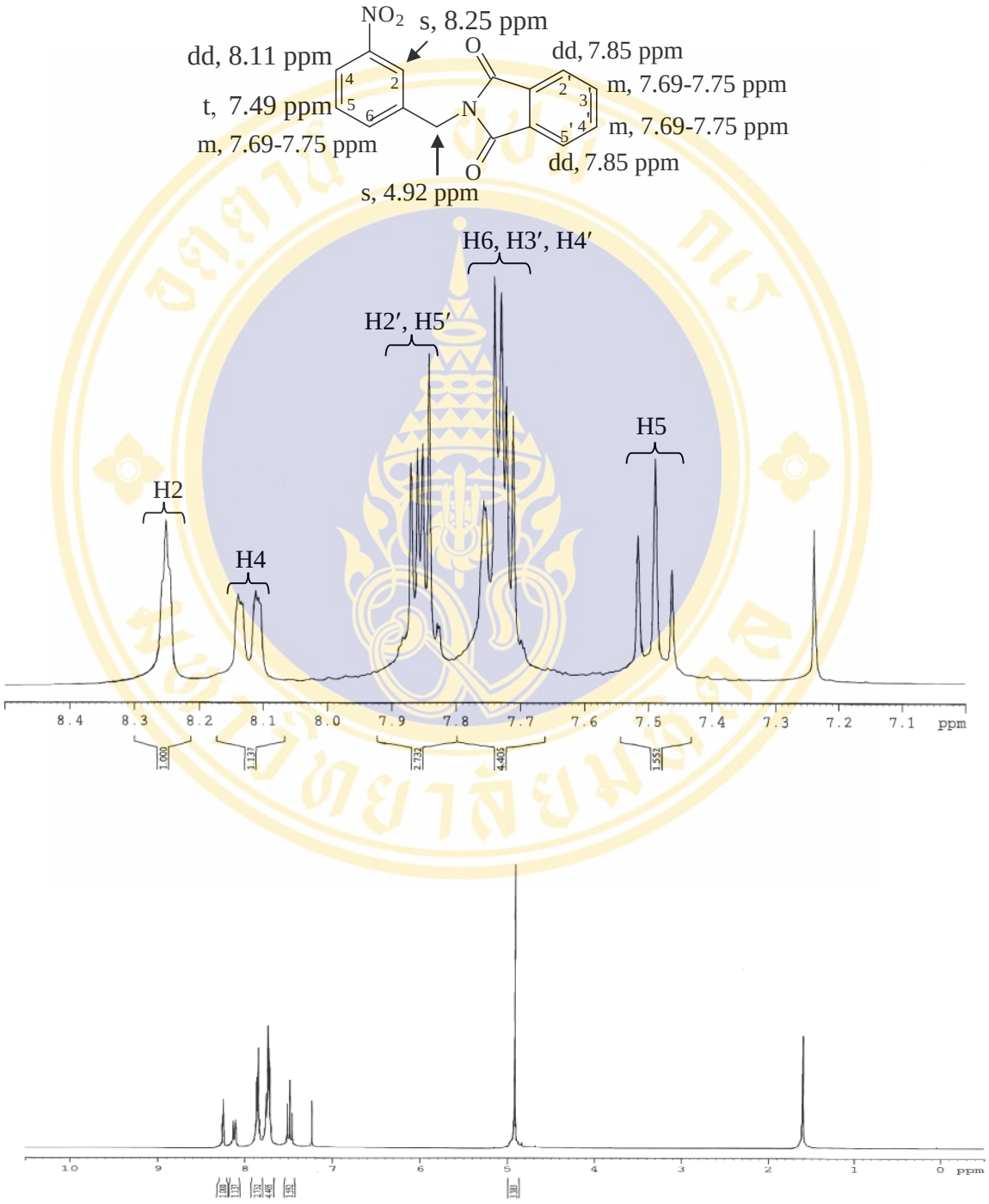

Figure 22. The ^{1}H NMR spectrum (300 MHz, $CDCl_3$) of 1-phthalimidomethyl-3-nitrobenzene **38**

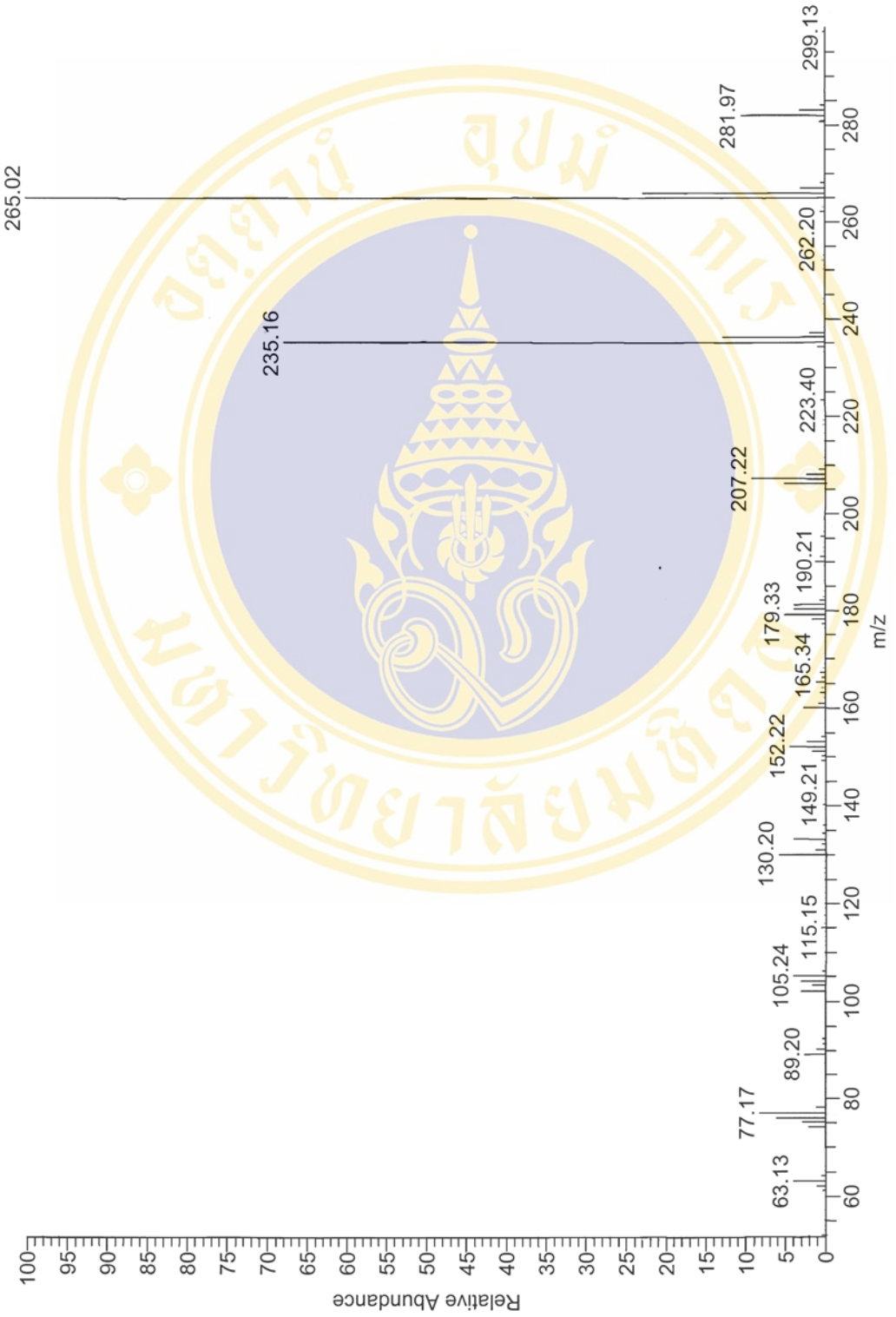

Figure 23. The EI mass spectrum of 1-phthalimidomethyl-3-nitrobenzene **38**

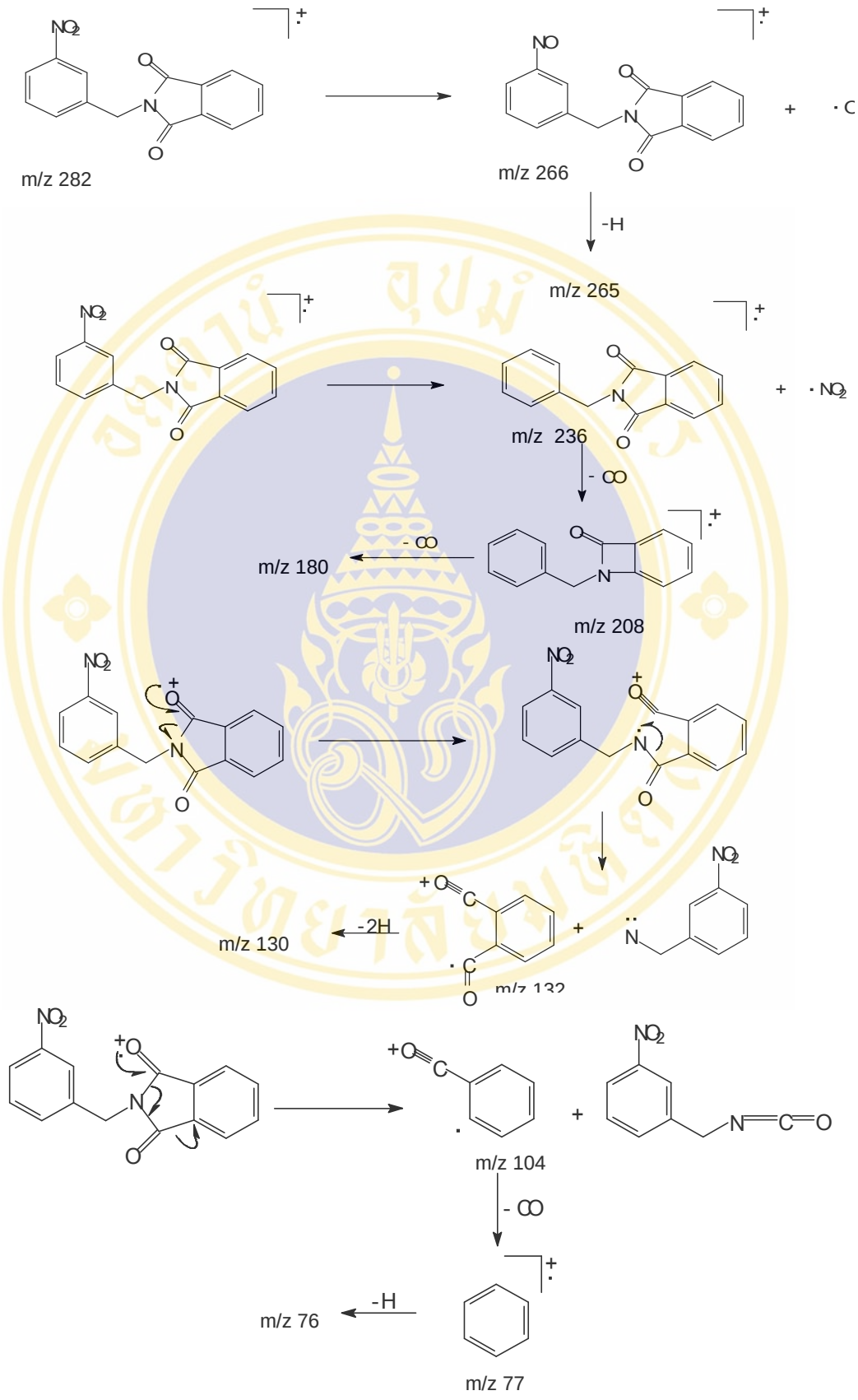

Figure 24. Fragmentation patterns of 1-phthalimidomethyl-3-nitrobenzene **38**

C. Evaluation of HIV-1 reverse transcriptase inhibitory activity

Radioactivity test

The 6 newly synthesized compounds were tested for HIV-1 RT activity with homopolymeric poly(rA).oligo(dT) as a template-primer and [^{3}H]dTTP as substrate. The details of the principle and procedure of this assay were discussed in Chapter II and Chapter IV respectively. The reactions were performed under the condition described for the HIV-1 RT RNA dependent DNA polymerase activity assay (140). The results of this assay were reported as percentage of relative inhibitory activity ratio (%IR) which were determined based on count per minute of incorporated ^{3}H labeled substrates into a polymer fraction by RT in the presence of the sample. The %IR was calculated as followed:

$$(\%)\ IR = \left[1 - \frac{[cpm(complete\ system) - cpm(complete\ system\text{-}RT)]}{[cpm(complete\ system\text{-}sample) - cpm(complete\ system\text{-}RT)]} \right] \times 100$$

where: (%) IR = percent of relative inhibitory ratio

cpm = count per minute

complete system = reaction mixture which consisted of RT, template-primer, substrate, sample, and other reagents.

complete system-RT = reaction mixture which consisted of template-primer, substrate and other reagents.

complete system-sample = reaction mixture which consisted of RT, template-primer, substrate and other reagents.

Doxorubicin hydrochloride (adriamycin) at 1.25 mM (678.8 μg/mL) was used as a positive control substance which exhibited 99.9% enzyme inhibition. The tested compounds were evaluated in triplicate at concentration 200 μg/mL. All of the tested compounds were dissolved in DMSO and were adjusted to the final concentration of DMSO of 5%. The result of activity testing was shown in Table 4.

Table 4. The inhibitory activity of the test compounds at concentration 200 µg/mL.

cpd	Structure	%IR
34	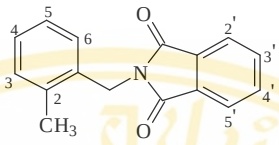 (0.80 mM)	12.5
35	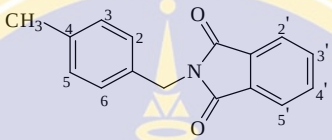 (0.80 mM)	12.4
36	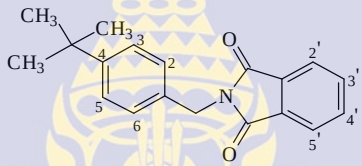 (0.68 mM)	22.9
37	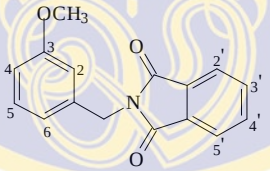 (0.75 mM)	18.9
38	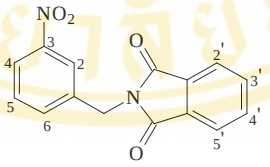 (0.71 mM)	14.6
39	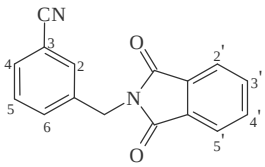 (0.76 mM)	7.9

Note: Doxorubicin hydrochloride at concentration 678.8 µg/mL (1.25 mM) exhibited 99.9% IR

Compounds in this series showed low inhibitory activity between 7.9-22.9 %IR. However, the concentrations of the tested compounds used in this assay was between 0.68-0.80 mM which were still lower of the positive control, doxorubicin, 1.25 mM

It should be mentioned that if different template-primer is used in the experiment, it might end up with different %IR (146-147). NNRTIs usually bind to the allosteric binding site which is clearly distinct from the substrate-binding site of enzyme, indicating that the binding of the enzyme with substrate is not influenced by the inhibitor. NNRTIs are noncompetitive with respect to the template-primer. However, mechanism of inhibition, i.e., competitive or noncompetitive is also depending on the template-primer, substrate, and divalent cation used in the assay (146). The unsatisfactory inhibitory activity of the synthesized derivatives might due to unappropriated assay condition. The more efficient template-primer as well as other optimal experimental conditions should be found out for the further study. Moreover, the low activity of these derivatives may resulted from the shape and size of the substituent of the benzene ring. The considered bulky group at meta or para position (designed from CoMFA and CoMSIA studies) does not provide appropriate steric effect for better activity. Bulkier substituent(s) should be tried to put at meta or para or both positions to improve the activity. The contour map of electrostatic field should be considered as well for modifying structures to obtain more potent derivatives.

D. Evaluation of cytotoxic activity

The cytotoxicity was determined by using MTT colorimetic assay. The three cell lines, human epidermoid carcinoma (KB), human cervical carcinoma (HeLa), and african green monkey kidney cell (vero) were used in the assay. The previously and newly synthesized derivatives were evaluated for cytotoxic activity. The details of the principle and procedure of this assay were discussed in Chapter II and Chapter IV respectively. The results were shown as the percentage of cell viability calculated by following equation.

$$\% \text{ viability} = \frac{(\text{OD of sample at 550 nm})}{(\text{OD of control at 550 nm}).} \times 100$$

Where: % viability = percent of the cell survival

OD = optical density (absorbance) units

The tested compounds were evaluated in triplicate at concentration 0.1-100 μg/mL. All of the tested compounds were dissolved in DMSO and were adjusted to the final concentration of DMSO of 5%. As shown in Table 5 most of the compounds showed similar cytotoxic activity with IC_{50} values over 100 μg/mL, except for compound **36**. The IC_{50} values of compound **36** for KB and HeLa cell lines were 50 and 62 μg/mL (0.17 and 0.21 μM) respectively and higher than 100 μg/mL for vero cell line. Therefore, there was no correlation between HIV-1 RT and cytotoxic activity found in this phthalimide series.

Table 5. The cytotoxic activity of the phthalimide derivatives

Cpd	R	IC_{50} (μg/mL)		
		KB	**HeLa**	**vero**
1		ND	ND	ND
2	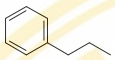	>100	>100	>100
3		>100	>100	>100
4	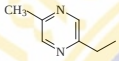	ND	ND	ND
5	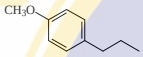	>100	>100	>100
6		>100	>100	>100
7	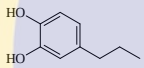	>100	>100	>100
8	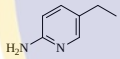	>100	>100	>100
9	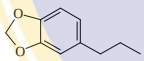	>100	>100	>100
10	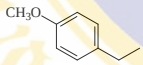	>100	>100	>100
11	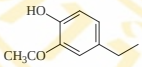	ND	ND	ND
12	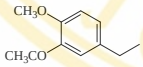	>100	>100	>100
13	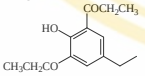	>100	>100	>100
14	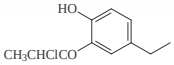	>100	>100	>100
15	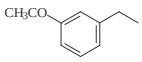	ND	ND	ND
16	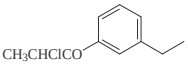	>100	>100	>100
17	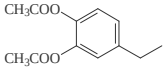	>100	>100	>100
18	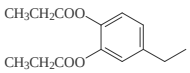	>100	>100	>100
19	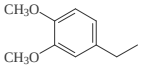	>100	>100	>100
20	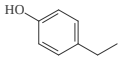	>100	>100	>100
21	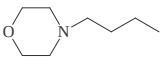	ND	ND	ND

Table 5. The cytotoxic activity of the phthalimide derivatives (continue)

Cpd	R	IC_{50} (μg/mL)		
		KB	**HeLa**	**vero**
22	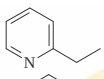	>100	>100	>100
23	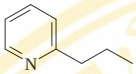	ND	ND	ND
24	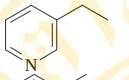	>100	>100	>100
25		>100	>100	>100
26	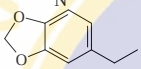	>100	>100	>100
27	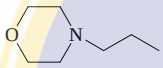	>100	>100	>100
28	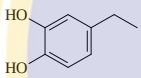	>100	>100	>100
29	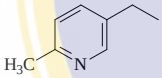	ND	ND	ND
30	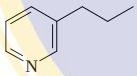	>100	>100	>100
31	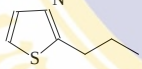	ND	ND	ND
32	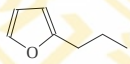	>100	>100	>100
33	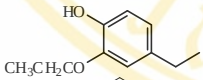	>100	>100	>100
34	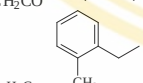	>100	>100	>100
35	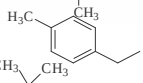	>100	>100	>100
36	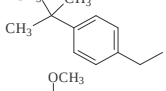	50 (0.17 μM)	62 (0.21μM)	>100
37	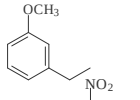	>100	>100	>100
38	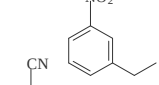	>100	>100	>100
39	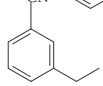	>100	>100	>100

Note: ND = not determined

CHAPTER VI

CONCLUSION

Six new derivatives in the phthalimide series have been designed and synthesized (based on the previous 3D QSAR, CoMFA and CoMSIA studies). These derivatives were synthesized using phthalimide and substituted benzyl halide in the presence of potassium hydroxide. The RT inhibitory activity assay were determind by radiometric method, using 200 μg/mL of the inhibitors. The assay was performed using poly(rA).oligo(dT) as template-primer, [^{3}H]dTTP as substrate, and doxorubicin (adriamycin) 1.25 mM as a positive control. The synthesized compounds showed low inhibitory activity in the range of 7.9-22.9 % inhibition. The unsatisfactory activity of there derivatives may be due to the inappropriated assay conditions or the bulkiness of the substituent at meta or para position of the benzene ring still not adequate for better activity.

The previously and newly synthesized phthalimide derivatives have been subjected to cytotoxic activity testing using MTT colorimetric method against the cancer cell lines KB and HeLa and normal vero cell line. Only 1-phthalimidomethyl-4-*tert*-butylbenzene, compound **36** showed promising cytotoxic activity with less toxic to normal cell.

REFERENCES

1. Sleasman JW, Goodenow MM. HIV-1 infection. J Allergy Clin Immun 2003; 111(2): 582-92.
2. HIV. Available from: http://www.medicalhelpers.com/medical_illness/hiv.html [Accessed 2006 July 13].
3. Global AIDS epidemic continues to grow. Available from: http://www.who.int/hiv/ mediacentre/news62/en/index.html [Accessed 2006 November 27].
4. Rabkin CS. AIDS and cancer in the era of highly active antiviral therapy(HAART).Eur J Cancer 2001; 37: 1316-9.
5. Rabkin CS. Association of non-acquired immunodeficiency syndrome-defining cancers with human immunodeficiency virus infection. J Natl Cancer I Monographs 1998; 23: 23-5.
6. Levine AM. Hodgkin's disease in the setting of human immumodeficiency virus infection. J Natl Cancer I Monographs 1998; 23: 37-42.
7. Fiorelli V, Gendelman R, Sirianni MC, Chang HK, Colombini S, Markham PM, et al. Γ- Intereron produced by $CD8^+$ T cells infiltrating Kaposi's sarcoma induces spindle cells with angiogenic phenotype and synergy with human immunodeficiency virus-1 Tat protein: an immune response to human herpesvirus-8 infection? Blood 1998; 91 (3): 956-67.
8. Sgadart C, Barillari G, Toschi E, Carlei D, BaciGalupo I, Baccarini S, et al. HIV protease inhibitors are potent anti-angiogenic molecules and promote regression of Kaposi sarcoma. Nat Med 2002; 8 (3): 225-31.
9. Darnawski JW, Goulette FA. 3'-Azido-3'-deoxythymidine cytotoxicity and metabolism in the human colon tumor cell line HCT-8. Biochem Pharmacol 1994; 48 (9): 1797-805.
10. Ilezoe T, Daar ES, Hisatake J, Taguchi H, Koeffler HP. HIV-1 protease inhibitors decrease proliferation and induce differentiation of human myelocytic leukemia cells. Blood 2000; 96 (10): 3553-9.

11. Wagner CR, Ballato G, Akanni AO, McIntee EJ, Larson RS, Chang S, et al. Potent growth inhibitory activity of zidovudine on cultured human breast cancer cells and rat mammary tumors. Cancer Res 1997; 57: 2341-5.
12. Petit F, Fromenty B, Owen A, Estaquier J. Mitochondria are sensors for HIV drugs. Trends Pharmacol Sci 2005; 26 (5): 259-64.
13. Strayer DS, Akkina R, Bunnell BA, Dropulic B, Planelles V, Pomerantz RJ, et al. Current status of gene therapy strategies to treat HIV/AIDS. Mol Ther 2005; 11 (6): 823-42.
14. Otto MJ. New nucleoside reverse transcriptase inhibitors for the treatment of HIV infections. Curr Opin Pharmacol 2004; 4: 431-6.
15. Pauwels R. New non-nucleoside reverse transcriptase inhibitors (NNRTIs) in development for the treatment of HIV infections. Curr Opin Pharmacol 2004; 4: 437-46.
16. Turner SR. HIV protease inhibitors-the next generation. Curr Med Chem 2002; 1 (2): 141-61.
17. Ridky TW, Cameron CE, Cameron J, Leis J. Human immunodeficiency virus, type 1 protease substrate specificity is limited by interactions between substrate amino acids bound in adjacent enzyme subsites. J Biol Chem 1996; 271 (9): 4709-17.
18. Drugs approved by the FDA: aptivue (tipranavir). Available from: http://www.centerwatch.com/patient/drug/dru880.htm [Accessed 2006 June 6].
19. Darunavir. Available from: http://www.hivinsite.ucst.edu/InSite?page=ar-rr-03 [Accessed 2006 July 13].
20. Fung HB., Guo Y. Enfuvirtide: a fusion inhibitor for the treatment of HIV infection. Clin Ther. 2004; 26 (3): 352-78.
21. Liu S, Lu H, Niu J, Xu Y, Wu S, Jiang S. Different from the HIV fusion inhibitor C34, the anti-HIV drug fuzeon (T-20) inhibits HIV-1 entry by targeting multiple sites in gp41 and gp120. J Biol Chem 2005; 280 (12): 11259-73.
22. Samee W, Ungwitayatorn J, Matayatsak C, Pimthon J. 3D-QSAR studies on phthalimide derivatives as HIV-1 reverse transcriptase inhibitors. Science Asia 2004; 30: 81-8.

23. Bentwich Z, Kalinkovich A, Weisman Z, Grossman Z. Immune activation in the context of HIV infection. Clin Exp Immunol 1998; 111: 1-2.
24. HIV. Available from: http://www.en.wikipedia.org/wiki/HIV [Accessed 2006 July 13].
25. Pieribone D. The HIV life cycle. ACRIA update 2002; 12 (1): 1-4.
26. Human inmumodeficiency a globle pandemic. Available from: http:// www. stanford.edc/group/virus/retro/2005gongishmail/HIV.html [Accessed 2006 July 23].
27. Epidemiology of HIV. Available from: http:// www.critpath.org/aric [Accessed 2006 July13].
28. HIV structure and genome. Available from:http://en.wikipedia.org/wiki/HIV_ structure_and_genome#Structure [Accessed 2006 July13].
29. Ramon SS, Bellon JM, Resino S, Nogues CC, Gurbindo D, Ramon JT, et al. Low blood $CD8^+$ T-lymphocytes and high circulating monocytes are predictors of HIV-1 associated progressive encephalopathy in children. Pediatrics. 2003; 111 (1): 168-75.
30. Stricker JD. Drugs in development: new promise. ACRIA. 2002-3; 12: 5-19.
31. Clercq ED. New development in anti-HIV chemotherapy. BBA 2002; 1587: 258-75.
32. Clercq ED. HIV-chemotherapy and -prophylaxis: new drugs, leads and approaches. IJCCB 2004; 36: 1800-22.
33. Griffeeith R, Luu TTT, Garner J, Keller PA. Combining structure-base druge design and pharmacophores. J Mol Graph Model 2005; 23: 439-46.
34. Girard MP, Osmanov SK, Kieny MP. A review of vaccine research and development: the human immunodeficiency virus (HIV). Vaccine 2006; 24: 4062-81.
35. Yeni P. Update on HAART in HIV. J Hepatol 2006; 44: S100-3.
36. Pauwels R. Aspects of successful drug discovery and development. Antiviral Res 2006; 71: 77-89.
37. Wainbery MA. The emergence of HIV resistance and new antivirals: are we winning? Drug Resist Update 2004; 7: 163-7.

38. Sanrafianos SG, Hughes SH, Arnold E. Designing anti-AIDS drugs targeting the major mechanism of HIV-1 RT resistance to nucleoside analog drugs. IJBCB 2004; 36:1706-15.

39. Cremer NS, Alpay N, Bahar I. Conformational changes in HIV-1 reverse transcriptase induced by nonnucleoside reverse transcriptase inhibitor binding. Curr HIV Res 2004; 2: 323-32.

40. Ren J, Stammers DK. HIV reverse transcriptase structures: designing new inhibitors and understanding mechanisms of drug resistance. Trends Pharmacol Sci 2005; 26 (1): 4-7.

41. Das K, Lewi PJ, Hughes SH, Arnold E. Crystallography and design of anti-AIDS drugs: conformational flexibility and positional adaptability are important in the design of non-nucleoside HIV-1 reverse transcriptase inhibitors. Prog Biophys Mol Bio 2005; 88; 209-31.

42. Hughes SH. Molecular matchmaking: NNRTIs can enchance the dimerization of HIV type 1 reverse transcriptase. PNAS 2001; 98 (13): 6991-2.

43. Leung D, Abbenante G, Fairlie DP. Protease inhibitors: current status and future prospects. J Med Chem 2000; 43 (3): 305-41.

44. Tomasselli AG, Heinrikson RL. Targeting the HIV-protease in AIDS therapy: a current clinical perspective. BBA 2000; 1477: 189-214.

45. Pettit SC, Lindquist JN, Kaplan AH, Swanstron R. Processing site in the human immunodeficiency virus type1 (HIV-1) Gap-Pro-Pol precursor are cleave by the viral protease at different rats. Retrovirol 2005; (11): 1-6.

46. Zidovudine. Available from: http://www.aidsinfo.nif.gov/DrugsNew/DrugDatail NT.aspx?int_id=0004 [Accessed 2006 July 13].

47. Lozano JS, McCoig CC, Cao Y, Vitetta ES, Ramilo O. Zidovudine, lamivudine, and abacavir have different effects on resting cells infected with human immunodeficiency virus in vitro. Antimicrob Agents Ch 2004; 48 (8): 2825-30.

48. Francke S, Orosz C, Hayes KA, Mathes LE. Effect of zidovudine on the primary cytolytic T-lymphocyte response and T-cell effector fungtion. Antimicrob Agents Ch 2000; 44 (7): 1900-5.

49. Didanosine. Available from: http://www.aidsinfo.nif.gov/Drugs New/pdfdrug_nt.asp?int_id=16 [Accessed 2006 July 13].

50. Meng Q, Walker DM, Olivero OA, Shi X, Antiochos BB, Poirier MC, et al. Zidovudine-didanosine coexposure potentiates DNA incorporation of zidovudine and mutagenesis in human cells. PNAS 2000; 97 (23): 12667-71.

51. Perry CM, Moble S. Didanosine: an updated review of its use in HIV infection. Drugs 1999; 58 (6): 1099-135.

52. Zalcitabine. Available from: http://www.aidsinfo.nif.gov/Drugs New/DrugDatailNT.aspx?MenuItem=Drugs&sear [Accessed 2006 July 13].

53. Izopet J, Sailler L, Sandres K, Pasquier C, Bonnet E, Aquilina C, et al. Intermittent selection presure with zidovudine plus zalcitabine treatment reduces the emergence in vivo of zidovidine resistance HIV mutations. J Med Virol 1999; 57 (2): 163-8.

54. Stavudine. Availalble from: http//www.aidinfo.nif.gov/DrugsNew/DrugDetailNT.aspx?MenuItem=Drug&searhtm [Accessed 2006 July 13].

55. Nitanda T, Wang X, Kumamoto H, Haraguchi K, Tanaka H, Cheng YC, et al. Anti-human immunodeficiency virus type1 activity and resistance profile of 2',3'-difehydro-3'-deoxy-4'-ethynythymidine in vitro. Antimicrob Agents Ch 2005; 49 (8): 3355-60.

56. Lamivudine. Available from: http//wwwaidinfo.nif.gov/DrugsNew/DrugDetailNT.aspx?MenuItem=Drug&sear htm [Accessed 2006 July 13].

57. Balzarint J, Pelemans H, Karlssons A, Clercq ED, Kleim JP. Concomitant combination therapy for HIV infection preferable over sequential therapy with 3TC and nonnucleoside reverse transcriptase inhibitors. Proc Nalt Acad Sci USA 1996; 93: 13152-7.

58. Sarafianos SG, Das K, Arthur D. Clark JR, Ding J, Boyer PL, et.al. Lamivudine (3TC) resistance in HIV-1 reverse transcriptase involves steric hindrance with beta-branched amino acids. PNAS 1999; 96: 10027-32.

59. Abacavir. Available from: http://www.aidsinfo.nif.gov/Drugs New/Drug DatailNT.aspx?MenuItem=Drugs&sear [Accessed 2006 July 13].

60. Clay PG. The abacavir hypersensivity reaction: a review. Clin Ther 2003; 24 (10): 1502-14.

61. Ray AS, Basavapathruni A, Anderson AS. Mechanistic studies to understand the progressive development of resistance in human immunodeficiency virus type 1 reverse transcriptase to abacavir. J Biol Chem 2002: 277 (43): 40479-90.

62. Tenofovir disproxil fumarate. Available from: http//www.aidinfo.nif.gov/ Drugs New/DrugDetailNT.aspx?MenuItem=Drug&sear [Accessed 2006 July 13].

63. Stone C, Khaled MA, Craig C, Griffin P, Tisdale M. Human immunodeficiency virus type 1 reverse transcriptase mutation selection dure in vitro exposure to tenofovir alone or combined abacavir or lamivudine. Antimicrob Agents Ch 2004; 48 (4): 1413-5.

64. Emtricitabine. Available from: http//www.aidinfo.nif.gov/ DrugsNew/Drug Detail NT.aspx?MenuItem=Drug&sear [Accessed 2006 July 13].

65. Frampton JE, Perry CM. Emtricitabine: a review of its use in the management of HIV infection. Drugs 2005; 65 (10): 1427-48.

66. Furman PA, Painter G, Wilson JE, Cheng N, Hopkins S. Substrate inhibition of the human immunodeficiency virus type 1 reverse transcriptase. PNAS 1991; 88: 6013-7.

67. Harrigan PR, Salim M, Stammers DK, Wynhoven B, Brumme Z, McKenna P, et al. A mutation in the 3 region of human immunodeficiency virus type 1 reverse transcriptase (Y318F) associated with nonnucleoside reverse transcriptase inhibitor resistance. J Virol 2002; 76 (13): 6836-40.

68. Ambrose Z, Julias JG, Boyer PL, Kewal VNR, Hughes SH. The level of reverse transcriptase (RT) in human immunodeficiency virus type 1 particles affects susceptibility to nonnucleoside RT inhibitors but not to lamivudine. J Virol 2006; 80 (5): 2578-81.

69. Motakis D, Parniak MA. A tight-binding mode of inhibition is essential for anti-human immunodeficiency virus type1 virucidal activity of nonnucleoside reverse transcriptase inhibitors. Antimicrob Agents Ch 2002; 46 (6): 1851-6.

70. Nevirapine. Available from: http://www.aidsinfo.nif.gov/DrugsNew/DrugDatail NT.aspx?MenuItem=Drugs&sear [Accessed 2006 July 13].

71. Jarvir B, Faulds D. Nevirapine, a review of its therapeutic efficacy in HIV infection. Drugs 1998; 56 (1): 147-67.

72. Delavirdine. Available from: http://www.aidsinfo.nif.gov/Drugs New/Drug DatailNT.aspx?MenuItem=Drugs&sear [Accessed 2006 July 13].

73. Scott LJ, Perry MJ. Delavirdine: a review of its use in HIV infections. Drugs 2002; 60 (6): 1411-44.

74. Drugs approved by the FDA: sustiva. Available from: http:// www. centerwatch. com/patient/drug/dru758.htm [Accessed 2006 October 26].

75. Mutlib AE, Chen H, Nemeth G, Gan LS, Christ DD. Liquid chromatography/ mass spectrometry and high-field nuclear magnetic resonance characterization of novel mixed diconjugates of the non-nucleoside human immunodeficiency virus-1 reverse transcriptase inhibitor, efavirenz. Drug Metab Dispos 1999; 27 (9): 1045-56.

76. Crespa E, Locatelli GA, Cancio R, Hubscher U, Spadari S, Maga G. Drug resistance mutations in the nucleotide binding pocket of human immunodeficiency virus type 1 reverse transcriptase differentially affect the phosphorolysis-dependent primer unblocking activity in the presence of stavudine and zidovudine and its inhibition by efavirenz. Antimicrob Agents Ch 2005; 49 (1): 342-9.

77. Young SD, Britcher SF, Tran LO, Payne LS, Lumma WC, Lyle TA, et. al. L-743,726(DMP-266): A novel, highly potent nonnucleoside inhibitor of the human inmumodeficiency virus type 1 reverse transcriptase. Antimicrob Agents Chemother 1995; 39; 2602-2.

78. Patick AK, Boritzki TJ, Bloom LA. Activities of the human deficiency virus type 1 (HIV-1) protease inhibitor nelfinavir mesylate in combination with reverse transcriptase and protease inhibitors against acute HIV-1 infection in vitro. Antimicrob Agents Chemother 1997; 1: 2159-64.

79. Saquinavir. Available from: http://www.aidsinfo.nif.gov/Drugs New/DrugDatail NT.aspx?MenuItem=Drugs&sear [Accessed 2006 July 13].

80. Graves BJ, Hatada MH, Miller JK, Graves MC, Roy S, Cook CM, et al. The three-dimensional x-ray crystal structure of HIV-1 protease complexed with a hydroxyethylene inhibitor. Adv Exp Med Biol 1991; 306: 455-60.

81. Kravcik S. Pharmacology and clinical experience with saquinavir. Expert Opin Pharmacother 2001; 2: 303-15.

82. Figgitt DP, Plosker GL. Saquinavir soft-gel capsule: an updated review of its use in the management of HIV infection. Drugs 2000; 60: 481-516.

83. Vanhove GF, Gries JM, Verotta D, Sheiner LB, Coombs R, Collier AN, et al. Exposure-response relationships for saquinavir, ziduvudine and zalcitabine in combination therapy. Antimicrob Agents Ch 1997; 41 (11): 2433-8.

84. Ritonavir. Available from: http://www.aidsinfo.nif.gov/Drugs New/DrugDatail NT.aspx?MenuItem=Drugs&sear [Accessed 2006 July 13].

85. Mikus G, Schowel V, Drzewinska M, Rengelshausen J, Ding R, Riedel K, et al. Potent cytochrome P450 2C19 genotype–related interaction between voriconazole and the cytochrome P450 3A4 inhibitor ritonavir. Clin Pharmacol Ther 2006; 80 (2): 126-35.

86. Koudriakova T, Iatsimirskaia E, Utkin I, Gangl E, Vouros P, Storozhuk E, et al. Metabolism of the human immunodeficiency virus protease inhibitors indinavir and ritonavir by human intestinal microsomes and xxpressed cytochrome P4503A4/3A5: mechanism-based inactivation of cytochrome P4503A by ritonavir. Drug Metab Dispos. 1998; 26 (6): 552-61.

87. Indinavir. Available from: http://www.aidsinfo.nif.gov/Drugs New/DrugDatail NT.aspx?MenuItem=Drugs&sear [Accessed 2006 July 13].

88. Rose MJ, Merschman SA, Eisenhandler R, Woolf EJ, Yeh KC, Lin l, et al. High-throughput simultaneous determination of the HIV protease inhibitors indinavir and L-756423 in human plasma using semi-automated 96-well solid phase extraction and LC–MS/MS. J Pharm Biomed Anal. 2000; 24 (2): 291-305.

89. Plosker GL, Noble S. Indinavir: a review of its use in the management of HIV infection. Drugs 1999; 58: 1165- 203.

90. Nelfiravir. Available from: http://www.aidsinfo.nif.gov/Drugs New/DrugDatail NT.aspx?MenuItem=Drugs&sear [Accessed 2006 July 13].

91. Creus TM, Meda MJM, Jane CC, Garcia IN, Sala RJ. Nelfinavir: review of its pharmacokinetics and drug interactions. Farm. Hosp. 1999; 23: 79-93.

92. Drugs approved by the FDA: agenerase (amprenavir). Available from: http:// www.centerwatch.com/patient/drug/dru526.htm [Accessed 2006 October 26].

93. Fung HB, Kirschenbaum HL, Hameed R. Amprenavir: a new human immunodeficiency virus type 1 protease inhibitor. Clin Ther 2000; 22 (5); 549-72.

94. Maguire M, Ahortino D, Klein A, Harris W, Manohitharajah V, Tisdale M, et, al. Emergence of resistance to protease inhibitor amprenavir in human immunodeficiency virus type 1-infected patients: selection of four alternative viral protease genotype and influence of viral susceptibility to coadminitered reverse transcriptase nucleoside inhibitors. Antimicrob Agents Ch 2002; 46(3): 731-8.

95. Lopinavir/ritonavir. Available from: http://www.aidsinfo.nif.gov/Drugs New/ Drug DatailNT.aspx?MenuItem=Drugs&sear [Accessed 2006 July 13].

96. Cvetkovic RS, Goa KL. Lopinavir/ritonavir: a review of its use in the management of HIV infection. Drugs 2003; 63 (8): 769-802.

97. HIV and AIDS treatment: kaletra. Available from: http:// www.hivandhepatitis. com/hiv_andaids/kaletra_1.html [Accessed 2006 November 11].

98. Kumar GN, Dykstra J, Roberts EM, Jayanti VK, Hickman D, Uchic J, et al. Potent inhibition of the cytochrome P-450 3A-mediated human liver microsomal metabolism of a novel HIV protease inhibitor by ritonavir: a positive drug-drug interaction. Drug Metab Dispos 1999; 27: 902-8.

99. Wlodawer A. Rational approach to AIDS drug design through structural bio - logy. Annu Rev Med 2002; 53: 595-614.

100. Drugs approved by the FDA: reyataz (atazanavir sulfate): Available from: http:// www.centerwatch.com/patient/drug/dru835.htm [Accessed 2006 October 26].

101. Colonno RJ, Thiry A, Limoli K, Parkin N. Activities of atazanavir (BMS-232632) against a large panal of human immunodeficiency virus type 1 clinical isolates resistant to one or more approved protease inhibitors. Antimicrob Agents Ch 2003; 47 (4): 1324-33.

102. Orrick JJ, Corklin R, Steinhart CR. Atazanavir. Annal Pharmacother 2004; 38: 1664-70.

103. Colonno R, Rose R, McLaren C, Thiry A, Parkin N. Identification of I50L as the signature atazanavir (ATV) resistance mutation in treatment-naive HIV-1 infected patients receiving ATV-containing regimens. J Infect Dis 2004; 189: 1802-10.

104. Drugs approved by the FDA: lexiva (fosamprenavir calcium). Available from: http://www.centerwatch.com/patient/drug/dru844.htm [Accessed 2006 October 26].

105. Ellis JM, Roos JW, Coleman CI. Fosamprenavir a novel protease inhibitor and prodrug of amprenavir. Formulary 2004; 39: 151-60.

106. Zhao Z, Koeplinger KA, Peterson T, Conradi RA, Burton PS, Suarato A, et al. Mechanism, structure-activity studies, and potential applications of glutathione *s*-transferase-catalyzed cleavage of sulfonamides. Drug Metab Dispos 1999; 27(9): 992-8.

107. Chapman TM, Plosker GL, Perry CM. Fosamprenavir: a review of its use in the management of antiretroviral therapy-naive patients with HIV infection. Drugs 2004; 64 (18): 2101-24.

108. Antiretroviral combination therapy. Available from: http://www.hivmanagement.org/enfuvirtide.html [Accessed 2006 October 26].

109. Doyon L, Tremblay S, Bourgon L, Wardrop E, Cordingley MG. Selection and characterization of HIV-1 showing reduced susceptibility to the non-peptidic protease inhibitor tipranavir. Antivir Res 2005; 68: 27-35.

110. Colombo S, Beguin A, Marzolini C, Telenti A, Biollaz J, Decosterd LA. Determanation of the nevel non-petidic HIV-protease inhibitor tipranavir by HPLC-UV after solid-phase exteaction. J Chromatogr B 2006; 832: 138-43.

111. Rusconl A, Catamancio SLS, Citterio P, Kurtagic S, Violin M, Balotta C, et al. Susceptibility to PNU-140690 (tipranavir) of human immunodeficiency virus type 1 isolated from patients with multidrug resistance to other protease inhibitors. Antimicrob Agents Ch 2000; 44 (5): 1328-32.

112. Mukwaya G, Gregor TM, Hoelscher D, Heming T, Legg D, Kavanaugh K, et al. Interaction of ritonavir-boosted tipranavir with loperamide dose not result in loperamide-associated neurologic side effects in healthy volunteers. Antimicrob Agents Ch 2005; 49 (12): 4903-10.

113. Prezista™ (Tibotec, Inc.): darunavir description. Available from: http://www.fda.gov/cder/foi/label/2006/021976lbl.pdf [Accessed 2005 August 28].

114. Koh Y, Nakata H, Maeda K, Ogata H, Bilcer G, Devasamudram T, et al. Nevel *bis*-tetrahydrofuranylurethane-containing nonpeptidic protease inhibitor (PI) UIC-94017 (TMC114) with potent activity against multi-PI-resistant human immunodeficiency virus in vitro. Antimicrob Agents Ch 2003; 47 (10): 3123-9.

115. King NM, Jeyabalan MP, Nalivaika EA, Wigerinck P, Bethune MP, Schiffer CA. Structural and thermodynamic basis for the binding of TMC114, a next-generation human immunodeficiency virus type 1 protease inhibitor. J Virol 2004; 78 (21): 12012-21.

116. Kovalevsky AY, Liu F, Leshchenko S, Ghosh AK, Louis JM, et al. Ultra-high resolution crystal structure of HIV-1 protease mutant reveals two binding sites for clinical inhibitor TMC114. JMB 2006; 363: 161-73.

117. Sekar VJ, Guzman S, Pauw MD, Paepe ED, Vangeneugden T, Hoetelmans R, et al. The pharmacokinetic interaction between clarithromycin and TMC114/ritonavir in healthy subjects. Clin Phamacol Ther 2006; 79 (2): 23.

118. Meyer SD, Azijin H, Surleraux D, Jochmans D, Tahri A, Pauwels R, et al. TMC114, a novel human immunodeficiency virus type 1 protease inhibitoractive against protease inhibitor-resistant viruses, including a broad range of clinical isolates. Antimicrob Agents Ch 2005; 49 (6): 2314-21.

119. Price OT, Erical N, Nakaoke R, Banks WA. HIV-1 viral proteins gp120 tat induce oxidative stress in brain endothelial cell. Brain Res 2005; 1045: 57-63.

120. Conti L, Fantuzzi L, Corno MD, Belardelli F, Gessani S. Immunomodulatory effects of the HIV-1 gp120 protein on antigen presenting cell: implication for AIDS pathologesis. Immunology 2004; 209: 99-115.

121. Eraikhuemen N, Branch E, Boston N, Honeywell M, Sneed K. Enfuvirtide: a novel agent for inhibiting the entry of HIV-1 into immune cells. Drug Forcast 2003; 28: 571-83.

122. Heidenreich O, Kruhoffer M, Gross F, Eckstein F. Inhibition of human immunodeficeincy virus 1 reverse transcriptase by 3'-azido thymidine triphosphate. Eur J Biochem 1990; 192: 621-5.

123. Vrang L, Oberg B, Lower J, Kurth R. Reverse transcriptase from human immunodeficiency virus type 1 (HIV-1), HIV-2, and simian immunodeficiency virus (SIV_{MAC}) are suscreptible to inibition by foscarnet and 3'-azido-3'-deoxythymidine triphosphate. Antimicrob Agents Ch 1988; 32 (11): 1733-4.

124. Pimthon J. Synthesis and in vitro HIV-1 reverse transcriptase inhibitory activity of phthalimide derivatives. [M.S. Thesis in Pharmacy]. Bangkok: Faculty of Graduate Studies, Mahidol University, 2001.

125. Rabkin CS, Yellin F. Cancer incidence in a population with a high prevalence of infection with human immunodeficiency virus type 1. J Nalt Cancer Inst 1994; 86 (22): 1711-6.

126. Gescher A, Pastorino U, Plummer SM, Mansom MM. Suppression to tumor development by substances derived from the diet-mechanism and clinical implications. Br J Clin Pharmacol 1998; 45: 1-12.

127. Houghton P, Fang R, Techatanawat I, Steventon G, Hylands PJ, Lee CC. The sulphorhodamine (SRB) assay and other approaches to testing plant extracts and derived compounds for activities related to reputed anticancer activity. Methods 2007; (24): 377-87.

128. Bigl K, Schmitt A, Meiners I, MÜnch G, Arendt T. Comparison of results of the CellTiter Blue, the tetrazolium (3-[4,5-dimethylthioazol-2-yl]-2,5- diphenyl tetrazolium bromide), and the lactate dehydrogenase assay applied in brain cells after exposure to advanced glycation endproducts. Toxicology in Vitro 21 2007; (21): 962-71.

129. Padrón JM, Wilt CL, Smid K, Wilms ES, Backus HHJ, Pizao PE , et al. The multilayered postconfluent cell culture as a model for drug screening. Oncology Hematology 2000; (36): 141-57.

130. Hunter AC. Molecular hurdles in polyfectin design and mechanistic background to polycation induced cytotoxicity. Advanced Drug Delivery Reviews 2006; (58): 1523-31.

131. Beridge MV, Herst PM, Tan AS. Tetrazilium dye as tools in cell biology: new insights into their cellular reduction. Biotecnol Annu Rev 2005; 11: 127-52.

132. Scudiero DA, Shoemaker RH, Paull KD, Monks A, Tierney S, Nofziger TH, et al. Evaluation of soluble tetrazolium/formazan assay for cell growth and drug sensitivity in culture using human and other tumor cell lines. Cancer Res 1988; 48 (17): 4827-33.

133. Machida H, Ashida N, Ikeda T, Sakata S, Baba M, Shigeta S. In vitro drug combination of 1-(-D-arabinofuranosyl-E-5-(2-bromovinyl)uracil with anti-human immunodeficiency virus or anticancer nucleosides. Antimicrob Agents Ch 1992; 36 (1): 214-6.

134. Mosmann T. Rapid colorimetric assay for cellular growth and survival: application to proliferation and cytotoxicity assays. J Immunol Methods 1983; 65 (1-2): 55-63.

135. Yu FR, Lian XH, Guo HY, McGuire PG, Li RD, Wang R, et al. Isolation and characterization of methyl esters and derivatives for Euphorbia kansui (Euphorbiaceae) and their inhibitory effects on the human SGC-7901 cells. J Pharm Pharmaceut Sci 2005; 8 (3): 528-35.

136. Bezivin C, Tomasi S, Devehat FL, Boustie J. Cytotoxic activity of some lichen extracts on murine and human cancer cell lines. Phytomedicine 2003; 10: 499-503.

137. Liu Y, Schubert D. Steroid hormones block amyloid fibril-induced 3-(4,5-dimrthylthiazol-2-yl)-2,5-diphenyltetrazolium bromide (MTT) formazan exocytosis: relationship to neurotoxicity. J Neurochem 1998; 71 (6): 2322-9.

138. Silva GVJ, Heleno VCG, Constantino MG. Reduction and preparation of a phthalimide derivative from a furo-heliangolide. Molecules 2000; 5: 908-15.

139. Lawrence NJ, Busell SM. The asymmetric synthesis and stereochemical assignment of chelonin B. Tetrahedron Lett 2001; 42: 7671-4.

140. Ungwitayatorn J, Wiwat C, Matayatsuk C, Sripha K, Kamalanonth P, et al. Synthesis and evaluation of phthalimide and benzofuran derivatives as potential HIV-1 reverse transcriptase inhibitors. Songklanakarin J Sci Technol 2001; 23(2): 235-45.

141. Machado AL, Lima LM, Araujo-Jr JX, Fraga CAM, Koatz VLG and Barreiro EJ. Design, synthesis and antiinflammatory activity a novel phthalimide derivative, structurally related to thalidomide. Bioorg Med Chem Lett 2005; 15: 1169-72.

142. Shinji C, Nakamura T, Maeda S, Yoshida M, Hashimoto Y, Miyachi H. Design and synthesis of phthalimide-type histone deacetylase inhibitors. Bioorg Med Chem Lett 2005; 15: 4427-31.

143. Vermeulen M, Zwanenburg B, Chittenden GJF, Verhagen H. Synthesis of isothiocyanate-derived mercapturic acids. Eur J Med Chem 2003; 38: 729-37.

144. Barrett AGM, Braddock DC, James RA, Procopiou PA. Nucleophilic substitution of (alkoxymethylene) dimethylammonium chloride with potassium phthalimide; a convenient procedure for the synthesis of imides with invesrsion of configuration. Chem Commum 1997: 433-4.

145. Yavari I, Alizadeh A, Abbasinejad AA, Bijanzadeh HR. Reaction between alkyl isocyanides and dibenzoylacetylene in the presence of strong NH-acids: synthesis of highly functionalized aminofurans. Tetrahedron 2003; 59: 6083-6.

146. Balzarini J, Pere-Perez MJ, San Felix AS, Camarasa MJ, Bathurst IC, Barr PJ, et al. Kinetic of inhibition of human immunodeficiency virus type 1 (HIV-1) reverse transcriptase by the novel HIV-1 specific nucleoside analogue [2′,5′-bis-*O*-(*tert*-butyldimethylsilyl)-*ß*-D-ribofuranosyl]-3′-spiro-5"-(4"-amino, 2"-oxathiole-2",2"-dioxide)thymine (TSAO-T). J Biol Chem 1992; 267 (17): 11831-8.

147. Clercq ED. HIV-1 specific RT inhibitors: Highly selective inhibitors of human immunodeficiency virus type 1 that are specifically targeted at the viral reverse transcriptase. Med Res Rev 1993; 13 (3): 229-58.

APPENDIX

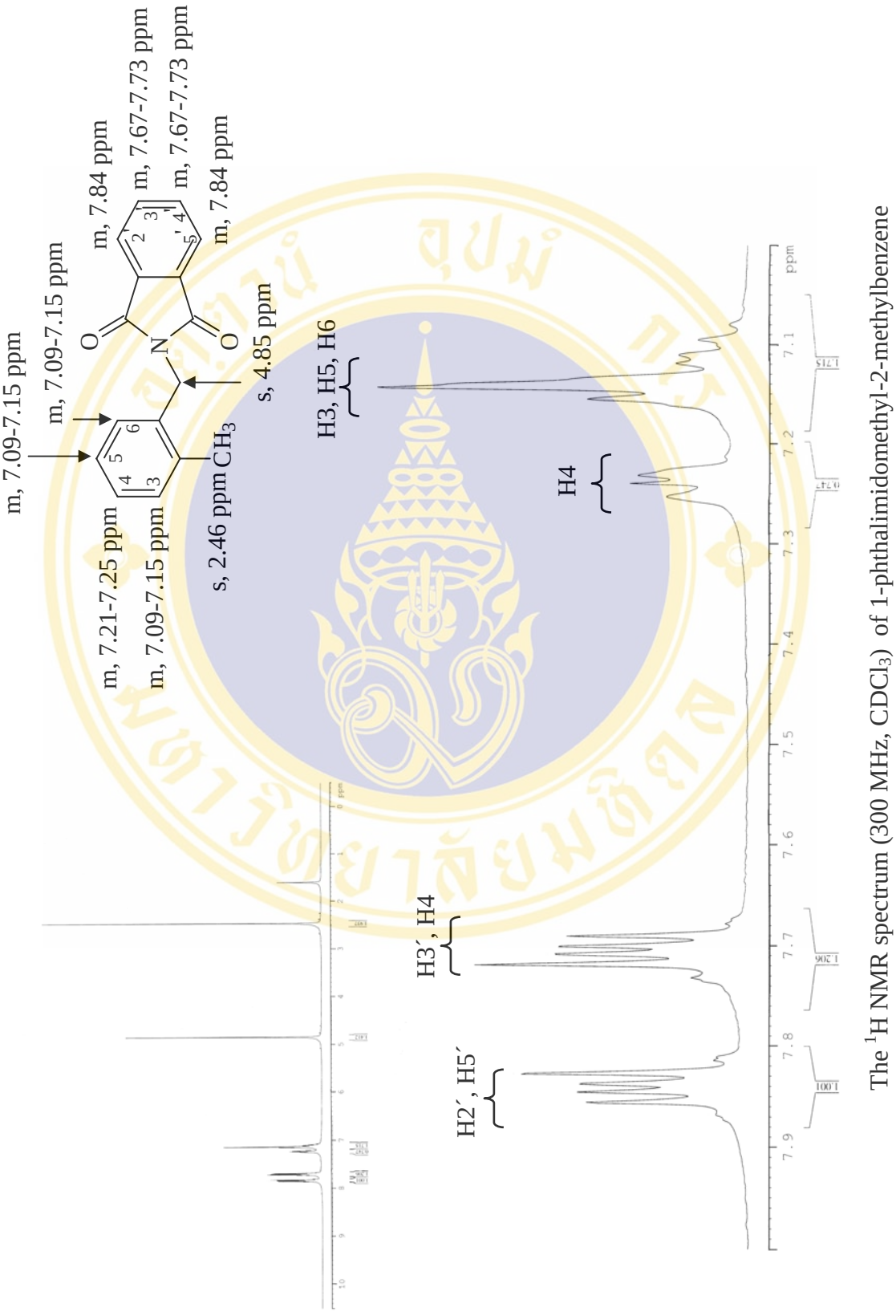

The ^{1}H NMR spectrum (300 MHz, $CDCl_3$) of 1-phthalimidomethyl-2-methylbenzene

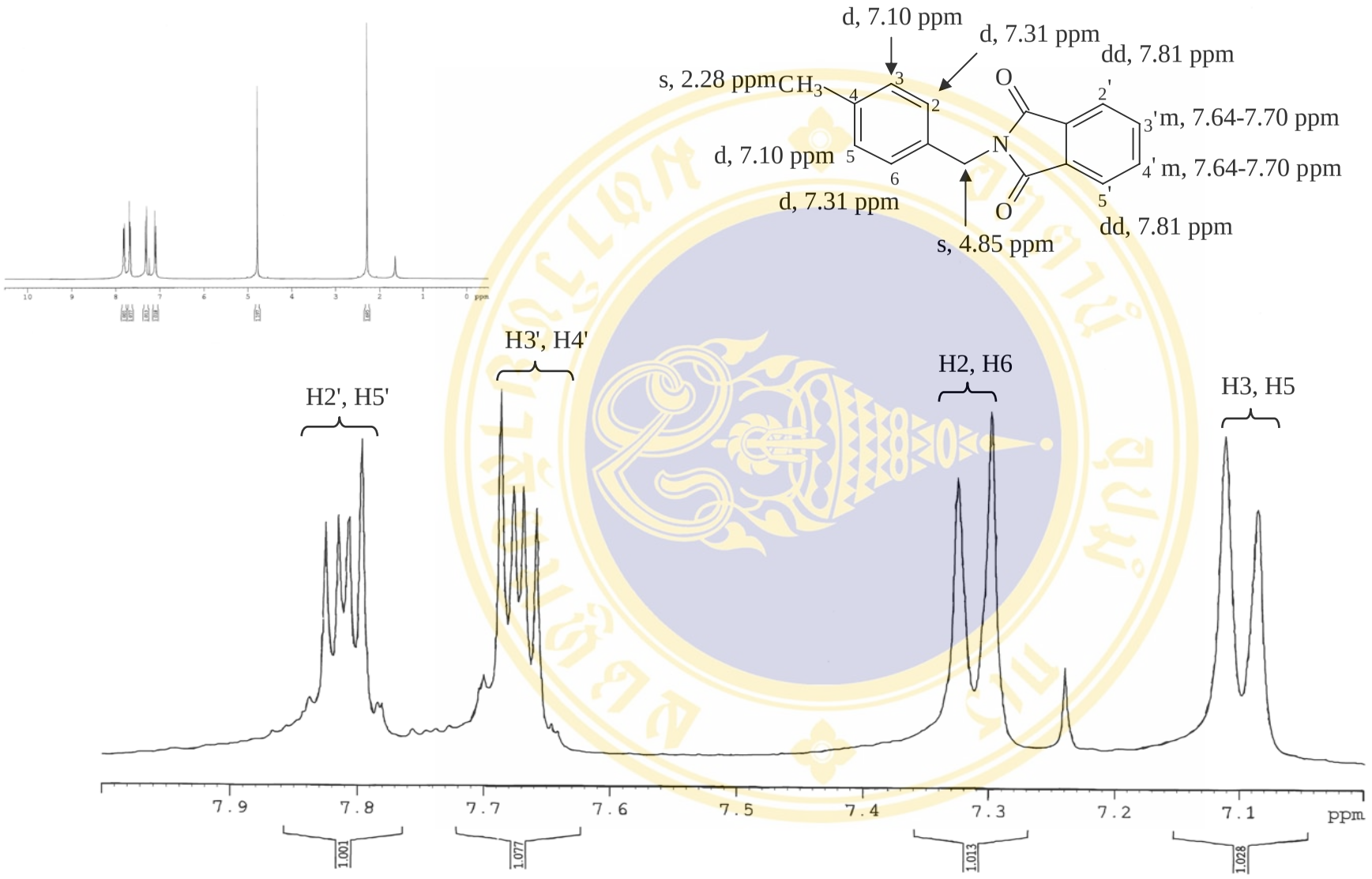

The ^{1}H NMR spectrum (300 MHz, $CDCl_3$) of 1-phthalimidomethyl-4-methylbenzene

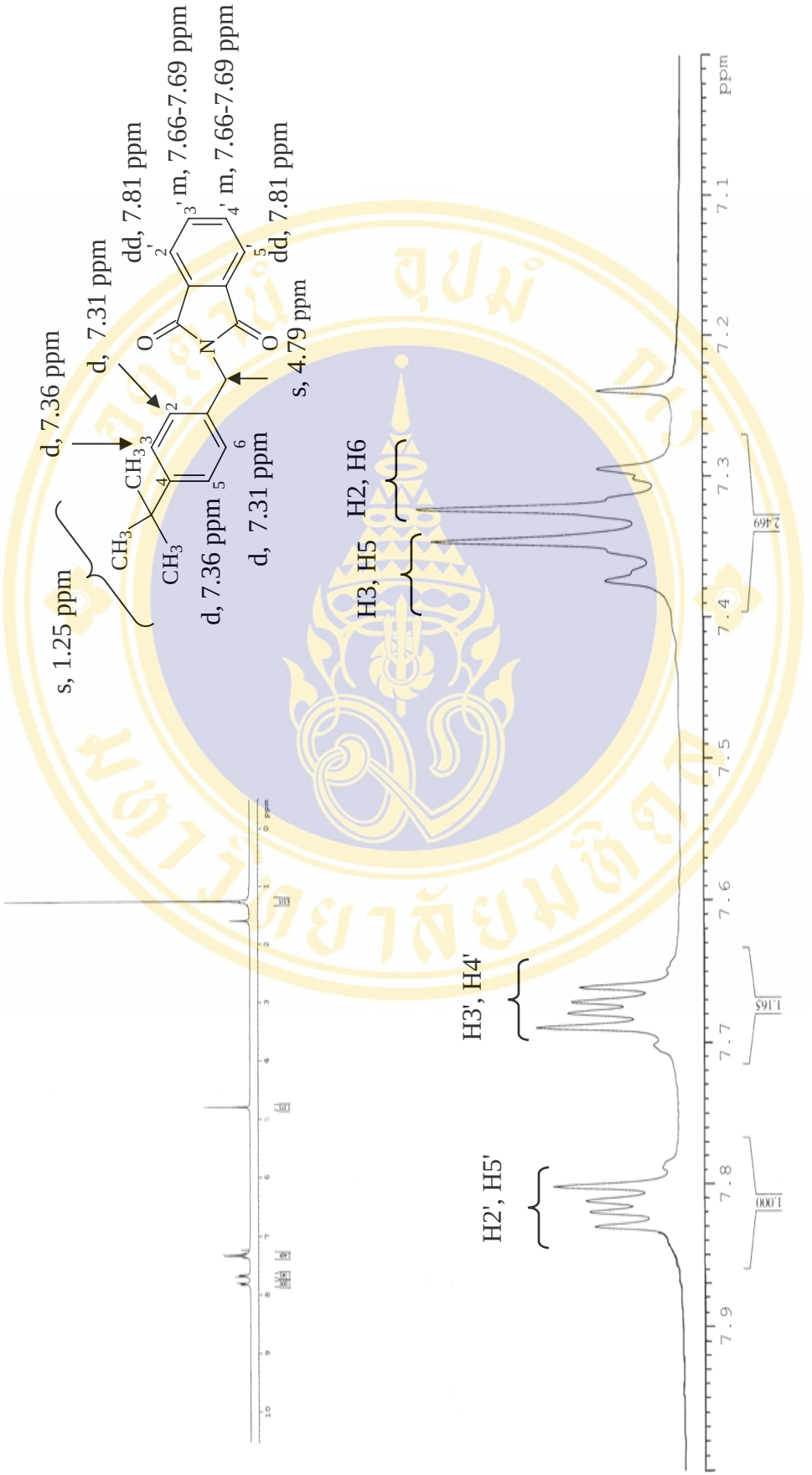

The ^{1}H NMR spectrum (300 MHz, $CDCl_3$) of 1-phthalimidomethyl-4-*tert*-butylbenzene

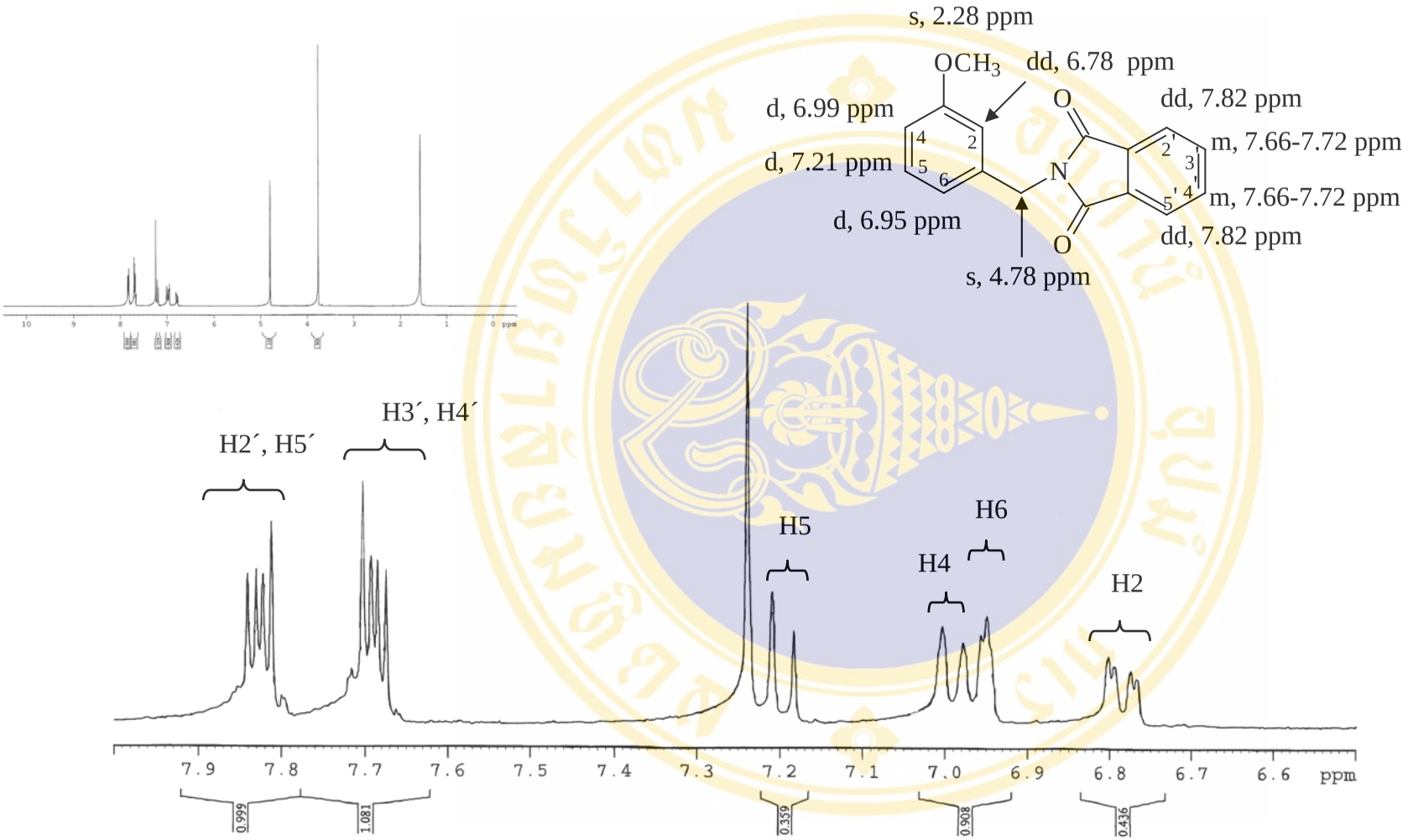

The ^{1}H NMR spectrum (300 MHz, $CDCl_3$) of 1-phthalimidomethyl-3-methyloxybenzene

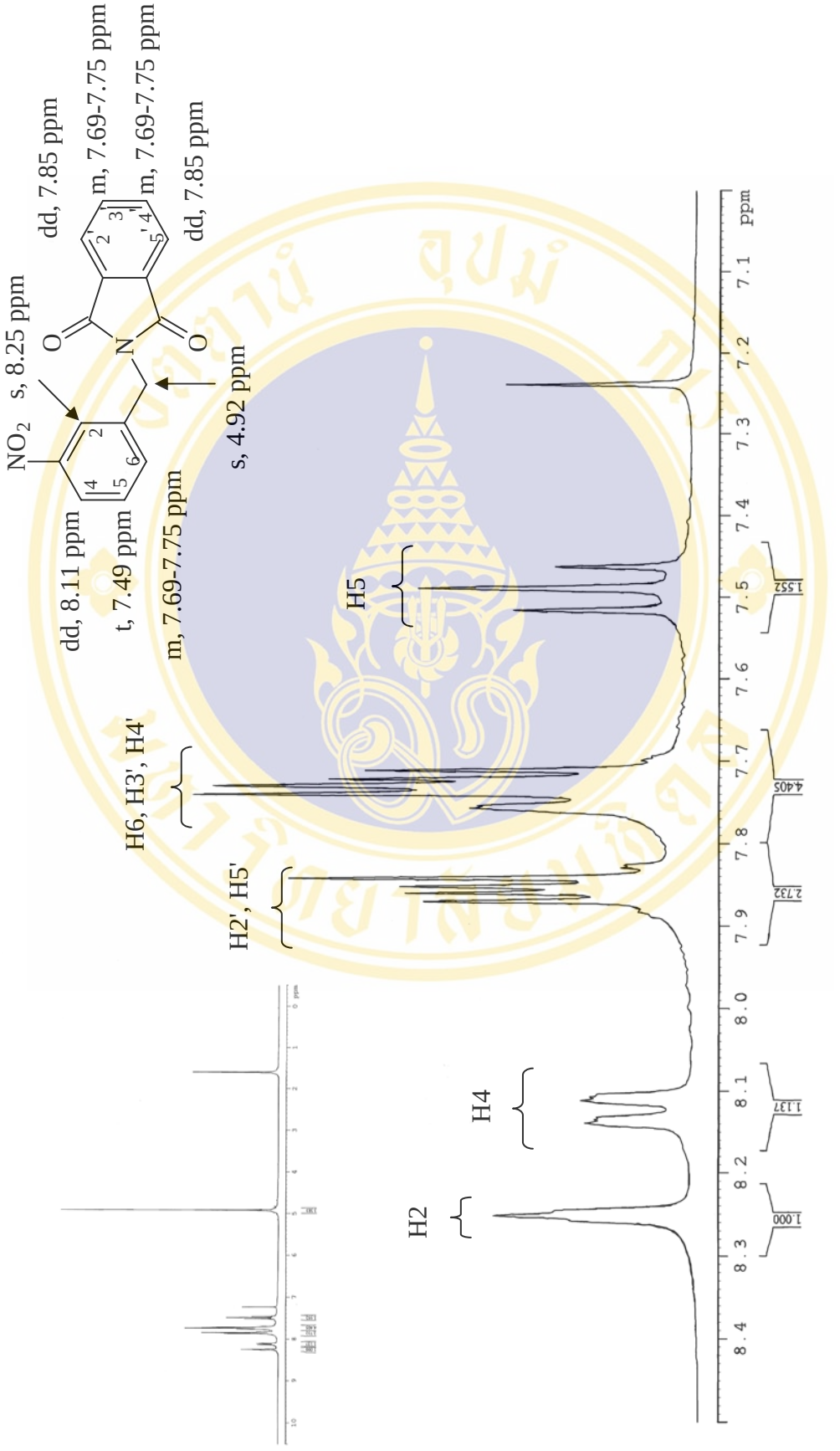

The ^{1}H NMR spectrum (300 MHz, $CDMCl_3$) of 1-phthalimidomethyl-3- nitrobenzene

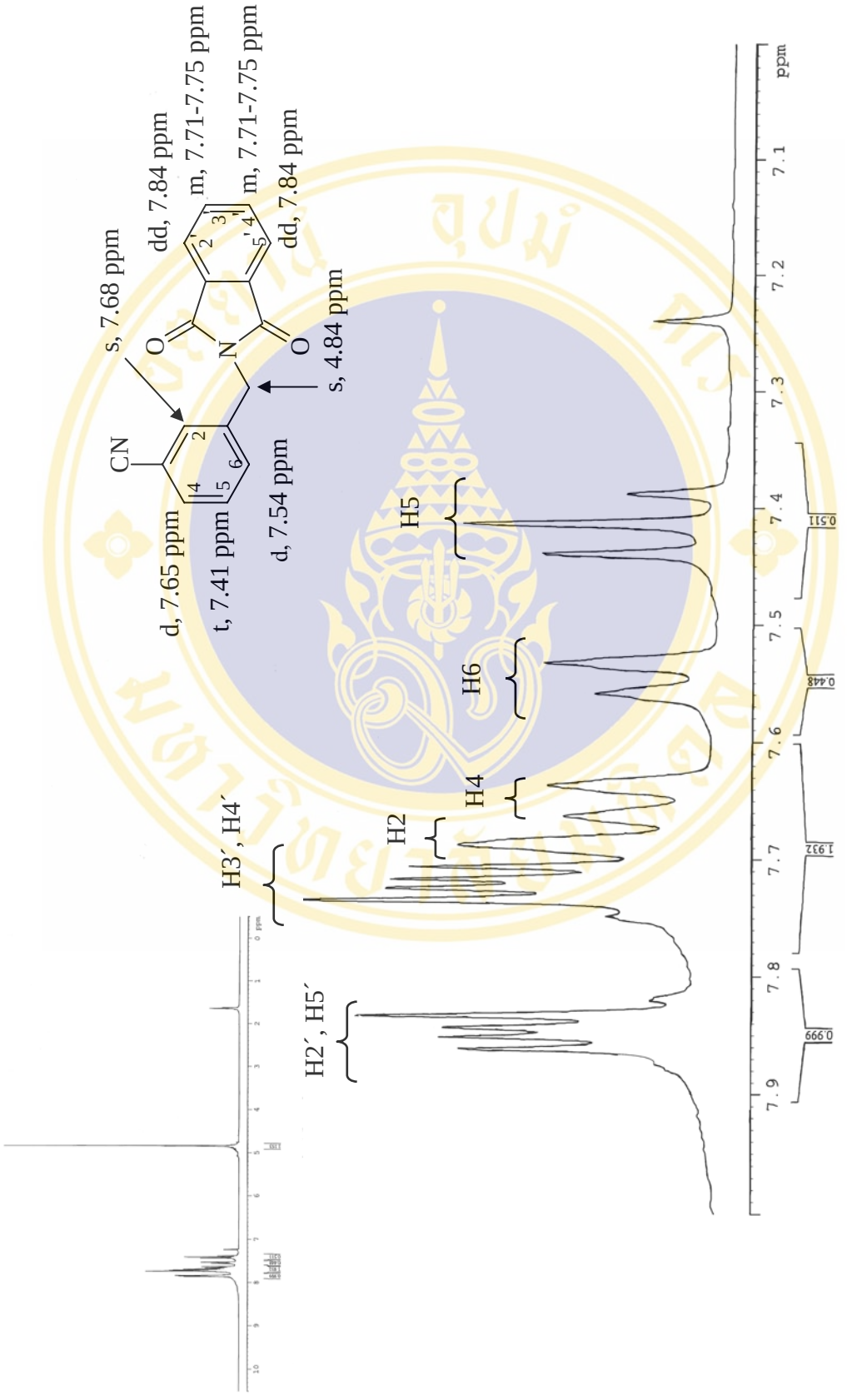

The ^{1}H NMR spectrum (300 MHz, $CDCl_3$) of 1-phthalimidomethyl-3- cyanobenzene

BIOGRAPHY

NAME	Ms. Suratsawadee Piyaviriyakul
DATE OF BIRTH	18 November 1973
PLACE OF BIRTH	Krabee, Thailand
INSTITUTION ATTENDED	Ramkhamhaeng University, Bachelor of Science in Science Mahidol University,: Master of Science in Pharmaceutical Chemistry and Phytochemistry
RESEARCH GRANT	Supported in part by the Thesis Grant, Faculty of Graduate Studies, Mahidol University